UNIVERSITY OF SÃO PAULO

Faculty of Pharmaceutical Sciences

Departament of Pharmacy

Post Graduate Program in Drug and Medicinal Products

Concentration area: Pharmaceutical Production and Control

Dapsone nanocrystals for leprosy treatment: preparation and physicochemical characterization

NATALY PAREDES DA ROCHA

MS. Thesis to obtain the title of Master of Pharmaceutical Sciences

Supervisor: Prof. Dr. Nádia Araci Bou Chacra

São Paulo

2021

UNIVERSITY OF SÃO PAULO

Faculty of Pharmaceutical Sciences

Departament of Pharmacy

Post Graduate Program in Drug and Medicinal Products

Concentration area: Pharmaceutical Production and Control

Dapsone nanocrystals for leprosy treatment: preparation and physicochemical characterization

NATALY PAREDES DA ROCHA

Original Version

MS. Thesis to obtain the title of Master of Pharmaceutical Sciences

Supervisor: Prof. Dr. Nádia Araci Bou Chacra

São Paulo

2021

Nataly Paredes da Rocha

Dapsone nanocrystals for leprosy treatment: preparation and physicochemical characterization.

Examination Board
Of
Thesis to obtain the title of MASTER of Pharmaceutical Science

Prof. Dr.
Supervisor/President

_____
1st examinator

_____
2nd examinator

_____
3rd examinator

_____
4th examinator

São Paulo, _____ de _____ 2021.

Ficha Catalográfica elaborada eletronicamente pelo autor, utilizando o programa desenvolvido pela Seção Técnica de Informática do ICMC/USP e adaptado para a Divisão de Biblioteca e Documentação do Conjunto das Químicas da USP

Bibliotecária responsável pela orientação de catalogação da publicação:
Marlene Aparecida Vieira - CRB - 8/5562

R672d

Rocha, Nataly Paredes da
Dapsone nanocrystals for leprosy treatment: preparation and physicochemical characterization. / Nataly Paredes da Rocha. - São Paulo, 2021.
140 p.

Dissertação (mestrado) - Faculdade de Ciências Farmacêuticas da Universidade de São Paulo. Departamento de Farmácia.
Orientador: Bou-Chacra, Nádia Araci

1. nanotecnologia. 2. nanopartículas. 3. nanosuspensão. 4. hanseniase. 5. nanotechnology. I. T. II. Bou-Chacra, Nádia Araci, orientador.

“Você tem que agir como se fosse possível transformar radicalmente o mundo.
E você tem que fazer isso o tempo todo.”

Angela Davis

DEDICATION

I dedicate this work to the One who strengthens me, to my beloved parents for their unconditional love, example and strength, and to my husband, my partner, with whom I share my dreams.

ACKNOWLEDGMENTS

First of all, I would like to thank God for blessing my life and enabling me to make this dream come true.

I would like to thank and express my admiration for the Prof. Dr. Nádia A. Bou Chacra, for her guidance and confidence. This work faced many challenges over a critical period in history, and only their enthusiasm combined with several hours of hard work made its conclusion possible. As your undergraduate student, through your example I fell in love with the pharmaceutical industry, and as your master's student, I fell in love with science. She made me understand that I must not limit myself, but always believe.

I would also like to thank to Doctors Gabriel Lima de Barros Araújo, Iolanda Midea Cuccovia, Kelly Ishida, Humberto Gomes Ferraz, their students Mariana Miyagi, Thayna Barreto, Paloma Sousa, Katherine Melo, and the laboratory technician Eremita Santos for their availability, help and contribution to my work. I would like to extend my thanks to the Department of Pharmacy, Faculty of Pharmaceutical Sciences, University of São Paulo, especially to the administrative technicians David de Lima Filho and Alexandre Spitalere for their support.

I am thankful to CAPES (Coordenação de Aperfeiçoamento de Pessoal de Nível Superior) for providing the scholarship for completion of this MS degree under Faculty of Pharmacy and Pharmaceutical Sciences of University of São Paulo.

My gratitude goes to the current and former colleagues in the laboratory: Aline, Maria Christina, Isabela, Megumi, Mirla, Beatriz, Eduardo, Osvaldo, Lis, Luiza, for your friendship, patience and exchanges.

I am especially grateful to Julio Rocha, my father, my first and unconditional lifelong support. He gave me courage to go further, and is my loving safe haven during in worries. I express my gratitude to Harley Souza, my husband, who always encourages me, reassures me, and was my spectator for countless hours. One special thanks to my mother, Agostinha Rocha, my example of woman and strength, your memory will always be in me. I can never thank them enough.

I am also thankful to my friends and family, who always believed in my potential, and supported me throughout the years with a lot of love and joy. To all the people who were part of my life and somehow contributed for me to this achievement, my eternal thanks.

RESUMO

ROCHA, N.P.D. Nanocristais de dapsona para o tratamento de hanseníase: preparação e caracterização físico-química. 2021. Tese (Mestrado) ‑ Faculdade de Ciências Farmacêuticas, Universidade de São Paulo, São Paulo, 2021.

A hanseníase é uma das doenças mais antigas da humanidade e, embora não seja mais considerada um problema de saúde pública globalmente, ainda é endêmica em vários países. O Brasil é o segundo país em novos casos, sendo responsável por 12,8% do total detectado. A dapsona é um dos fármacos da poliquimioterapia (PQT), mas seu uso está comumente relacionado à ocorrência de efeitos adversos graves, resultando em abandono do tratamento. Segundo o Sistema de Classificação Biofarmacêutica (SCB), esse fármaco pertence à classe II, e sua baixa solubilidade em água pode limitar sua biodisponibilidade. Portanto, a redução do tamanho de partícula do fármaco para a produção de nanocristais promove um aumento da razão entre a área superficial e o volume, o que permite um incremento da solubilidade de saturação e da taxa de dissolução. Além disso, a aplicação de uma abordagem sistemática durante a fase de desenvolvimento é fundamental, garantindo um melhor entendimento de um produto por meio da qualidade por design (QbD). No presente estudo, a seleção da concentração ideal de Povacoat®, da velocidade de agitação e do tempo de processo, até a redução das partículas foi realizada pelo planejamento de experimentos (DoE). A formulação otimizada obtida pela técnica de moagem por via úmida em escala reduzida resultou em um tamanho médio de 206,3 ± 6,7 nm, IP de 0,132 ± 0,012 e potencial zeta de -9,8 ± 0,3 mV, com distribuição monomodal. A análise térmica (DSC) e a difração de raios X (DRX) da formulação liofilizada revelaram a manutenção da estrutura cristalina do fármaco após o processo de moagem, e a ausência de interação entre fármaco e excipientes. A nanosuspensão apresentou baixa variabilidade de tamanho de partícula ao longo dos 4 meses de estudos de longa duração e 3 meses de estudos de estabilidade acelerada. Os nanocristais de dapsona demostraram uma melhoria na solubilidade de saturação de 3,78 vezes em água, comparado à matéria-prima. Estudos de toxicidade realizados em larvas de *galleria mellonella* indicam baixa toxicidade a uma dose de 20 mg/kg da formulação. Finalmente, uma tentativa inicial de aumentar a escala, de laboratorial para piloto, resultou em nanopartículas promissoras para um produto comercial. Portanto, o presente estudo permitiu o desenvolvimento de

uma nanosuspensão de dapsona, com potencial para melhorar a adesão ao tratamento para hanseníase.
Palavras-chave: nanocristais, nanosuspensão, hanseníase, dapsona, desenho de experimentos.

ABSTRACT

ROCHA, N.P.D. Dapsone nanocrystals for leprosy treatment: preparation and physicochemical characterization. 2021. MS. Thesis – School of Pharmaceutical Sciences, University of São Paulo, São Paulo, 2021.

Leprosy is one of humanity's oldest diseases, and even though it is no longer considered a public health problem globally, it is still endemic in several countries. Brazil is the second country in new cases detected, being responsible for 12.8% of the total. Dapsone is one of Multidrug treatment (MDT), but its use is commonly related to the occurrence of serious adverse effects, resulting in treatment abandonment. According to Biopharmaceutics Classification System, this drug belongs to class II, and its low solubility in water may limit bioavailability. Hence, reducing particle size to produce drug nanocrystals promotes an increase of surface area to volume ratio, which allows an increment of saturation solubility and dissolution rate. In addition, the use of a systematic approach during the development phase is paramount, guaranteeing a better understanding of a product through quality by design appeal. In the present study, the selection of optimal Povacoat^{TM} concentration, stirring speed, and process time to particle reduction was carried out by the design of experiment (DoE). The optimized formulation obtained by small-scale wet bead milling technique resulted in an average size of 206.3 ± 6.7 nm, PdI of 0.132 ± 0.012, and zeta potential of -9.8 ± 0.3 mV and monomodal distribution. Thermal analysis (DSC) and X-ray diffraction (XRD) of lyophilized formulation revealed the maintenance of the drug substance crystal structure after the milling process and the absence of interaction between drug and excipients. The nanosuspension presented low particle size variability over the 4 months of long-term and 3 months of accelerated stability studies. Dapsone nanocrystals showed an improvement in saturation solubility of 3.78 in water compared to raw material. Toxicity studies performed in *galleria mellonella* larvae indicates low toxicity at dose of 20 mg/kg of formulation. Finally, an initial attempt to scale up from lab to pilot resulted in promising nano-sized particles for a commercial product. Therefore, the present study allowed the development of dapsone nanosuspension with the potential to improve adherence to leprosy treatment.

Keywords: nanocrystals, nanosuspension, leprosy, dapsone, design of experiments.

PREFACE

This thesis is an original work by Nataly Paredes da Rocha completed under the supervision of Prof. Dr. Nádia Araci Bou-Chacra at the Faculty of Pharmaceutical Sciences. Most parts of the work were performed at the Dr. Bou-Chacra lab facilities. Some experiments were also carried out at different lab facilities at the University of São Paulo, as Dr. Humberto Gomes Ferraz and Dr. Gabriel Lima Barros de Araujo at the Faculty of Pharmaceutical Sciences - University of São Paulo, Dr. Kelly Ishida at the Microbiology Department of Institute of Biomedical Sciences, Dr. Iolanda Midea Cuccovia at the Institute of Chemistry, and LCT - Technological Characterization Laboratory at Polytechnic School, all of them at University of São Paulo.

Chapter 1 of this thesis focuses on the challenges faced for leprosy elimination in the world. The chapter compiles the findings of recent studies and disease statistics while underscoring the importance of a treatment more safe and effective. It was adapted from an article submitted as Nataly Paredes da Rocha, Gabriel Lima de Barros Araújo, Eduardo José Barbosa, Nádia Araci Bou-Chacra, with the title of Leprosy diagnosis and treatment: update and challenges in **Brazilian Journal of Pharmaceutical Sciences** (impact factor:0.814).

Chapter 2 is composed by the adaptation of a submitted mini review in adittion to the results of the development of dapsone nanocrystal applying a design space approach and its chemical-physical characterization. The mini review article untitled “Innovative drug delivery systems for Leprosy treatment” is in review in the **Indian Journal of Dermatology, Venereology and Leprology** (impact factor: 2.545). The experimental article is resulting from this dissertation is being finalized and will be submitted in **Journal of Pharmaceutical Sciences** (impact factor: 3.534).

Appendices presented the articles submitted during the master degree period. Appendix A corresponds to the article referenced in chapter 1, while appendix B refers to the article used to compose chapter 2. On the other hand, Appendix C presents an article that will be submitted as Nataly Paredes da Rocha, Osvaldo Cirilo da Silva, Eduardo José Barbosa, Gidel Soares, Roberto Oliveira, Raimar Löbenberg, Lis Marie Monteiro, Nádia Araci Bou-Chacra, untitled “Statistical process control of manufacturing tablets for antiretroviral therapy” in **Brazilian Journal of Pharmaceutical Sciences**. In addition, the appendix D “Cancer treatment in the

lymphatic system: A prospective targeting employing nanostructured systems" contain the abstract of the article published as Megumi Nishitani Yukuyama, Gabriel Lima Barros de Araujo, Aline de Souza, Raimar Löbenberg, Eduardo José Barbosa, Mirla Anali Bazán Henostroza, Nataly Paredes da Rocha, Isabela Fernandes de Oliveira, Beatriz Rabelo Folchini, Camilla Midori Peroni, Jessica Fagionato Masiero, Nádia Araci Bou-Chacra in **International Journal of Pharmaceutics**.

LIST OF FIGURES

LIST OF TABLES

LIST OF EQUATIONS

SUMMARY

1. CHAPTER 1: Leprosy and the challenges for its elimination

1.1. Introduction

Leprosy is one of humanity's oldest diseases, an infectious-contagious and chronic disease caused by *Mycobacterium leprae*, an obligate intracellular parasite (SCHNEIDER; FREITAS, 2018). The bacillus has a tropism for macrophages presents in the skin and for Schwann cells in nerves, which determines the main areas affected by the disease (TIWARI et al., 2017). As well as, the damage caused in peripheral nerves may provoke sensory and motor impairment with deformities and disability, which is characteristic of the patient committed by leprosy (BRITTON; LOCKWOOD, 2004). Leprosy is the second mycobacteria disease most common in the world (CARDONA-PEMBERTHY et al., 2018).

In 2019, a total of 202,185 new cases were reported, according to WHO. India, Brazil, and Indonesia are the first three countries in the number of new cases reported, in this order, concentrating approximately 80% of them (Figure 1). Brazil is responsible for 13.8% of total globally reported and for 93,1% of Americas countries (WHO, 2020). The WHO guideline "Global Leprosy Strategy 2016–2020: accelerating towards a leprosy-free world" aimed to eliminate leprosy and visible deformities among children (WHO, 2016). The incidence of a disease in children reveals a disease active foci and the endemic transmission force, guiding government decisions on epidemiological surveillance (DE SOUZA et al., 2018; SCHNEIDER; FREITAS, 2018). In addition, the presence of disabilities during diagnosis indirectly indicates delayed detection. Although both indexes have been reduced globally, Brazil showed a 28% increase in the number of children with severe dysfunctions compared to the previous year (WHO, 2019, 2020).

Figure 1: Leprosy new cases: most prevalent countries in the world (2019) according to the WHO.

Source: the author

1.2. Infection development

The transmission occurs by the aerosol spread of droplets, especially during close and prolonged contact with untreated patients, to susceptible individuals (MANE ABHAY B, 2014; CUNHA et al., 2015). The susceptibility to infection seems to be low (about 20%), but gene mutations in myeloid protein zero (MPZ) and in mannose-binding lectin 2 (MBL_2) receptors may increase the infection risk in family members of leprosy patients (BLOK et al., 2018; CARDONA-PEMBERTHY et al., 2018). Moreover, the close contact and exposure time are aggravating factors for contamination (CUNHA et al., 2015). Therefore, in order to mitigate the risk of contagion, chemoprophylaxis and immunoprophylaxis treatments can be proposed for patients' households (PALIT; KAR, 2020).

The disease pathogenesis is not fully understood; meantime, recent studies have progressed in elucidating different aspects of leprosy. For example, it is now known that the extraordinarily complexity of the disease is determined by the immune response modulation by the bacillus (DE SOUSA et al., 2017). For a long period, it

was known that a paradigm between Th1 and Th2 responses determines the severity and the disease manifestation (ANTONIO; QUARESMA, 2017). Thus, patients who present strong Th1 immune response, a high cell-mediated immunity, will narrow the disease's progression. In contrast, the Th2 response, predominantly humoral and with high titles of antibodies, would impair the bacillus multiplication control, worsening the disease (REIBEL; CAMBAU; AUBRY, 2015). Nevertheless, Th9, Th17, Th22, Treg, and different subsets of pro-inflammatory cytokines were recently identified as additional modulators of leprosy (ANTONIO; QUARESMA, 2017; FABEL et al., 2019). Additionally, metabolic alterations, overproduction of reactive oxygen species (ROS) and B-cells are also involved in leprosy progression (MATTOS et al., 2011; MADIGAN et al., 2017; FABEL et al., 2019). These numerous mechanisms involved may explain the clinical spectrum of the disease.

1.3. Leprosy classification

Ridley and Jopling proposed in 1966 a classification based on immunity and considering clinical, histological, and bacteriological aspects (RIDLEY, D S; JOPLING, 1966). Tuberculoid leprosy (TT) patients have a strong pro-inflammatory response, with Th1 and Th17 responses aiming to control the infection; however, this vigorous response may affect the body's own cells, mimicking autoimmunity (GELUK, 2018). In the other spectrum extreme, Lepromatous leprosy (LL) patients have no cell-mediated immunity, with Th2 polarization and down-regulation of Th1 response, lacking *M. leprae*-specific T cells and allowing pathogen reproduction (ANTONIO; QUARESMA, 2017; GELUK, 2018). Between the two extremes are the majority of the patients, classified as borderline: Borderline Tuberculoid (BT), Mid-borderline (BB), and Borderline Lepromatous (BL), respectively, showing decrease in cell-mediated immunity, and an increase in the bacillary load (RIDLEY, D S; JOPLING, 1966; GELUK, 2018; LEGUA, 2018). These patients are immunologically unstable, with characteristics varying between TT and LL forms (ANTONIO; QUARESMA, 2017).

The WHO proposed a clinical classification for therapy purposes. The patients started to be classified as Multibacillary (MB), presenting more than five skin patches (including BB, BL, and LL) or Paucibacillary (PB), with 1 to 5 skin patches (including TT and BT) (YAWALKAR, 2009; LEGUA, 2018). This method is practical and

inexpensive, being essential in underdeveloped regions and with insufficient Public Health infrastructure. However, this diagnostic method is effective for only 70% of patients and tends to overestimate MB cases (MOURA et al., 2008; RODRIGUES JÚNIOR et al., 2016). This fact becomes a concern since the treatments are different for the two clinical forms, and can result in overtreatment for PB patients and incomplete for MB (PARDILLO et al., 2007).

Based on the difference in treatments, the assertive diagnosis is vital to decrease leprosy transmission since untreated patients are able to disseminate the bacillus (WALKER; LOCKWOOD, 2007; CUNHA et al., 2015). Additionally, as previously mentioned, the early detection is crucial to prevent physical disabilities (RAO; SUNEETHA, 2018).

1.4. The importance of assertive and early diagnosis

The clinical diagnosis, based on the number of skin lesions, was recommended by WHO, but its limitations and the corresponding impact on the success of therapy must be considered (LASTÓRIA; DE ABREU, 2014). Besides the challenges of under and overtreatment, an incorrect classification can trigger drug resistance (PARDILLO et al., 2007). When available, microbiological assessment of slit skin smears (SSSs) and histopathology can be appropriate tools for correct diagnosis (JIAN et al., 2020). The bacterial index is especially useful to confirm MB diagnosis, since its low sensitivity could not be assertive for PB cases (LASTÓRIA; DE ABREU, 2014; MINISTÉRIO DA SAÚDE, 2016). The SSSs, together with clinical examination, is recommended in areas which present a high frequency of MB cases (PARDILLO et al., 2007). The histopathology examination, performed in fragments of skin lesions or nerves, may disagree with the clinical aspect, indicating the evolution of the disease towards one of the extremes (LASTÓRIA; DE ABREU, 2014).

Furthermore, the early diagnosis is important to avoid the occurrence of reactions, which may lead to disabilities, deformities and morbidity often associated with leprosy (NERY et al., 2013). These reactions can be divided in type I and II, according to immune response, and may happen before or after the treatment (EICHELMANN et al., 2013). Initiating anti-inflammatory therapy early has potential to prevent nerve damage (NERY et al., 2013).

Although clinical and histopathological tests may be helpful to diagnosis leprosy, they cannot, for example, confirm the PB suspected cases (BARBIERI et al., 2019). Aiming at assertive and early diagnosis, recent research attempts to identify specific molecular markers for *M. leprae* and develop a sensitive laboratory test (LASTÓRIA; DE ABREU, 2014). Sorological and molecular diagnosis methods have presented as promising choices for differential leprosy diagnosis (GARNIER et al., 2001; RIBEIRO-ALVES; SARNO; OZO, 2011). Among them, the kit NDO-LID® may be highlighted due to its low-cost and simplicity, which does not require a laboratory setup (DEVIDES et al., 2018). And, the quantitative PCR (qPCR) assays may be applicable regarding their higher specificity, sensitivity and faster turnaround time, as long as the cost and laboratory equipment are not limiting factors (RIBEIRO-ALVES; SARNO; OZO, 2011; SOTO; TORRES MUÑOZ, 2015).

1.5. Leprosy treatment and its challenges

The treatment is important to cure the patient individually but also to contain the disease transmission. For centuries, no drug substance was effective against leprosy. Only in 1946 dapsone was used intramuscularly for leprosy treatment, and orally in 1947 (YAWALKAR, 2009). Dapsone was used as monotherapy until the reports of relapsed patients, in the 1960s, and the definitive proof of the selection of dapsone-resistant *Mycobacterium leprae* was obtained in 1964, with the adapting Shepard's mouse foot-pad technique, due to the impossibility of bacillus to grow in a culture medium (PEARSON; REES; WATERS, 1975; JI, 1985; BRITTON; LOCKWOOD, 2004). Since 1981, the WHO has recommended multidrug therapy (MDT) regimens to minimize resistance to the single drugs themselves used as monotherapy (CAMBAU et al., 1997). MDT consists of dapsone, rifampicin, and clofazimine, with a different duration between clinical classifications (WORLD HEALTH ORGANIZATION, 2018). The inclusion of clofazimine in PB treatment occurred in 2018 to reduce the impact of misdiagnosis and is still questionable (WORLD HEALTH ORGANIZATION, 2018; ALEMU BELACHEW; NAAFS, 2019). The MDT posology is shown in Table 1.

Table 1: Doses of MDT medications and treatment duration (for adults), recommended by the WHO, according to clinical classification.

Classification	Drug substance (mg)			Duration (months)
	Dapsone (daily)	Rifampicin (monthly)	Clofazimine (daily/ monthly)	
Multibacillary	100	600	50/300	12
Paucibacillary	100	600	50/300	6

Source: Adapted from ALEMU BELACHEW; NAAFS, 2019.

Dapsone (DAP, $C_{12}H_{12}N_2O_2S$) is a structural analog of para-aminobenzoic acid (PABA) presenting bacteriostatic action (KAI et al., 1999; GOULART et al., 2005). It acts as a competitive inhibitor of dihydropteroate synthase enzyme, decreasing or blocking bacterial folic acid synthesis (GOULART et al., 2005). DAP has multiple activities, namely antibacterial, anti-inflammatory, antiprotozoal, and antifungal (FERNANDES et al., 2017). Therefore, DAP can also be indicated for the treatment of several diseases, such as malaria, rheumatoid arthritis, granuloma annulare, dermatitis herpetiformis, and other vesiculobullous diseases (FERNANDES et al., 2017).

Rifampicin (RIF, $C_{43}H_{58}N_4O_{12}$) is a macrocyclic antibiotic with bactericidal action (ANGIOLINI et al., 2017; ANGIOLINI; COHEN; DOUHAL, 2019). It is used mainly against mycobacterial infections (e.g., tuberculosis and leprosy) and a wide range of Gram-positive and Gram-negative bacteria (ANGIOLINI; COHEN; DOUHAL, 2019). RIF forms a stable drug-enzyme complex with RNA polymerase enzyme, suppressing chain formation during the RNA synthesis, causing bacteria death (ANGIOLINI et al., 2017; GURAGAIN; UPADHAYAY; BHATTARAI, 2017).

Clofazimine (CFZ, $C_{27}H_{22}Cl_2N_4$) is a phenazine derivative, active in *M. leprae* dapsone-resistant cases, working slowly on bacillus and destroying 99% of them in approximately five months (CRUZ et al., 2017). CFZ is a repository drug, thus, it continues to be stored in the body after administration and is slowly excreted (WORLD HEALTH ORGANIZATION, 2003). This feature explains the monthly additional administration of CFZ to ensure the optimal concentration maintenance in cases of daily missed dose (WORLD HEALTH ORGANIZATION, 2003). Additionally, CFZ has also anti-inflammatory activity, being used in leprosy reactions to manage the corticosteroid doses (EICHELMANN et al., 2013; CRUZ et al., 2017). The CFZ exact mechanism of action is not entirely understood, but it probably acts in different

targets, such as generation of reactive oxygen species, inhibition of respiratory chain, and reduction of ATP for cellular processes (MIRNEJAD et al., 2018).

All MDT drugs are classified as Class II drug substances, according to Biopharmaceutics Classification System (BCS), and present low solubility in water and high permeability, impairing its bioavailability (LINDERSTRØM-LANG; NAYLOR, 1962; AGRAWAL; PANCHAGNULA, 2005; BOLLA; NANGIA, 2012). Accordingly, water solubility is the limiting factor for oral absorption, and may aggravate the occurrence of adverse effects and resistance, finally resulting in treatment abandonment.

Despite the solubility challenge, MDT still faces the emergence of bacterial resistance in some patients. For DAP, 55% of monitored patients developed resistance, whose mutations occurs in codon 55 and 53 from the *folp1 M. leprae* gene encode DHPS (KAI et al., 1999; DALAWI et al., 2017). Similarly, the *rpoB* gene, which encodes the β subunit of the RNA polymerase, is responsible for the bacterial mutation in RIF resistance cases (REIBEL; CAMBAU; AUBRY, 2015). The percentage of RIF resistance cases differs, but it is less than 5% (DALAWI et al., 2017; CAMBAU et al., 2018). Assuming the rifampicin resistance rate in non-compliant patients of 89%, the RIF resistance may be mainly related to treatment compliance (SISKAWATI et al., 2018). Unlikely, resistance is less critical for CFZ, observed in only 0.2% of patients (DALAWI et al., 2017). The bacillus survival may be attributed to several CFZ mechanisms of action (KAR; GUPTA, 2015).

In contrast, CFZ is commonly associated with adverse effects in MDT. Reddish-brown skin discoloration, which is common when using iminophenazine dye, is manifested in 75-100% of patients (KAR; GUPTA, 2015; CRUZ et al., 2017). Ichthyosis and dryness are less prevalent, and acneiform eruptions, subacute intestinal obstruction, and Bull's-eye retinopathy are rare (KAR; GUPTA, 2015). Patients under DAP treatment can present skin hyperpigmentation, hemolytic anemia, methemoglobinemia, hepatotoxicity, peripheral neuropathy, and rarely agranulocytosis and toxic epidermal necrolysis (BHENGRA; KUMAR; SUNDAR CHAUDHARY, 2016; GURAGAIN; UPADHAYAY; BHATTARAI, 2017). Severe adverse effects DAP-related are Steven-Johnson syndrome, toxic epidermal necrolysis, or dapsone hypersensitivity syndrome (BHENGRA; KUMAR; SUNDAR CHAUDHARY, 2016). DAP metabolites may produce ROS through a dose-dependent reaction, causing hemolysis (REILLY; WOSTER; SVENSSON, 1999). RIF

may also present adverse effects, such as hepatotoxicity, thrombocytopenia, orange discoloration (of sweat, saliva, urine, feces, and tears) (GOULART et al., 2005; HOWARD et al., 2015). According to the various possible adverse effects, the inclusion of CFZ in the treatment of PB patients to minimize misdiagnosis, may end up resulting in treatment abandonment.

In summary, the present study aims to improve the leprosy treatment by improving the bioavailability of the main MDT drug, dapsone, reducing the occurrence of adverse effects and bacterial resistance. This measure enables the therapy compliance enhancement, promoting the cure of patients and reducing the occurrence of new cases.

1.6. REFERENCES

AGRAWAL, S.; PANCHAGNULA, R. Implication of biopharmaceutics and pharmacokinetics of rifampicin in variable bioavailability from solid oral dosage form. **Biopharmaceutics and Drug Disposition**, v. 26, n. 8, p. 321–334, 2005.

ALEMU BELACHEW, W.; NAAFS, B. Position statement: LEPROSY: Diagnosis, treatment and follow-up. **Journal of the European Academy of Dermatology and Venereology**, v. 33, n. 7, p. 1205–1213, 2019.

ANGIOLINI, L. et al. Formation, characterization and pH dependence of rifampicin: heptakis(2,6-di-O-methyl)-β-cyclodextrin complexes. **International Journal of Pharmaceutics**, v. 531, n. 2, p. 668–675, 2017.

ANGIOLINI, L.; COHEN, B.; DOUHAL, A. Ultrafast dynamics of the antibiotic Rifampicin in solution. **Photochemical and Photobiological Sciences**, v. 18, n. 1, p. 80–91, 2019.

ANTONIO, J.; QUARESMA, S. Leprosy As a Complex infection : Breakdown of the Th1 and Th2 immune Paradigm in the immunopathogenesis of the Disease. **Frontiers in Immunology |**, v. 8, n. November, p. 18–21, 2017.

BARBIERI, R. R. et al. Quantitative polymerase chain reaction in paucibacillary leprosy diagnosis: A follow-up study. **PLoS neglected tropical diseases**, v. 13, n. 3, p. 1–12, 1 mar. 2019.

BHENGRA, M. P.; KUMAR, P.; SUNDAR CHAUDHARY, S. **An unusual case of dapsone hypersensitivity syndrome in a leprosy patientJournal of Pakistan Association of Dermatologists**.

BLOK, D. J. et al. Minimum requirements and optimal testing strategies of a diagnostic test for leprosy as a tool towards zero transmission: A modeling study. **PLOS Neglected Tropical Diseases**, v. 12, n. 5, p. e0006529, 25 maio 2018.

BOLLA, G.; NANGIA, A. Clofazimine mesylate: A high solubility stable salt. **Crystal Growth and Design**, v. 12, n. 12, p. 6250–6259, 2012.

BRITTON, W. J.; LOCKWOOD, D. N. Leprosy. **The Lancet**, v. 363, n. 9416, p. 1209–1219, abr. 2004.

CAMBAU, E. et al. Multidrug-resistance to dapsone, rifampicin, and ofloxacin in Mycobacterium leprae. **Lancet**, v. 349, n. 9045, p. 103–104, jan. 1997.

CAMBAU, E. et al. Antimicrobial resistance in leprosy: results of the first prospective open survey conducted by a WHO surveillance network for the period 2009–15. **Clinical Microbiology and Infection**, v. 24, n. 12, p. 1305–1310, 2018.

CARDONA-PEMBERTHY, V. et al. Genetic variants, structural, and functional changes of Myelin Protein Zero and Mannose-Binding Lectin 2 protein involved in immune response and its allelic transmission in families of patients with leprosy in Colombia. **Infection, Genetics and Evolution**, v. 61, p. 215–223, 1 jul. 2018.

CRUZ, R. C. da S. et al. Leprosy: Current situation, clinical and laboratory aspects, treatment history and perspective of the uniform multidrug therapy for all patients. **Anais Brasileiros de Dermatologia**, v. 92, n. 6, p. 761–773, 1 nov. 2017.

CUNHA, C. et al. A historical overview of leprosy epidemiology and control activities in amazonas, brazil. **Revista da Sociedade Brasileira de Medicina Tropical**, v. 48, n. September 2014, p. 55–62, 2015.

DALAWI, I. et al. Drug resistance pattern of Mycobacterium leprae from mouse footpad cultivation between 1997 to 2013 in Malaysia. **Leprosy Review**, v. 88, n. 4, p. 463–477, 2017.

DE SOUSA, J. R. et al. Th9 cytokines response and its possible implications in the immunopathogenesis of leprosy. **Journal of Clinical Pathology**, v. 70, n. 6, p. 521–527, 1 jun. 2017.

DE SOUZA, E. A. et al. Leprosy and gender in Brazil: Trends in an endemic area of the Northeast region, 2001-2014. **Revista de Saude Publica**, v. 52, 2018.

DEVIDES, A. C. et al. Can anti–PGL-1 and anti–NDO-LID-1 antibody titers be used to predict the risk of reactions in leprosy patients? **Diagnostic Microbiology and Infectious Disease**, v. 91, n. 3, p. 260–265, 1 jul. 2018.

EICHELMANN, K. et al. Leprosy. An Update: Definition, Pathogenesis, Classification, Diagnosis, and Treatment. **Actas Dermo-Sifiliográficas (English Edition)**, v. 104, n. 7, p. 554–563, set. 2013.

FABEL, A. et al. Pathogenesis of Leprosy : An Insight Into B Lymphocytes and Plasma Cells. **The American Journal of Dermatopathology**, v. 41, n. 6, p. 422–427, 2019.

FERNANDES, T. R. M. de O. et al. **Dapsone-induced agranulocytosis in patients**

with Hansen's diseaseAnais Brasileiros de Dermatologia Sociedade Brasileira de Dermatologia, , 1 nov. 2017.

GARNIER, T. et al. Massive gene decay in the leprosy bacillus. **Nature**, v. 409, p. 1007–1011, 2001.

GELUK, A. **Correlates of immune exacerbations in leprosySeminars in Immunology**Academic Press, , 1 out. 2018.

GOULART, I. M. B. et al. Efeitos adversos da poliquimioterapia em pacientes com hanseníase: um levantamento de cinco anos em um Centro de Saúde da Universidade Federal de Uberlândia. **Revista da Sociedade Brasileira de Medicina Tropical**, v. 35, n. 5, p. 453–460, 26 abr. 2005.

GURAGAIN, S.; UPADHAYAY, N.; BHATTARAI, B. M. Adverse reactions in leprosy patients who underwent dapsone multidrug therapy: A retrospective study. **Clinical Pharmacology: Advances and Applications**, v. 9, p. 73–78, 29 jun. 2017.

HOWARD, P. et al. Rifampin (INN Rifampicin). **Journal of Pain and Symptom Management**, v. 50, n. 6, p. 891–895, 2015.

JI, B. H. Drug resistance in leprosy--a review. **Leprosy review**, v. 56, n. 4, p. 265–78, 1985.

JIAN, L. et al. Evaluation of antibody detection against the NDO-BSA, LID-1 and NDO-LID antigens as confirmatory tests to support the diagnosis of leprosy in Yunnan province, southwest China. **Transactions of the Royal Society of Tropical Medicine and Hygiene**, v. 114, n. 3, p. 193–199, 2020.

KAI, M. et al. Diaminodiphenylsulfone resistance of Mycobacterium leprae due to mutations in the dihydropteroate synthase gene. **FEMS Microbiology Letters**, v. 177, n. 2, p. 231–235, 15 ago. 1999.

KAR, H. K.; GUPTA, R. Treatment of leprosy. **Clinics in Dermatology**, v. 33, n. 1, p. 55–65, 1 jan. 2015.

LASTÓRIA, J. C.; DE ABREU, M. A. M. M. Leprosy: Review of the epidemiological, clinical, and etiopathogenic aspects - Part 1. **Anais Brasileiros de Dermatologia**, v. 89, n. 2, p. 205–218, 2014.

LEGUA, P. Leprosy. **International Journal of Infectious Diseases**, v. 73, n. 2018, p. 66, ago. 2018.

LINDERSTRØM-LANG, C.; NAYLOR, R. 4,4′-Diaminodiphenyl sulphone: solubility and distribution in blood. **Biochemical Journal**, v. 83, n. 3, p. 417–420, 10 ago. 1962.

MADIGAN, C. A. et al. A Macrophage Response to Mycobacterium leprae Phenolic Glycolipid Initiates Nerve Damage in Leprosy. **Cell**, v. 170, n. 5, p. 973- 985.e10, 24 ago. 2017.

MANE ABHAY B. Leprosy on the rise in India: need to adopt enhanced strategy for its control. **Primary Health Care: Open Access**, v. 04, n. 1, p. 1–2, 2014.

MATTOS, K. A. et al. Modulation of lipid droplets by Mycobacterium leprae in Schwann cells: A putative mechanism for host lipid acquisition and bacterial survival in phagosomes. **Cellular Microbiology**, v. 13, n. 2, p. 259–273, 2011.

MINISTÉRIO DA SAÚDE. **Diretrizes para vigilância, atenção e eliminação da hanseníase como problema de saúde pública 2016**. Brasília: MINISTÉRIO DA SAÚDE, 2016.

MIRNEJAD, R. et al. Clofazimine: A useful antibiotic for drug-resistant tuberculosis. **Biomedicine and Pharmacotherapy**, v. 105, p. 1353–1359, 1 set. 2018.
MOURA, R. S. de et al. Leprosy serology using PGL-I: a systematic review. **Revista da Sociedade Brasileira de Medicina Tropical**, v. 41 Suppl 2, p. 11–8, 2008.

NERY, J. A. da C. et al. Compreender melhor o estado reacional tipo 1 para o diagnóstico e tratamento precoces: Uma forma de se evitar as incapacidades na hanseníase. **Anais Brasileiros de Dermatologia**, v. 88, n. 5, p. 787–792, 2013.

PALIT, A.; KAR, H. K. Prevention of transmission of leprosy: The current scenario. **Indian Journal of Dermatology, Venereology and Leprology**, v. 86, n. 2, p. 115–123, 2020.

PARDILLO, F. E. F. et al. Methods for the Classification of Leprosy for Treatment Purposes. **Clinical Infectious Diseases**, v. 44, n. 8, p. 1096–1099, 2007.

PEARSON, T. M. H.; REES, R. T. W.; WATERS, M. F. R. SULPHONE RESISTANCE IN LEPROSY. A Review of One Hundred Proven Clinical Cases. **The Lancet**, v. 306, n. 7924, p. 69–72, 12 jul. 1975.

RAO, Pn.; SUNEETHA, S. Current situation of leprosy in India and its future implications. **Indian Dermatology Online Journal**, v. 9, n. 2, p. 83, 2018.
REIBEL, F.; CAMBAU, E.; AUBRY, A. **Update on the epidemiology, diagnosis, and treatment of leprosyMedecine et Maladies Infectieuses**Elsevier Masson SAS, 1 set. 2015.

REILLY, T. P.; WOSTER, P. M.; SVENSSON, C. K. Methemoglobin formation by hydroxylamine metabolites of sulfamethoxazole and dapsone: implications for differences in adverse drug reactions. **The Journal of pharmacology and experimental therapeutics**, v. 288, n. 3, p. 951–9, 1999.

RIBEIRO-ALVES, M.; SARNO, E. N.; OZO, M. Evaluation of qPCR-Based Assays for Leprosy Diagnosis Directly in Clinical Specimens. **PLOS Neglected Tropical Diseases**, v. 5, n. 10, p. 1–8, 2011.

RIDLEY, D S ; JOPLING, W. H. Classification of Leprosy According to Immunity. **Internacional Journal o Leprosy**, v. 34, n. 3, p. 255–273, 1966.

RODRIGUES JÚNIOR, I. A. et al. Leprosy classification methods: A comparative study in a referral center in Brazil. **International Journal of Infectious Diseases**, v. 45, p. 118–122, 1 abr. 2016.

SCHNEIDER, P. B.; FREITAS, B. H. B. M. de. Tendência da hanseníase em menores de 15 anos no Brasil, 2001-2016. **Cadernos de Saúde Pública**, v. 34, n. 3, 12 mar. 2018.

SISKAWATI, Y. et al. Poor treatment compliance leads to a higher mutation for rifampicin resistance in multibacillary leprosy patients. **Medical Journal of Indonesia**, v. 27, n. 4, p. 237, 31 dez. 2018.

SOTO, A.; TORRES MUÑOZ, P. Leprosy Diagnosis: An Update on the Use of Molecular Tools Lucrecia. **Molecular Biology**, v. 04, n. 04, 2015.

TIWARI, V. et al. Evaluation of polymerase chain reaction in nerve biopsy specimens of patients with Hansen's disease. **Journal of the Neurological Sciences**, v. 380, p. 187–190, 2017.

WALKER, S. L.; LOCKWOOD, D. N. J. Leprosy. **Clinics in Dermatology**, v. 25, n. 2, p. 165–172, 6 mar. 2007.

WHO. Global Leprosy Strategy 2016-2020: accelerating towards a leprosy-free world.Weekly Epidemiological record.

WHO. Weekly epidemiological record - Global leprosy update, 2018: moving towards a leprosy-free world.

WHO. Global leprosy (Hansen disease) update, 2019: time to step-up prevention initiatives. Weekly epidemiological record, v. 95, n. 36, p. 417–440, 2020

WORLD HEALTH ORGANIZATION. The final push strategy to eliminate leprosy as a public health problem: questions and answers.WHO.

WORLD HEALTH ORGANIZATION. Guidelines for the Diagnosis, Treatment and Prevention of Leprosy Report of the literature review ii. 2018.

YAWALKAR, S. J. **Leprosy for Medical Practitioners and Paramedical Workers**. American Medical Association (AMA), 2009. v. 8

2. CHAPTER 2: Drug delivery systems in Leprosy treatment

Leprosy elimination is still a challenge mainly due to low adherence to treatment. Among the causes can be highlighted the patients socioeconomic condition, inadequate health care services, and issues from MDT drugs (HEUKELBACH et al., 2011). The occurrence of resistance and adverse effects related to MDT drugs directly impair therapy compliance (DEPS et al., 2007; CAMBAU et al., 2018; DE ANDRADE et al., 2019). An extensive study from endemic countries showed 8.0% of *M. leprae* strains presenting mutations, which results in MDT resistance (CAMBAU et al., 2018). Regarding the relevance of drugs adverse effects to patients, a Brazilian study revealed 37.9% manifesting at least one adverse effect MDT-related (GOULART et al., 2005).

Besides, from a pharmaceutical development point of view, the low water solubility of all MDT drugs limits their bioavailability (LINDERSTRØM-LANG; NAYLOR, 1962; AGRAWAL; PANCHAGNULA, 2005; BOLLA; NANGIA, 2012). The adverse effects may be aggravated by the administration of high doses to reach therapeutic blood levels. In addition, drugs' poor water solubility may cause high variability of drug concentration in the serum, increasing the likelihood of bacterial resistance (DE SOUSA et al., 2012; SINGH et al., 2015; HUSSAIN et al., 2016). Thus, to overcome these issues and solve the challenges of MDT adherence, new formulations are being proposed for leprosy therapy.

In general, the formulations for oral administration proposed focused on two main strategies: increasing the apparent drug water solubility or modifying the drug's release (Table 2). Focusing on the MDT drug substance chosen for this study, three dapsone (DAP) innovative formulations have been proposed in the last years to increase its solubility: salt, cocrystal, and solid dispersion (CHAVES et al., 2015; CHAPPA et al., 2018; LI et al., 2020). Among the improvements, it is possible to highlight the enhancement of more than 7.5-fold of solid dispersion compared to free DAP (CHAVES et al., 2015), leading to a hypothetical dose reduction. The modified drug release approach was proposed for DAP using hydrogels, nanofibers, and polymeric nanoparticles, the last associated with CFZ (LI et al., 2017; CHAVES et al., 2019; RANJBAR et al., 2019). *In vivo* results of polymeric nanoparticles proved that

the sustained co-delivery of DAP/CFZ could reduce their doses improving the safety (LI et al., 2017).

Table 2: Innovative formulations containing dapsone, proposed in the last years: summary of in vitro evaluation and in vivo performance.

DAP innovative formulations	***In vitro* evaluation (Drug release/ Solubility assessment)**	***In vivo* performance**	**Reference**
Solid dispersion	Drug release was nearly 1.9-fold compared to physical mixture and 7.5-fold compared to pure DAP (in first 10 min).	-	(CHAVES et al., 2015)
Polymeric nanoparticles	Sustained release: after 24h, 82% of DAP and 68% of CFZ.	NP was more effective than the same dose of the drugs.	(LI et al., 2017)
Cocrystal	Best solubility achieved: 1.5 times, compared to pure DAP.	-	(CHAPPA et al., 2018)
Hydrogel	In the first hours, up to 5%, after 4h 10% and sustained release (up to 20%) in the next 22h.	-	(CHAVES et al., 2019)
Nanofibers	After 400 min, 77.71%, compared to 80.61% of DAP nanoemulsion.	-	(RANJBAR et al., 2019)
Salt and Eutectics	Dissolution rate of salt nearly 2-fold and eutectics 1.7-fold than pure DAP (in first 10 min).	-	(LI et al., 2020)

The present study aims to obtain DAP nanocrystals, an innovative drug delivery formulation, never before proposed for dapsone to the best of our knowledge. Nanocrystals present no carrier material being stabilized using surfactants or polymeric stabilizers. Additionally, the nanosuspensions are defined as drug nanocrystals stabilized and dispersed in liquid media (JUNGHANNS; MÜLLER, 2008). Nanocrystals can address the low water solubility of hydrophobic drugs substances, which are most of the compounds in the development pipelines at present (MOHAMMAD et al., 2019; JACOB; NAIR; SHAH, 2020). Approximately 70% of the developmental drugs are class II, as well as dapsone (Figure 2), according to Biopharmaceutical Classification System (BCS). Their poor water-solubility impacts dissolution rate, limiting bioavailability and biodistribution (MOHAMMAD et al., 2019). Besides the enhanced saturation solubility and dissolution, food-effects elimination, safe dose escalation, and safety and efficacy enhancement inherent of nanoparticles,

nanocrystals still offer the additional advantage of 100% drug loading due to the absence of a matrix (RAGHAVA SRIVALLI; MISHRA, 2016).

Figure 2: Molecular structure of dapsone – main drug substance used to treat leprosy – and its chemical properties.

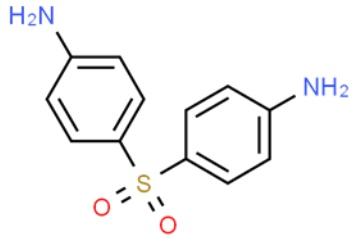

Dapsone
Molecular formula: $C_{12}H_{12}N_20_2S$
Molar mass: 249.3 g/mol
Solubility in water: 0.16 mg/mol at 25ºC
logD: 1.27, pH > 4.6
pKa: 2.41
logP: 1.27

Source: adapted from Chemicalize.com and MARTINS; CALDERINI; PESSINE, 2012

Nanocrystals' increased saturation solubility, dissolution rate, and mucoadhesiveness occur due to physicochemical changes related to particle size reduction (MÜLLER; GOHLA; KECK, 2011). Furthermore, the Noyes Whitney dissolution model equation explains the background of these effects as follows (Equation 1) (NOYES; WHITNEY, 1897; PATRAVALE; DATE; KULKARNI, 2004). The dissolution rates are proportional to the difference between the concentration of the saturated solution (C_S) and that concentration of the solution present at the moment (C). Besides, as the saturation solubility increases, the concentration gradient between blood and gut lumen also increases, promoting higher absorption (JUNGHANNS; MÜLLER, 2008).

Equation 1

$$\frac{dC}{dt} = k\ (C - Cs), \text{where k is a constant}$$

Nanocrystals were developed at the beginning of the 1990s, and at the end of the same period, the first medicines were approved by regulatory agencies (MÜLLER; GOHLA; KECK, 2011; MALAMATARI et al., 2018). Among all nanocrystals products on the market, most are for oral administration, as it is a more popular and convenient route for these formulations (MALAMATARI et al., 2018).

These products are designed as liquid oral formulations (nanosuspensions) or solid dosage forms (capsules and tablets). For the latter, a solidification step is necessary, with freeze-drying (lyophilization) being commonly used. Thus, the dapsone nanocrystal formulation of this study was planned for oral administration due to the numerous well-known advantages of this route.

2.1. Preparation of drug nanocrystals

Methods for drug nanocrystals preparation may be divided basically into three categories: bottom-up (precipitation or crystal growth), top-down (nanonization), or a combination of them (JUNGHANNS; MÜLLER, 2008; MOHAMMAD et al., 2019). The bottom-up approaches involve two fundamental principles, precipitation, and evaporation (MOHAMMAD et al., 2019). In this method, the molecules in solution aggregate forming nanoparticles. As a result, particle size control, solvent removal, and low solubility drugs, even in organic solvents, are limiting factors for the industrial use of bottom-up technologies.

On the other hand, the top-down methods are predominantly used in pharmaceutical industries (MOHAMMAD et al., 2019). This approach starts from large crystals in microscale to the nano-sized range through media milling or high-pressure homogenization (MÜLLER; GOHLA; KECK, 2011; MOHAMMAD et al., 2019). The particle reduction occurs due to inter-particle collision, generating mechanical attrition and shear forces (KARAKUCUK; CELEBI, 2020). The wet milling technique stands out for generating well-defined shape particles, for its eco-friendly characteristic (water as solvent), and for the ease of scaling up (MALAMATARI et al., 2018; MOHAMMAD et al., 2019). Furthermore, it is the method behind most marketed products, such as Rapamune®, Ritalin LA®, Naprelan®, Emend® and Invega Sustenna® (MALAMATARI et al., 2018).

A down-scaled wet bead milling was recently proposed by Romero et al. (2016) (ROMERO; KECK; MÜLLER, 2016). In the present study, adapting from this method, the milling chamber consisted of an 8 mL glass vial, 3 magnetic stirring bars (5mm each) disposed of one over the other, and 2.0g of zirconium oxide beads (0.1 mm). This approach is cost-effective and exciting due to its simplicity, especially for laboratory applications. Besides, the small scale simplified the stabilizer selection

step (ROMERO; KECK; MÜLLER, 2016). In general, stabilizer screening is the initial step on nanocrystals development. The proper stabilizer avoids the drug particles agglomeration due to attractive forces between them and maintains formulation stability during the shelf-life (LESTARI; MÜLLER; MÖSCHWITZER, 2019). The stabilizer, which surrounds the drug solid core, is generally an amphiphilic surfactant or a polymer. The surfactants are divided into ionic and non-ionic, playing their role via electrostatic forces or steric stabilization. Additionally, the stabilization conferred by the polymers is also based on a steric hindrance (TUOMELA; HIRVONEN; PELTONEN, 2016).

Considering the ICH (International Conference on Harmonization, 2009) guidelines, adopting a systematic approach in the development of a drug product is encouraged (ICH Q8, 2009). The design of experiment (DoE) is an optimization strategy, which allows evaluating numerous variables simultaneously, with a limited number of experiments (LEWIS; MATHIEU; PHAN-TAN-LUU, 1998). Enhance the understanding of a product, and its manufacturing process guarantees a quality by design outlook, creating a solid basis for science- and risk-based submissions, and consequently more flexible regulatory perspectives (ICH Q8, 2009).

The objective of the present study is to prepare dapsone nanocrystals using a small-scale wet bead milling technique and its physicochemical characterization. Toxicity on *galleria mellonella* larvae and nanosuspension scale-up attempts were performed. The project scope is to develop a nanotechnology platform through a design space approach with the potential to improve DAP saturation solubility and dissolution rate. The new formulation presents potential to decrease adverse effects occurrence, improving treatment adherence against leprosy worldwide.

2.2. MATERIAL AND METHOD

2.2.1. Material

2.2.1.1. Raw material

- Dapsone - kindly provided by Fundação para o Remédio Popular “Chopin Tavares de Lima” (FURP)
- Poloxamer 407 (BASF, Germany)
- Poloxamer 188 (BASF, Germany)
- Soluplus® - polyvinyl caprolactam-polyvinyl acetate-polyethylene glycol graft copolymer (BASF, Germany)
- Povacoat® - polyvinyl alcohol-Acrylic acid-Methyl methacrylate copolymer (Daido Chemical, Japan)
- Klucel® - hydroxypropyl cellulose (Ashland, USA)
- Tween 80 - polysorbate 80 (Sigma-Aldrich™, USA)
- TGPS - tocopherol polyethylene glycol succinate (BASF, Germany)
- Kolliphor® EL - polyoxyl castor oil (BASF, Germany)
- Kolliphor® RH40 - polyoxyl 40 Hydrogenated Castor Oil (BASF, Germany)
- Mannitol (Cinética, Brasil)
- Ultrapure water Milli-Q™

2.2.1.2. Equipment

- 0.1mm zirconium beads (Retsch, Germany)
- Climatic chamber (Climacell 222, MMMGroup, Planegg, Germany)
- Christ Alpha 2-4 LSC (Martin Christ Gefriertrocknungsanlagen GmbH, Germany)
- Coating System MED-020 (Bal-tec, Liechtenstein)
- Eppendorf Centrifuge 5424 R (Eppendorf, United States)
- Evolution™ 201 UV-Visible spectrophotometer (Thermo Scientific™, USA)
- Glass vial (10 mL)
- Granulometer Cilas 1900 (Cilas, France)

- LabStar Neos® agitator Bead Mill (NETZSCH-Feinmahltechnik GmbH, Germany)
- Magnetic stirring bars (5mm each one)
- Magnetic stirring plate (IKA®-WERKE, Germany)
- Miniflex 600 (Rigaku, Tokyo, Japan)
- Optical microscopy (Motic SMZ / 165 Series, Motic®, China)
- Scanning electron microscope Quanta 650 FEG (Thermo Fisher Scientific Inc., USA)
- SevenExcellence Multiparameter Conductivity Meter (Mettler Toledo, USA)
- Shaker Tecnal TE-4080 (Tecnal, Brazil)
- Zetasizer Nano ZS 90 (Malvern Instruments, UK)

2.2.2. Methods

2.2.2.1. Preparation of dapsone nanocrystals using small scale wet bead milling

The dapsone nanocrystals were obtained using a small-scale top-down approach by wet bead milling, according to Romero, Keck, and Müller (2016)(ROMERO; KECK; MÜLLER, 2016). The apparatus consists of 3 magnetic stirring bars (5mm each) arranged on top of the other in a 10 mL glass vial, stirring by a magnetic stirring plate (IKA®-WERKE, Germany). The formulation proposed contains 4% (w/w) of dapsone (DAP), 1 to 3% (w/w) of aqueous surfactant solution for the total weight of 8 g. Additionally, 20% of vial volume was filled with 2,0 g (w/w) zirconium beads (size of 0.1 mm) (Retsch, Germany). The surfactant concentration, stirring speed, and process time of formulation were studied in this work and, therefore, were varied as described in the following sections.

Each tested surfactant was weighed and placed in initial stirring for 10 minutes with approximately half of the planned water to guarantee its complete solubilization. In sequence, the dapsone was weighed and added to the formulation along with the remaining water to complete 8 g of nanosuspension. At this moment, the processing time starts to count. The stirring was turned off at the end of studied time, and the formulation was collected after decanting the zirconium beads.

2.2.2.2. Preliminary and pre-optimization studies

During the preliminary screening, a total of 9 formulations were prepared (using Poloxamer 407, Poloxamer 188, Soluplus®, Povacoat®, Klucel®, Tween 80, TGPS, Kolliphor® EL, and Kolliphor® RH40) to select the stabilizer that allows the particle size reduction while ensuring the nanosuspension stabilization. The formulations were maintained under stirring (800 rpm) for 7 days. The particle size and polydispersion index (PdI) were analyzed every day.

Afterward, the second step of pre-formulation studies was determining the range of process parameters. This determination was done using Povacoat® with the concentration of 1%, 2%, and 3% (w/w), stirring speed of 800, 1000, and 1200 rpm, during 3 to 7 days.

The formulations were stored at room temperature to avoid dapsone precipitation. This phenomenon was observed in the concentrated DAP solution, which had been stored in a refrigerator. Probably the temperature decay causes the solubility reduction, altering the physical-chemical characteristics of this solution. The promising formulations were kept on stability study for 15 days to monitor the particle size using Zetasizer Nano ZS 90 (Malvern Instruments, Malvern, UK). .

2.2.2.3. Experimental design for DAP nanocrystals production process optimization

Aiming to obtain an optimized formulation is desirable the use of tools throughout the production process. Thus, this study applied an intelligent approach with design of experiment (DoE) to identify and quantify simultaneously, systematically, and speedily the effect of critical process parameters in the final formulation (SINGH et al., 2011; TALEKAR; HAWARE; DAVE, 2019). Factors with potential influence on the nanosuspension were selected in preliminary studies: surfactant concentration (Povacoat® (POVA); w/w), stirring speed (rpm), and process time (days). After that, a three factor-three level Box–Behnken design (BBD) was applied to maximize the experimental efficiency of the DAP nanocrystals production.

The three independent variables were studied with three levels for each one, as described in Table 3. The lower, medium and higher values were also determined

during the preliminary phase for each variable. All the other variables were kept constant, such as drug substance concentration (4%), quantity of zirconium beads (2.0 g), and 3 cylindrical stirring bars (3.0 x 5.0 mm). The experimental trials were tested in 20 formulations, and the experimental plan of results was conducted with Minitab® 18 (Minitab Inc., State College, PA, US) software.

Table 3: Independent and dependent variables with respective coded levels of the Box–Behnken design.

Factors	Coded levels		
Independent variables	Low (-1)	Medium (0)	High (+1)
% of surfactant (w/w)	1.0	2.0	3.0
Process time (days)	3	5	7
stirring speed (rpm)	800	1000	1200
Dependent variable	Constrains		
Mean particle size	Optimized (250 nm)		
Polydispersity Index (PdI)	PdI < 0.4		

2.2.2.4. Particle size hydrodynamic diameter and Polydispersity Index (PdI) by Dynamic Light Scattering (DLS)

Hydrodynamic diameter and polydispersity index (PdI) of nanocrystals were measured by Dynamic Light Scattering (DLS) at a 90° angle, employing Zetasizer Nano ZS90 (Malvern Instruments, Malvern, UK). DLS is a well-established technique for characterizing the particle size in a dispersed medium. It is used to measure the translational diffusion coefficient of particles undergoing Brownian motion. Assuming a spherical shape, the particle size is determined by the conversion of the diffusion coefficient in hydrodynamic diameter using the Stokes-Einstein relation (Equation 2):

Equation 2

$$D_H = \frac{k\,T}{3\pi\,\eta D}$$

where k corresponds to the Boltzmann's constant, T to the absolute temperature, and η to the dispersant viscosity (KASZUBA et al., 2008; BOLUK; DANUMAH, 2014).

Meanwhile, the term "polydispersity" (or "dispersity" as recommended by IUPAC) describes the degree of non-uniformity based on the distribution of particle sizes in a sample; therefore, PdI describes the sample heterogeneity (IGE; BARIA; GATTANI, 2013). It is calculated by the equation 3:

Equation 3

$$PdI = \left(\frac{\sigma}{Zavg}\right)^2$$

wherein σ = particle size distribution and Z_{avg} = average particle size.

Values less than 0.05 represent highly monodisperse standards. Values greater than 0.7 indicate that the sample has an extensive particle size distribution, which is probably not suitable for analysis by the DLS technique(DANAEI et al., 2018). PdI values between 0.1 and 0.4 proved effective for guaranteeing physical stability even with increasing particle surface area (KARAKUCUK; CELEBI, 2020).

First of all, the method development for determining the average of hydrodynamic diameter (Z-ave) of particle size and PdI were conducted, resulting in samples dilution of 1:100 ratios. Thus, the measurement was performed with 20 µL of each formulation for 2mL of total volume, being filled with dapsone saturated solution.

2.2.2.5. Particle size measurement of raw material dapsone by Laser diffraction (LD)

The initial particle size of the dapsone raw material was examinated by laser diffractometry (LD), with the equipment Granulometer Cilas 1900 (Cilas, Orléans, France). DAP saturated solution was previously filtered to be used as dispersing medium. The obtained results were exhibited as volume-weighted diameters - d(v;0.1), d(v;0.5), and d(v;0.9) - indicating the percentage of particles which are below the given size (nm).

2.2.2.6. Scanning electron microscopy (SEM)

The initial dapsone raw material inspection was performed through optical microscopy (Motic SMZ / 165 Series, Motic®, Kowloon, China). The program Imagem.j was used to generate the microscopic images.

In order to obtain the more detailed images that could demonstrate the morphology of the particles and the size, scanning electron microscopy (SEM) was chosen. The samples were covered with platinum using a Coating System MED-020 (Bal-tec, Liechtenstein). Moreover, the SEM was performed in a high-resolution scanning electron microscope Quanta 650 FEG (Thermo Fisher Scientific Inc., USA), with 10 kV of electron acceleration voltage. The DAP raw material and the nanocrystal were analyzed with an increase of 500 to 160,000 times, respectively.

2.2.2.7. Zeta potential (ZP)

The zeta potential was determined by Zetasizer Nano ZS 90 (Malvern Instruments, Malvern, UK). This equipment calculates the zeta potential through the Helmholtz-Smoluchowski equation below (Equation 4), using the measures of electrophoretic mobility, the relation between the particle's velocity, and the electric field applied.

Equation 4

$$U_E = \frac{2\varepsilon\zeta}{3\eta} f\,(ka)$$

wherein η corresponds to the viscosity, ε corresponds to the dielectric permittivity (both concerning solvent at 25ºC), UE to Electrophoretic Mobility, ζ to Zeta Potential, and f (ka) depends on the geometry of the particle (DESHIIKAN; PAPADOPOULOS, 1998).

The samples collected from the formulations were diluted in a NaCl aqueous solution with conductivity adjustment (~50 µS/cm). The pH of formulations was also measured using SevenExcellence Multiparameter Conductivity Meter (Mettler Toledo, USA).

2.2.2.8. Lyophilization of dapsone nanosuspension

The lyophilization of optimized dapsone nanosuspension was carried out to enable characterization tests, such as Scanning Electron Microscopy (SEM), thermal analysis (DSC), and X-ray diffraction (XRD). Aliquots of 1.5 mL of the nanosuspension were transferred to 8 mL flasks and diluted in 5% (w/w) of mannitol, a cryoprotectant agent. The lyophilization was performed using Christ Alpha 2-4 LSC (Martin Christ Gefriertrocknungsanlagen GmbH, Germany).

Initially, the samples were frozen at -40ºC. After that, the first drying was performed at -40°C (shelf temperature) for 48 hours, under 0.140 mbar of pressure. As a final step, the secondary drying was conducted at 10ºC and 0.140 mbar of pressure during 4 hours (MELO et al., 2020).

2.2.2.9. Thermal Analysis - Differential Scanning Calorimetry (DSC)

The differential scanning calorimetry (DSC) was conducted using Exstar DSC 7020 (Seiko Instruments, Tokyo, Japan) for dapsone raw material, povacoat® and mannitol, physical mixture (dapsone, povacoat®, and mannitol), and lyophilized dapsone nanocrystals. The equipment calibration was performed with metallic indium - melting point: 156.6 °C and ΔH fus = 28.57 J g−1. The samples were heated from 25 °C to 250 °C, with a heating rate of 10 °C/min.

2.2.2.10. Powder X-Ray Diffraction (XRD) analysis

The characterization of the crystalline state was carried out by Powder X-Ray Diffraction (XRD). The equipment Miniflex 600 (Rigaku, Tokyo, Japan) was used with a Cu kα (λ = 0.154 nm), radiated from 40 kV and 15 mA. The samples DAP raw material, povacoat®, mannitol, physical mixture, and lyophilized DAP nanocrystals were analyzed from 0º to 50º 2θ.

2.2.2.11. Verification of a spectrophotometric method for DAP quantification

Anjan and colleagues developed a quantification method for DAP in bulk, which was the basis of this study (ANJAN DE, SUDDHASATTYA DEY, PRASANNA KUMAR PRADHAN, FALGUNI CHAUDHARI, 2014). The UV-Vis spectrophotometric method was chosen and verified aiming at the DAP quantification, using the Evolution™ 201 UV-Visible spectrophotometer (Thermo Scientific™). The simplicity and the precision of this technique was the main reason for the choice. The method was verified regarding linearity, detection limit, quantification limit, precision, accuracy, and specificity, according to international and national guidelines, respectively ICH Q2 (R1) and RDC nº166/2017 (EMEA, 1995; MINISTÉRIO DA SAÚDE, 2017).

The stock solution was prepared by weighing 50 mg of DAP with further dissolution in 50 mL of a mixture of solvents - methanol:water (60:40, v/v). The solution was sonicated for 15 min for complete solubilization. The working solution was prepared to start from 1 mL of previous stock solution diluted in a 10 mL volumetric flask, producing a concentration of 100 µg/ml solution. Scanning was performed in the range of 200-400 nm.

2.2.2.11.1. Linearity

The linearity analysis aims to determine the ability of an analytical procedure to obtain results directly proportional to the concentration (EMEA, 1995). Statistical methods should evaluate the desirable linear relationship, and this study was conducted using Minitab18 software. Linearity of the method was obtained at 291 nm from 7 different concentrations, in a range between 2µg/mL and 8µg/mL. The different concentrations solutions were prepared by dilutions from the stock solution (100 µg/ml).

2.2.2.11.2. Detection limit and quantification limit

The detection limit (DL) is the lowest amount of the drug substance detected in the sample by this method. In contrast, the quantification limit (QL) is the lowest amount that can be quantitatively determined. In this study, these limits were mathematically determined through the regression line.

The detection limit was calculated using equation 5:

Equation 5

$$DL = \frac{3.3\ \sigma}{S}$$

Moreover, the quantification limit was calculated using equation 6:

Equation 6

$$QL = \frac{10\ \sigma}{S}$$

For these equations, σ is the standard deviation of the response, and S is the slope of the calibration curve.

2.2.2.11.3. Precision

Precision aims to verify the closeness between the results obtained from a series of measurements. It may be considered at three levels: repeatability, intermediate precision, and reproducibility. The last level was not performed because its objective was not applicable in this study regarding the ICH and Anvisa guidelines (EMEA, 1995; MINISTÉRIO DA SAÚDE, 2017).

a) Repeatability

It is also called intra-assay precision and was performed with six determinations of the test concentration (5,0 µg/mL).

b) Intermediate precision

It is also called inter-assay precision, performed with three repetitions of three different concentrations (2,0; 5,0 and 8,0 µg/mL), resulting in nine repetitions on different days.

2.2.2.11.4. Specificity

Specificity refers to the ability to assess the drug substance unequivocally in the presence of formulation components (EMEA, 1995). In this study, due to the simplicity of formulation, a solution of POVA was prepared to analyze the method specificity. Scanning was performed in the same range (200-400 nm).

2.2.2.11.5. Accuracy

As established in ICH Q2 (R1), the accuracy was not determined but inferred from precision, linearity, and specificity (EMEA, 1995).

2.2.2.12. Determination of saturation solubility

A saturation solubility test was performed for dried nanocrystals powder, dapsone raw material, and the physical mixture (dapsone, povacoat®, and mannitol at the same nanocrystal proportion) using the shake-flask method, shaker Tecnal TE 4080 (Tecnal, Sao Paulo, Brazil). Considering the pKa value of DAP as 2.41, the saturation solubility of DAP nanocrystals was determined in water, in hydrochloric acid buffer (pH 1.2), and in acetate buffer (pH 4.5), prepared according to the American Pharmacopeia and using SevenExcellence Multiparameter Conductivity Meter (Mettler Toledo, USA)(UNITED STATES PHARMACOPEIA AND NATIONAL FORMULARY, 2020). These different media were planned considering the presence of ionized species under the DAP pka, acid media, and unionized species above the pka.

Excess nanosuspension was added into 5-mL mediums and shook for 72h aiming the equilibrium state at 37°C. The aliquots were firstly centrifuged at 12,000 rpm for 10 min, using Eppendorf Centrifuge 5424 R (Eppendorf, United States), and filtered through a 0.22-µm microporous membrane (CHENG et al., 2020; MELO et al., 2020). Finally, the content of DAP was determined using the spectrophotometric method verified in this study at 291 nm.

2.2.2.13. Stability studies

The stability study for DAP nanosuspension was evaluated for 4 months at 30ºC and 65% relative humidity (RH), considering relevant guidelines (FDA, 2003; ICH Q8, 2009; BRASIL, 2019). Additionally, accelerated study stability was conducted for 3 months at 40ºC and 75% relative humidity, according to ANVISA and FDA requirements for drug substances storage under ambient conditions (BRASIL, 2019). Both studies were conducted in a climatic chamber (Climacell 222, MMMGroup, Planegg, Germany). The particle size, PdI, and zeta potential measurements were assessed at different times.

2.2.2.14. Toxicity on *Galleria mellonella* larvae

Galleria mellonella larvae were reared at the Laboratory of Antifungal Chemotherapy (Department of Microbiology, USP), being incubated at 30 ºC and fed with pollen and beeswax. Adult larvae were selected at the end of the development stage, with 2 to 2.5 cm of length and 150 to 200 mg of body weight (SPADARI et al., 2019).

The toxicity of free DAP and its nanocrystal at different concentrations were evaluated by injecting 10 µL of the solutions using a Hamilton® syringe. The following doses were applied: 2000, 200, and 20 mg/kg of DAP nanocrystal; 200 mg/kg of free DAP, and 100 mg/kg of POVA in the larvae last pro-leg and 10 µL of sterile distilled water in the control group (control for mechanical injection). The groups were incubated at 37 ºC in Petri dishes containing pollen and beeswax and evaluated for survival and morbidity, daily for 5 days (BASTIANI, 2018; BARRETO et al., 2020). Every 24 h, the number of surviving larvae and the health index were evaluated by analyzing mobility, pupal formation, and melanization. The morbidity curve was performed by summing these parameters, where the highest score (10) represents the best health condition of the larva (LOH et al., 2013; BASTIANI, 2018).

2.2.2.15. Scale-up from lab to pilot scale

An attempt was made to prove the effectiveness of scale up the formulation obtained by small scale lab-approach (MALAMATARI et al., 2018). LabStar Neos® agitator Bead Mill (NETZSCH-Feinmahltechnik GmbH, Germany) was employed to this attempt due to its ability to be precisely transferrable to production scale. The process parameters for small-scale and LabStar milling are described in Table 4. The proportion of drug substance and POVA was maintained.

Table 4: Main parameters of wet bead milling process: comparison between small scale approach and LabStar equipment.

Parameter	Small scale	Labstar
Water (ml)	8	3000
Milling speed (rpm)	1000	2600
Pump speed (rpm)	Not applicable	85
ZrO2 Beads (mm)	0.1	0.2 – 0.3
Beads loading (%)	20	85
Temperature (°C)	≈ 25	≈ 45
Milling time (h)	168	3.5

2.2.3. RESULTS AND DISCUSSION

2.2.3.1. Preparation of dapsone nanocrystals using small scale wet bead milling

2.2.3.2. Preliminary and pre-optimization studies

On preliminary stabilizer screening, Poloxamer 407, Poloxamer 188, Soluplus®, Povacoat®, Klucel®, Tween 80, TGPS, Kolliphor® EL, and Kolliphor® RH40 were tested. The surfactants or polymers play a fundamental role in the nanocrystals preparation due to a surface barrier formation and physicochemical stabilization of the nanosuspension, avoiding particle aggregation (FANGUEIRO et al., 2012). The average hydrodynamic diameter (Z-ave) size and PdI of each formulation are presented in Table 5. Promising formulations were stored at 25°C for 15 days, and their stability was evaluated by the determination of particle size.

Table 5: Particle size and PdI of formulations prepared for stabilizer selection – values expressed as mean ± standard deviation. Time milling: 72, 96, 120, 168 h. (n = 3)

Stabilizer	Time (h)	Z-ave (nm) ± SD	PdI ± SD	Z-ave (nm) ± SD after 15 days
Poloxamer 407	72	5841.7 ± 623.1	0.515 ± 0.181	-
	96	2249.0 ± 400.6	0.570 ± 0.499	
	120	3143.3 ± 348.3	0.211 ± 0.099	
	168	2851.7 ± 265.4	0.543 ± 0.159	
Poloxamer 188	72	2750.3 ± 257.4	0.275 ± 0.049	-
	96	4581.3 ± 1128.9	0.438 ±0.188	
	120	2866.3 ± 532.8	0.409 ± 0.169	
	168	2233.3 ± 1966.2	1.000 ± 0.000	
Soluplus®	72	2194.7 ± 399.7	0.416 ± 0.510	-
	96	1978.0 ± 628.3	1.000 ± 0.000	
	120	1851.3 ± 474.6	0.166 ± 0.076	
	168	1745.0 ± 452.4	0.086 ± 0.042	
Povacoat®	72	615.4 ± 16.7	0.224 ± 0.085	326.8 ± 3.1
	96	410.0 ± 43.3	0.197 ± 0.085	
	120	403.4 ± 26.1	0.120 ± 0.115	
	168	321.1 ± 14.4	0.272 ± 0.183	
Klucel®	72	950.1 ± 15.8	0.187 ± 0.020	671.5 ± 50.5
	96	610.7 ± 59.2	0.204 ± 0.190	
	120	498.6 ± 65.0	0.217 ± 0.106	
	168	565.0 ± 52.3	0.299 ± 0.301	
Tween 80	72	271.4 ± 9.4	0.303 ± 0.072	213.6 ± 7.3
	96	237.5 ± 9.5	0.289 ± 0.093	
	120	214.0 ± 5.9	0.307 ± 0.088	
	168	205.6 ± 2.7	0.327 ± 0.040	
TGPS	72	302.5 ± 29.1	0.466 ± 0.119	-
	96	298.7 ± 20.2	0.451 ± 0.049	
	120	288.5 ± 10.7	0.395 ± 0.039	
	168	275.8 ± 15.0	0.353 ± 0.080	
Kolliphor® EL	72	340.2 ± 11.4	0.289 ± 0.149	246.9 ± 11.2
	96	294.5 ± 16.4	0.258 ± 0.082	
	120	281.3 ± 7.4	0.321 ± 0.067	

Stabilizer	Time (h)	Z-ave (nm) ± SD	PdI ± SD	Z-ave (nm) ± SD after 15 days
Kolliphor® RH40	168	257.6 ± 8.1	0.206 ± 0.104	283.7 ± 12.2
	72	425.1 ± 10.3	0.361 ± 0.057	
	96	323.2 ± 27.8	0.208 ± 0.130	
	120	358.2 ± 19.1	0.204 ± 0.081	
	168	259.0 ± 11.0	0.226 ± 0.071	

H: hours, SD: standard deviation, PdI: polydispersity index.

The formulations containing Poloxamer 407, Poloxamer 188, and Soluplus® did not reach the nanoscale size until the maximum proposed process time (7 days). Thus, these formulations were discarded. Formulation containing TGPS presented a high attenuator on hydrodynamic diameter (HD) analysis, indicating a possible sample dilution. Through visual analysis, it was possible to observe drug particles in the supernatant (Figure 3). Therefore, for TGPS, the experimental conditions were not suitable for forming a nanosuspension. In summary, the stabilizers that presented satisfactory results were: Povacoat®, Klucel®, Tween 80, Kolliphor® EL, Kolliphor® RH40.

Figure 3: Formulation with TGPS: diluted appearance by visual evaluation.

Source: the author

Figure 4 shows the pre-optimization results of selected stabilizers graphically. Over time, it is possible to observe a decrease in the variation of particle size means, except for Klucel ®.

Figure 4: Boxplot of particle size measurements (Povacoat®, Klucel®, Tween 80, Kolliphor® EL, Kolliphor® RH40), by Dynamic Light Scattering (DLS) over time of milling process.

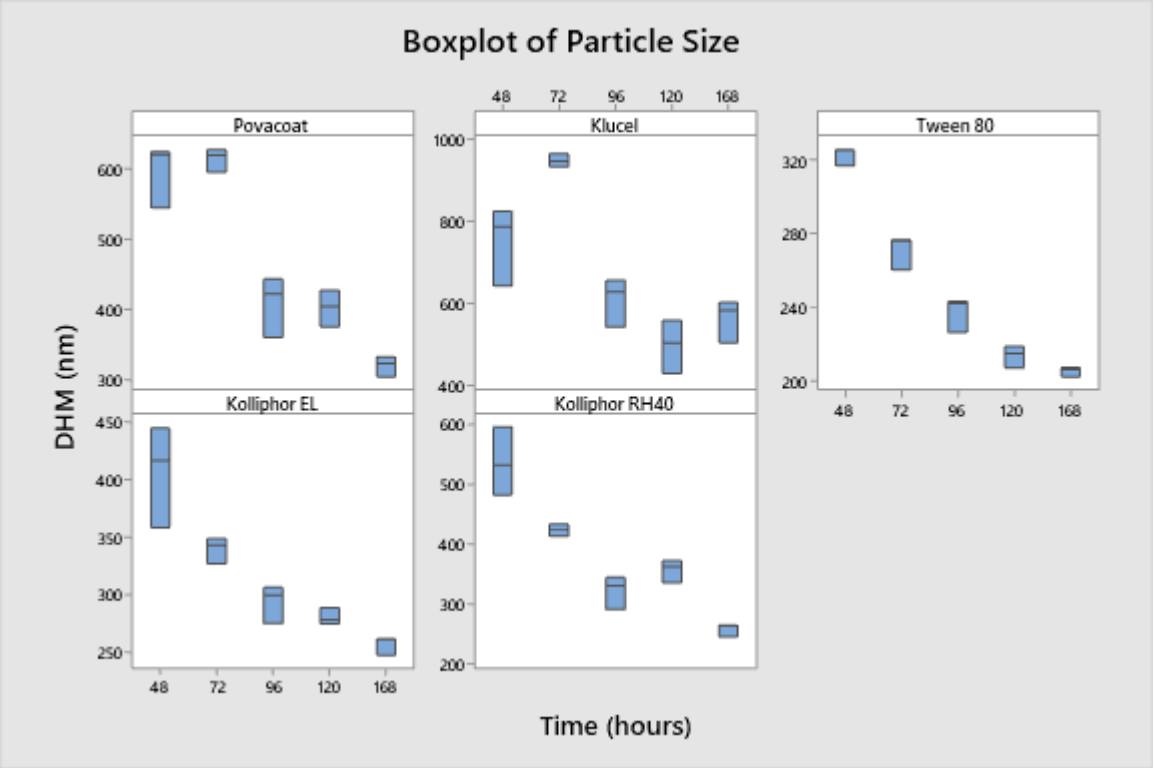

Source: the author

In Figure 5, the time series graph enables the evaluation of the long-term tendency of particle size means and the comparison of performances between stabilizers. The PdI of preliminary surfactant screening is shown in Table 5. It was expected that the stabilizer would gradually reduce the particle size over the process time, ensuring the uniformity of particle size distribution. However, this did not occur for Klucel® for example, as the PdI value increased over time (Figure 6). This occurrence may indicate that a prolonged milling time will not always be the most suitable for the process. The stabilizer Tween 80 presented the highest variability in PdI and was discarded.

Figure 5: Time Series graph to Z-Ave particle size for formulations with Povacoat®, Klucel®, Tween 80, Kolliphor® EL and Kolliphor® RH40), by Dynamic Light Scattering (DLS) over time of milling process.

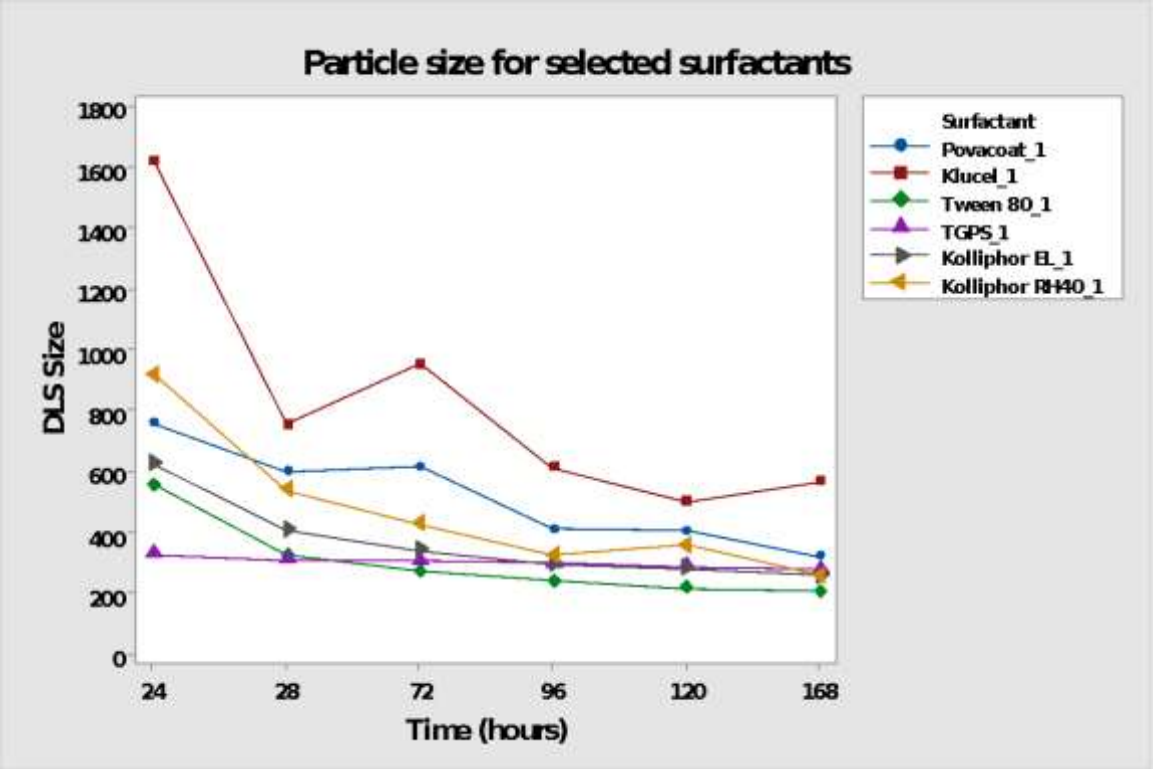

Source: the author

Considering that particles with PdI between 0.1 and 0.25 presented narrow size distribution since PdI is the square of the standard deviation divided by mean particle size, Povacoat® was chosen as the stabilizer for DAP nanosuspension (AGRAWAL; PATEL, 2011). The ideal process time was deeply evaluated during formulation optimization.

Figure 6: Boxplot of PdI measurements for selected surfactants (Povacoat®, Tween 80, Kolliphor® EL, Kolliphor® RH40), by Dynamic Light Scattering (DLS) over time of milling process.

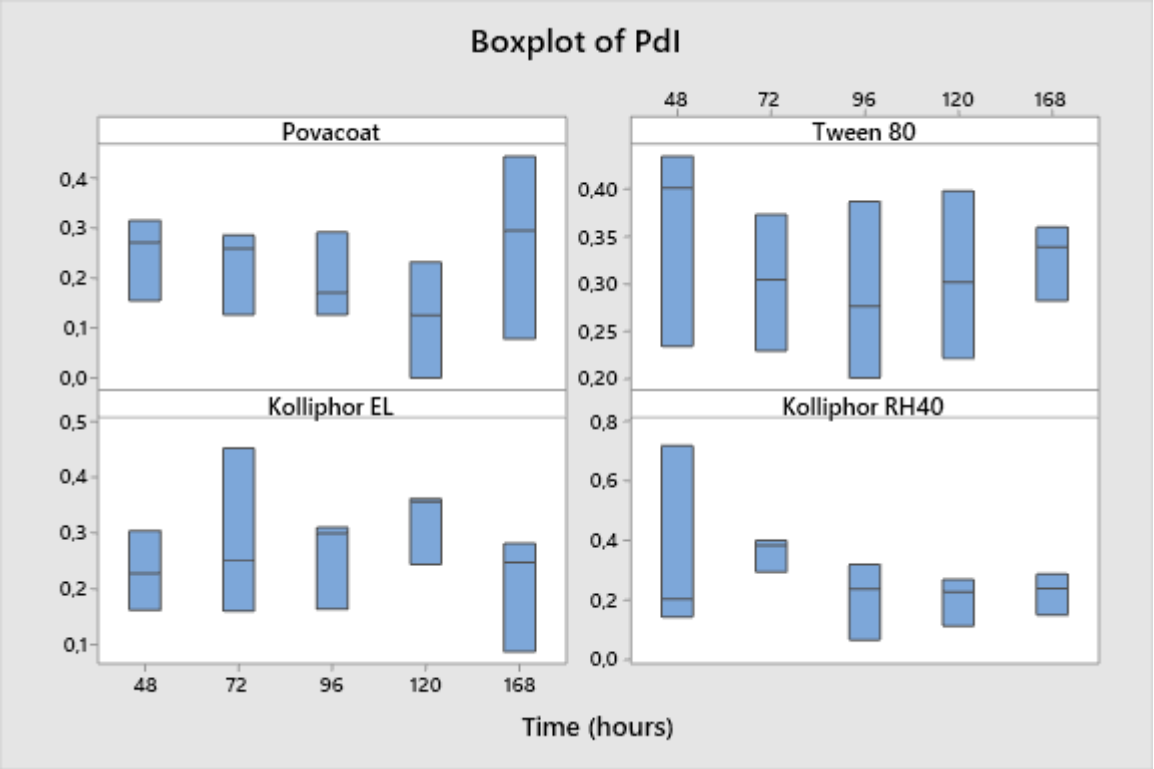

Source: the author

2.2.3.3. Experimental design for DAP nanocrystals production process optimization

The factors and levels for the factorial experiment were selected from a set of variables of the particle size reduction process. The relevant factors that directly influenced the process were selected based on prior knowledge of the development of the technique, namely concentration of POVA (% w/w), process time (days), and stirring speed of the magnetic bar (rpm). For the present study, a Box-Behnken statistical design (BBD) was carried out (including 6 central points) corresponding to the factorial design of three factors with three levels (3^3) to estimate the influence of factors in Z-ave and polydispersity index (PdI).

2.2.3.4. Average hydrodynamic diameter by Dynamic Light Scattering (DLS)

The results of experimental plan according to BBD were reported in Table 6.

Table 6: Mean particle size (Z-ave) and polydispersity index (PdI) of dapsone nanocrystals obtained from Box-Behnken experimental design.

F	Order	Level	Surfactant % (w/w)	Speed (rpm)	Time (days)	Z-ave ± SD	PdI ± SD
11	1	-1	2	800	5	313.0 ± 29.3	0.441 ± 0.027
5	2	1	1	800	7	196.4 ± 0.9	0.129 ± 0.004
8	3	1	3	1200	7	190.4 ± 1.1	0.120 ± 0.006
14	4	-1	2	1000	7	177.4 ± 1.7	0.150 ± 0.014
19	5	0	2	1000	5	216.1 ± 1.6	0.136 ± 0.012
4	6	1	3	1200	3	265.9 ± 8.8	0.150 ± 0.051
20	7	0	2	1000	5	239.9 ± 1.4	0.120 ± 0.035
18	8	0	2	1000	5	225.3 ± 2.1	0.104 ± 0.017
15	9	0	2	1000	5	228.2 ± 1.9	0.144 ± 0.007
13	10	-1	2	1000	3	265.3 ± 1.0	0.144 ± 0.024
16	11	0	2	1000	5	219.1 ± 2.0	0.143 ± 0.006
12	12	-1	2	1200	5	189.4 ± 0.7	0.127 ± 0.010
10	13	-1	3	100	5	234.6 ± 2.0	0.144 ± 0.011
3	14	1	1	1200	3	239.5 ± 1.7	0.144 ± 0.016
9	15	-1	1	1000	5	198.3 ± 1.4	0.157 ± 0.018
7	16	1	1	1200	7	171.9 ± 2.2	0.166 ± 0.011
2	17	1	3	800	3	416.6 ± 9.6	0.209 ± 0.030
17	18	0	2	1000	5	201.3 ± 1.0	0.109 ± 0.006
1	19	1	1	800	3	338.1 ± 3.4	0.147 ± 0.036
6	20	1	3	800	7	253.3 ± 2.1	0.156 ± 0.004

F: formula; SD: standard deviation

When the regression coefficients p-values were < 0.05, the factor was considered significant. In this model, three linear coefficients (POVA: concentration of Povacoat®, STIR: stirring speed of the magnetic bar and TIME: process time), one quadratic coefficient ($STIR^2$), and one interactive coefficient (STIR x TIME) were significant and described the interaction's pattern between factors (Table 7).

Table 7: Analysis of variance (ANOVA) - significance of terms - for particle Z-ave of DAP nanoparticles.

Source	DF	Adj SS	Adj MS	F-value	P-value
Model	5	57580.6	11516.1	25.57	0.000
Linear	3	49294.0	16431.3	36.49	0.000
POVA	1	4697.3	4697.3	10.43	0.006
STIR	1	21194.8	21194.8	47.07	0.000
TIME	1	23401.9	23401.9	51.97	0.000
Square	1	5009.7	5009.7	11.13	0.005
STIR*STIR	1	5009.7	5009.7	11.13	0.005
Interaction between 2 factors	1	3276.9	3276.9	7.28	0.017
STIR*TIME	1	3276.9	3276.9	7.28	0.017
Error	14	6304.3	450.3		
Lack-of-fit	9	5467.1	607.5	3.63	0.085
Pure error	5	837.2	167.4	*	*
Total	19	63884.9			

Summary of model	R^2	R^2 (adj)	R^2 (pred)
	95.54%	93.95%	87.71%

DF: degree of freedom; Adj. SS: Sum of the adjusted squares; Adj. MS: Adjusted quadratic mean, F-value: F statistic; p-value: significance level; POVA: concentration of Povacoat®, STIR: stirring speed of the magnetic bar, and TIME: process time.

The polynomial equation generated by this experimental model is given as follows in equation 7:

Equation 7

$$\text{Z} - \text{ave: } 1717 + 21{,}67\,P - 2{,}327\,S - 77{,}4\,T + 0{,}000922\,S*S + 0{,}0506\,S*T$$

where Z-ave (average of hydrodynamic diameter) is the dependent variable; 1717 is the intercept; P (POVA concentration, w/w), S (Speed of stirring, rpm), and T (Time of process, days) are the independent variables.

The polynomial equations were statistically evaluated through the analysis of variance (ANOVA).

The analysis of F-value (25.57) and associated p-value (0.0001; α=0.05) indicates the significance of the model. In addition, the lack of fit p-value of 0,085 was non-significant and demonstrated the model's accuracy (GAN; ABDUL MANAF; LATIFF, 2010; CHAVES et al., 2017; PENG et al., 2020). The well-correlated relationship between the response and the independent factors was denoted by the high values of R^2 (95.54%) and R^2 adj (93.95%) (PENG et al., 2020). The high R^2 value obtained also suggests a good fit to the mathematical model expressed by equation 7 (GAN;

ABDUL MANAF; LATIFF, 2010). Finally, the R^2 pred (87.71%) was in reasonable agreement with the R^2 adj (93.95%), suggesting a good prediction of results by the model (SINGARE et al., 2010).

Moreover, the analysis of the coefficients of equation 7 showed the more significant influence of the time process (-77.4), followed by POVA concentration (+21.67) and stirring speed (-2.327) on particle size. The quadratic term stirring influences little but positively the Z-ave and the interaction of stirring and time. The 3-D response surface and contour plots represent graphically equation 7 and visualize the relationship between experimental responses and levels (Figure 7).

Figure 7: (a) Contour plots and (b) response surface showing the effect of the concentration of Povacoat® (POVA), stirring speed (STIR), and process time (TIME) in hydrodynamic diameter.

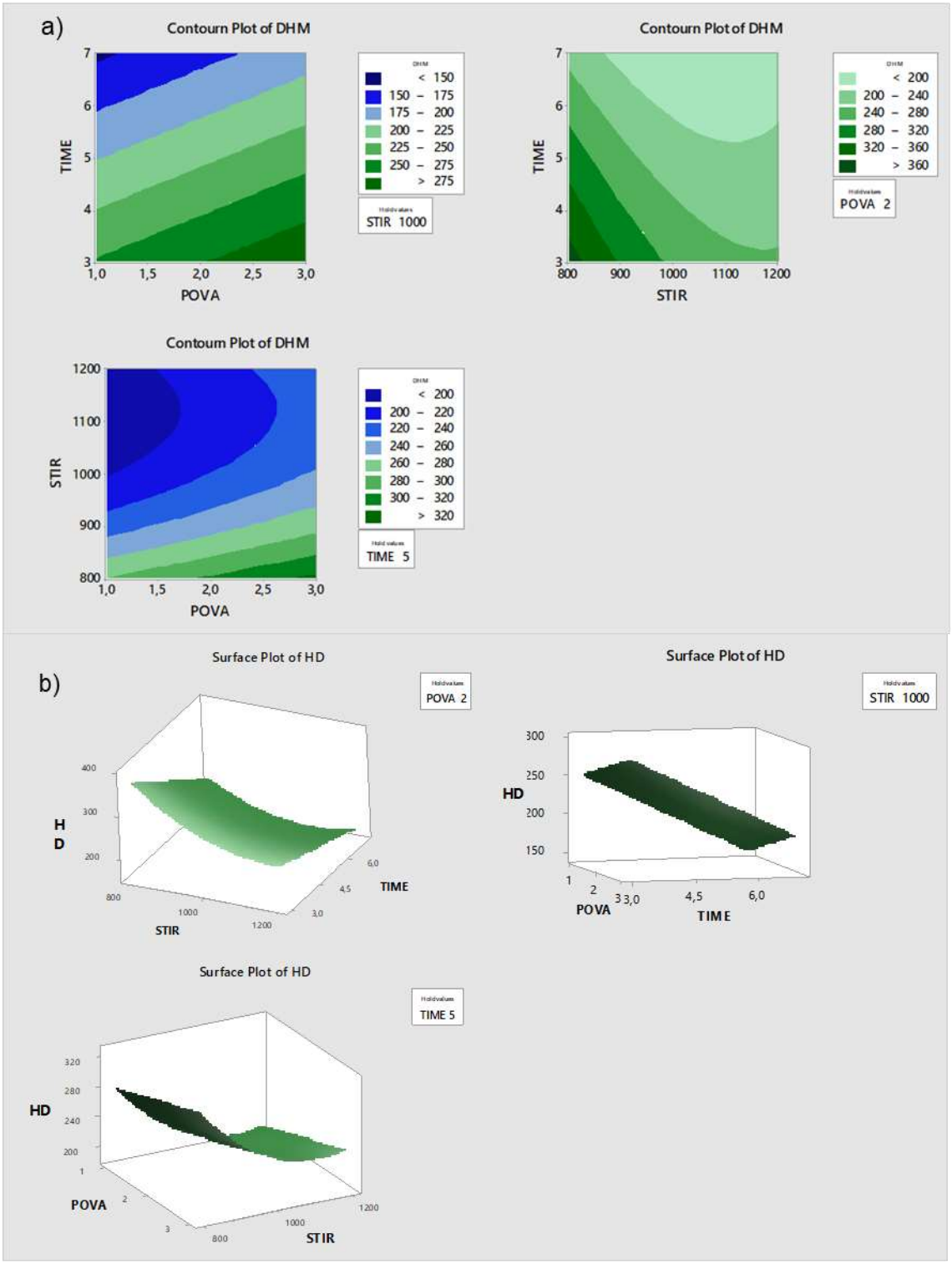

Source: the author

The graph analysis enables the identification of optimal conditions for obtaining the Z-ave of nanocrystals desired (~250 nm) depending on the process independent variables. These graphs may confirm the quadratic behavior and interaction of the equation 7. The optimal time estimated graphically to obtain nanocrystals with 200-250 nm Z-ave is between 5 and 7 days. The estimation of stirring speed is more difficult due to the quadratic and interaction effect. Furthermore, POVA concentration of 1-3% appears to be adequate and varies according to the variation of the other factors.

Even after the analysis of the mathematical model's accuracy, it is necessary to verify its predictability. The verification of the optimized model was conducted aiming at a nanocrystal formulation with 200nm. Thus, Figure 8 shows the graphs for DAP formulation optimization and the desired experimental conditions. The observed Z-ave result of the optimized formulation (O1) is close to the theoretical and is within the established 95% confidence interval (Table 8). Practical results demonstrated the validity of the mathematical model.

Figure 8: Z-ave optimization graphs of DAP nanocrystals containing the following variables: 2.0% of POVA, 1000 rpm of stirring speed and 5.766 days, prediction for 200.0 nm: O1.

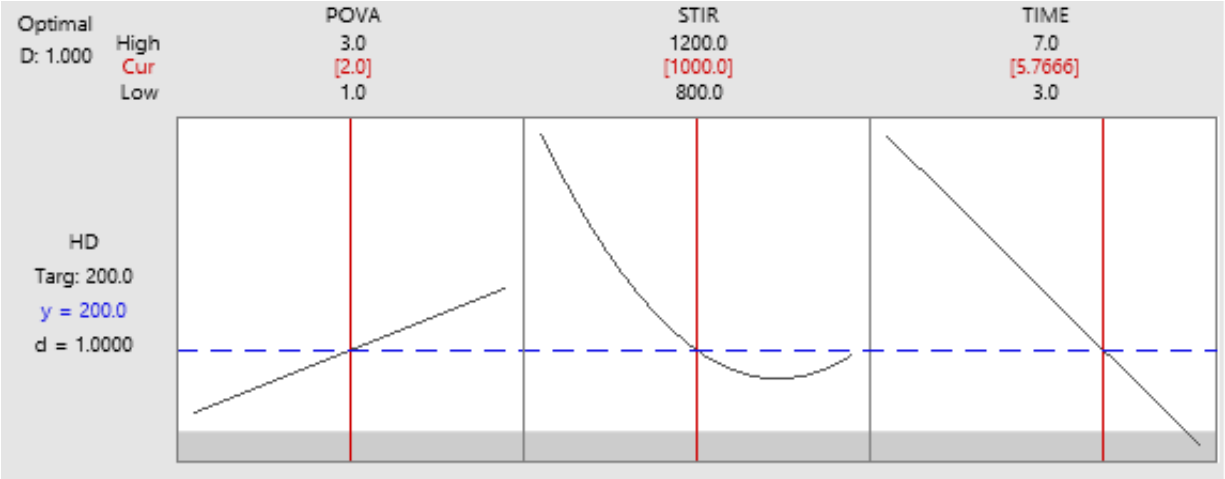

Source: the author

Table 8: Theoretical and observed Z-ave of DAP nanosuspension produced aiming the verification of response surface statistical design.

F	Sur% (w/w)	Speed (rpm)	Time (days)	Z-ave ± SD (nm)		95% CI	PdI ± SD	ZP ± SD (mV)
				T	O			
O1	2.0	1000	5.77	200.0	206.3 ± 6.7	(189.33; 210.67)	0.132 ± 0.012	-9.8 ± 0.3
O2	2.0	1000	6.51	180.0	192.3 ± 4.5	(167.51; 192.49)	0.107 ± 0.015	-9.9 ± 0.4

F: formula; Sur: surfactant; SD: standard deviation; T: Theoretical; O: Observed; CI: 95% confidence interval

Therefore, the experimental conditions stablished in this development step – POCA concentration: 2.0%, stirring speed: 1000 rpm, process time: 5.77 days - were applied to prepare all the tested formulations. Besides the particle size desired, the optimized formulation presented monomodal distribution and PdI < 0.4, indicating a monodisperse distribution of particles (Figure 9).

Figure 9: Particle size distribution of optimized DAP nanocrystals formulation.

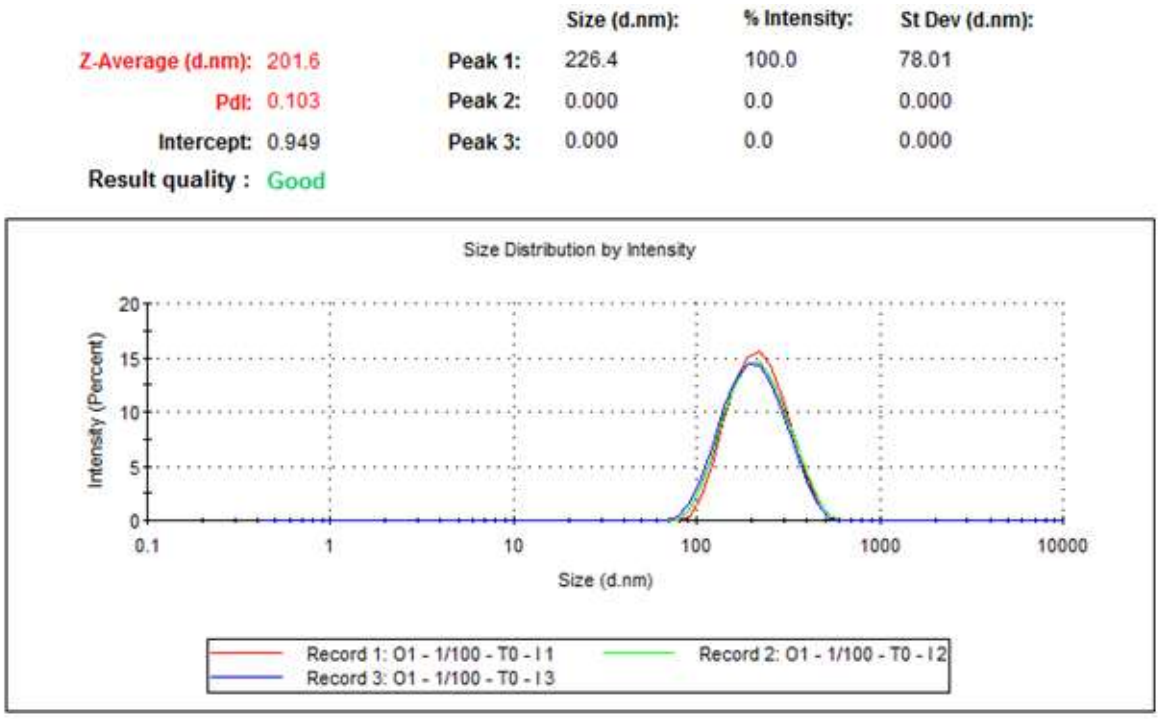

Source: author

2.2.3.5. Polydispersity Index (PdI) by Dynamic Light Scattering (DLS)

An attempt was made to understand the relationship of PdI and process variables through surface response methodology. Considering the PdI in Table 6, the ANOVA was conducted, and the results are presented in Table 9. The p-values regression coefficients of the model and the independent factors were all > 0.05; therefore, these factors may not be considered statistically significant. In summary, using this model, it is not possible to describe an interaction pattern between factors and PdI (Table 9).

Table 9: Analysis of variance (ANOVA) - significance of terms - for particle PdI of DAP nanoparticles.

Source	DF	Adj SS	Adj MS	F-Value	P-Value
Model	9	0.043091	0.004788	0.93	0.536
Linear	3	0.014690	0.004897	0.96	0.451
POVA	1	0.000126	0.000126	0.02	0.879
STIR	1	0.014046	0.014046	2.74	0.129
TIME	1	0.000518	0.000518	0.10	0.757
Square	3	0.024834	0.008278	1.62	0.247
POVA*POVA	1	0.004338	0.004338	0.85	0.379
STIR*STIR	1	0.024158	0.024158	4.72	0.055
TIME*TIME	1	0.005189	0.005189	1.01	0.338
2-Way Interaction	3	0.003567	0.001189	0.23	0.872
POVA*STIR	1	0.002113	0.002113	0.41	0.535
POVA*TIME	1	0.000953	0.000953	0.19	0.675
STIR*TIME	1	0.000501	0.000501	0.10	0.761
Error	10	0.051229	0.005123		
Lack-of-Fit	5	0.049679	0.009936	32.05	0.001
Pure Error	5	0.001550	0.000310		
Total	19	0.094320			

2.2.3.6. Particle size measurement of raw material dapsone by Laser diffraction (LD)

Table 10 and Figure 10 present the granulometric distribution of DAP raw material particle size and optimized nanocrystal formulation obtained by the small-scale wet bead milling. The laser diffraction measurement presented an obscuration around 15.

Table 10: Mean particle diameters of dapsone raw material (Dap) and optimized formulation (F1-Dap) by laser diffraction (LD) (n=10).

Samples	d (v; 0.1) (µm)	d(v; 0.5) (µm)	d(v; 0.9) (µm)	MD (µm)
Dap	8.74 ± 0.1	47.08 ± 0.1	116.11 ± 0.1	56.71 ± 0.1
O1-Dap	0.06 ± 0.1	0.18 ± 0.1	0.45 ± 0.1	0.23 ± 0.1

d(v;0.1), d(v;0.5), and d(v;0.9): volume-weighted diameters, MD: mean diameter.

Figure 10: Granulometric distribution of a) dapsone raw material b) optimized formulation of dapsone nanocrystals (F1- Dap). n = 10

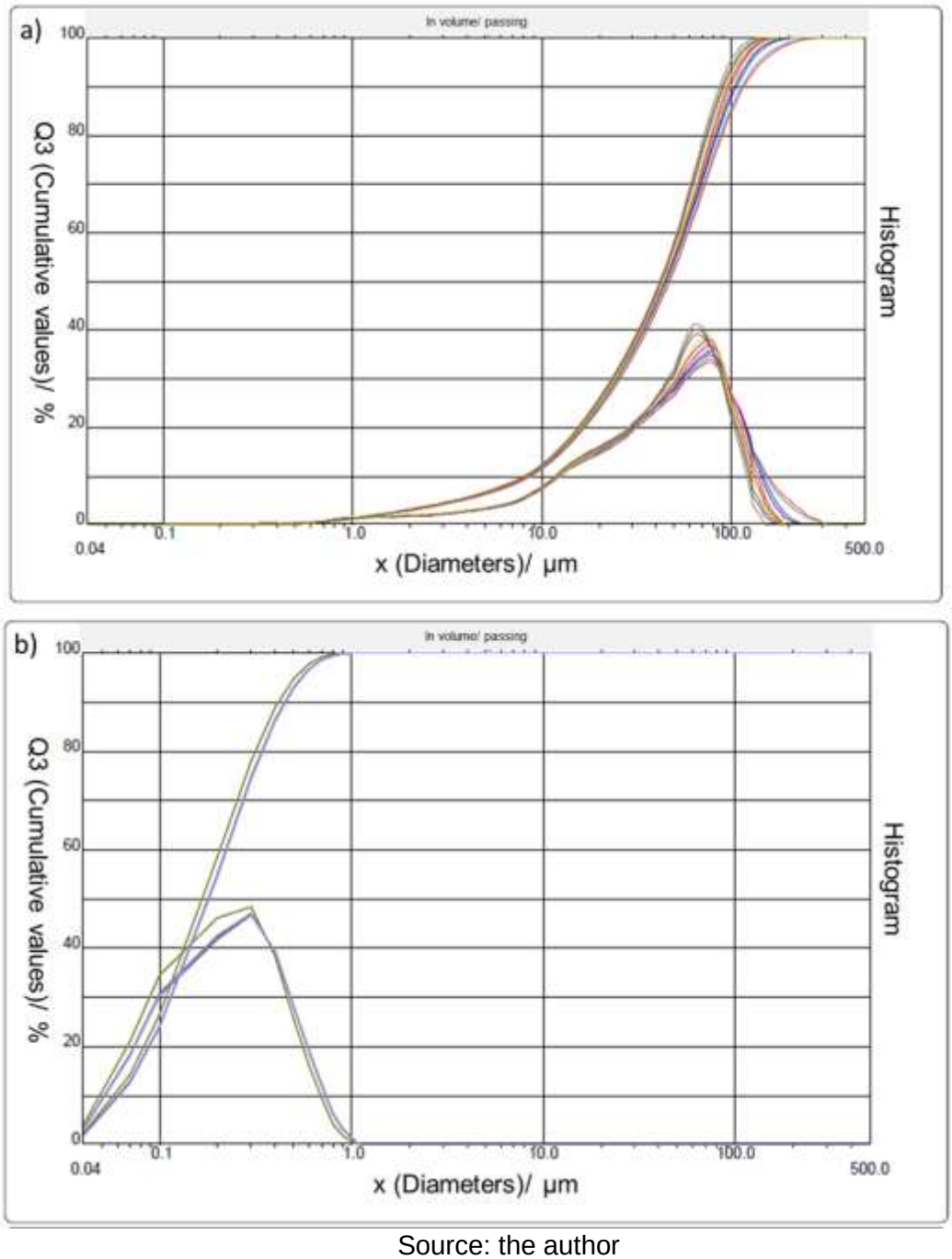

Source: the author

2.2.3.7. Scanning electron microscopy (SEM)

The SEM microphotographs presented the morphology of dapsone raw material (Figure 11a) and dapsone nanocrystals (Figure 11b). The microphotographs showed a shape change from prismatic irregular to spherical after the milling process. Besides, the images (Figure 11a and 12) confirm the particle size of raw material obtained by LD and figure 11b the particle size of nanocrystals by DLS.

Figure 11: Microphotograph of (a) dapsone raw material and (b) dapsone nanocrystal.

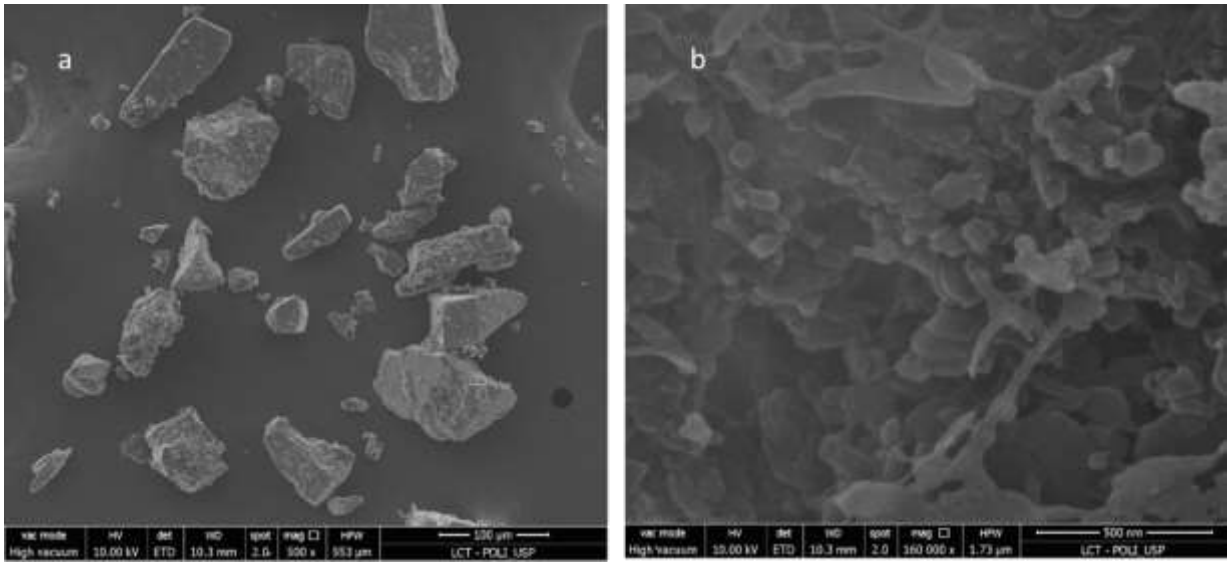

Source: the author

Figure 12: Optical microscopy of dapsone raw material in saturated DAP solution.

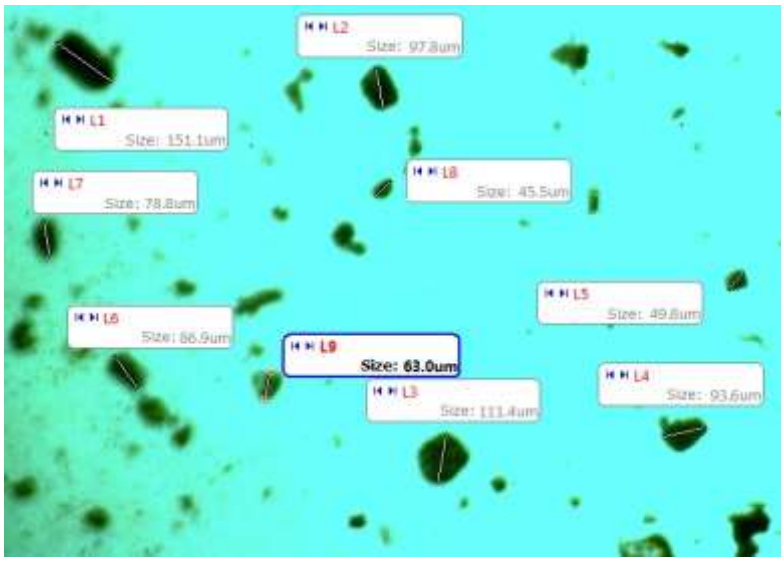

Source: the author

2.2.3.8. Zeta potential (ZP)

Zeta potential is used to predict the stability of nanosuspensions (KALEPU; NEKKANTI, 2016). The ZP obtained during stability studies are presented in Figure 22. DAP was neutral at the experimental conditions (pH 7.6); thus, the drug substance is not responsible for the negative charge observed. The other formulation component, Povacoat®, is a polyvinyl alcohol copolymer and usually promotes higher steric stability (Figure 13)(YUMINOKI et al., 2014, 2016).

Figure 13: Chemical structure of Povacoat®

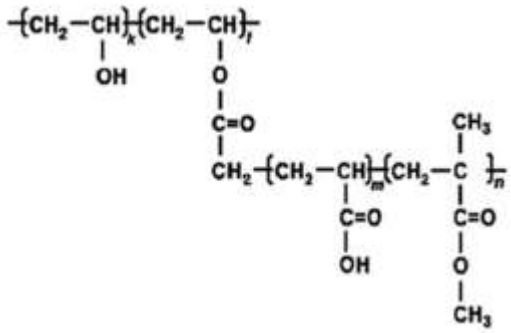

Source: YUMINOKI et al., 2014

The desirable ZP for steric stabilized systems are around -20 mV, near the observed results for DAP nanocrystals (KALEPU; NEKKANTI, 2016). Furthermore, the ZP were similar to previous studies using the same stabilizer, such as rifampicin and orotic acid nanocrystals (DE CÁSSIA ZAGHI COMPRI et al., 2019; MELO et al., 2020).

2.2.3.9. Lyophilization of dapsone nanosuspension and resuspension

The lyophilized formulation resulted in an elegant cake appearance (Figure 14). The lyophilized material was reconstituted (rehydrated) quickly in the same amount of water that was previously removed (MELO et al., 2020). After that, the particle size and the polydispersity index (PdI) were analyzed (Table 11). The results indicated the reduced variation of these physical attributes.

Figure 14: DAP nanosuspension lyophilized a) before and b) after lyophilization.

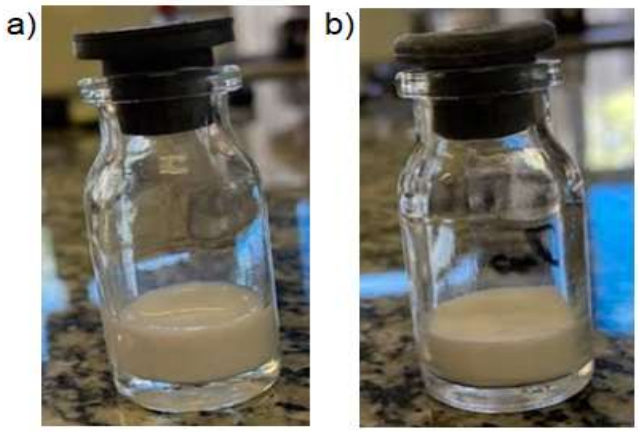

Source: the author

Table 11: Particle size (Z-ave) and polydispersion index (PdI) of nanocrystals in formulation before lyophilization (O1) and after resuspension (O1-R).

Formulation	Z-ave (nm) ± SD	PdI ± SD
O1	243.1 ± 8.0	0.175 ± 0.052
O1-R	239.0 ± 5.6	0.157 ± 0.014

SD: standard deviation

2.2.3.10. Thermal Analysis - Differential Scanning Calorimetry (DSC)

In Figure 15 are the DSC curves of dapsone raw material (DAP), the excipients povacoat® and mannitol (Pova+MN), physical mixture (PM), and dapsone nanocrystals (NC).

Figure 15: DSC curves of DAP raw material (DAP), Povacoat® and mannitol (Pova+MN), physical mixture (PM), and DAP nanocrystals (NC).

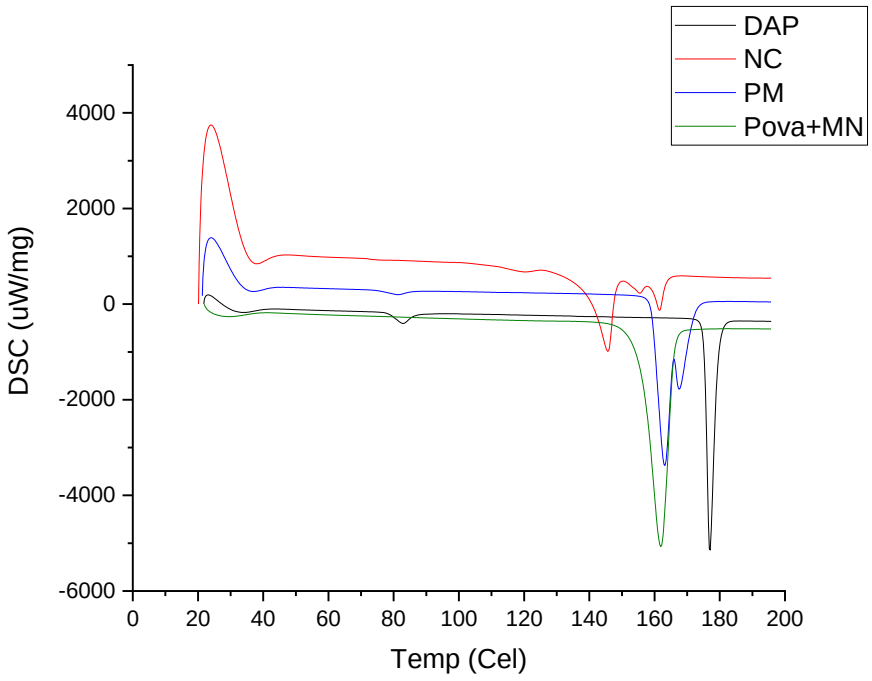

Source: the author

The dapsone sample showed two endothermic peaks, as described in the literature. The first peak, near 80 ºC corresponds to the polymorphic transition from the more stable form III to the form II. Furthermore, the second one, at 180 ºC, represents the melting point of the drug substance (VIEIRA et al., 2016; LI et al., 2020). For the mixture of excipients, the endothermic peak, from 160 ºC to 165 ºC, results mainly from the melting point of mannitol, as discussed in the next section (BRUNI et al., 2009; DE CÁSSIA ZAGHI COMPRI et al., 2019). The physical mixture curve is the superposition of all formulation components, as expected, and proves the compatibility among excipients. Similarly, the nanocrystal formulation showed a decreased enthalpy. The reduction of particle size may cause the temperature decrease of peaks, but even so, it is possible to identify them on nanocrystal DSC curves (XIA et al., 2010).

2.2.3.11. Powder X-Ray Diffraction (XRD) analysis

Powder X-ray diffraction was chosen to investigate the crystalline state of the formulation before and after the nanosizing process. This characterization method is considered a fingerprint to crystalline phases (LI et al., 2020). Figure 16 present the XRD diffractogram of dapsone (DAP), povacoat® (POVA), mannitol (MN), physical mixture (PM), and dapsone nanocrystals (NC).

The diffractogram of dapsone raw material presented narrow, intense, and numerous peaks, confirming the crystallinity of the drug substance before the milling process. Furthermore, specific intensities of DAP appeared, such as those observed between 10° and 30° (GREBOGI et al., 2012). Meantime, the absence of peaks in the POVA diffractogram showed a completely amorphous pattern, which confirms the DSC curve of mannitol.

Physical mixture maintained the crystalline pattern observed for DAP, as well as DAP nanocrystals. Therefore, it is possible to conclude that the nanosizing process did not change the crystallinity of the drug substance. However, it may have generated diffractogram peaks with lower intensity. This characteristic may have been caused by the “particle size broadening” phenomenon, applicable for crystalline materials with less than 1 μm (ZHANG et al., 2013). In addition, POVA presence or even the surface area increase may also contribute to the lower intensity peaks observed (KARAKUCUK; CELEBI, 2020).

Figure 16: X-ray diffractogram of dapsone (DAP), Povacoat® (POVA), mannitol (MN), physical mixture (PM), and dapsone nanocrystals (NC).

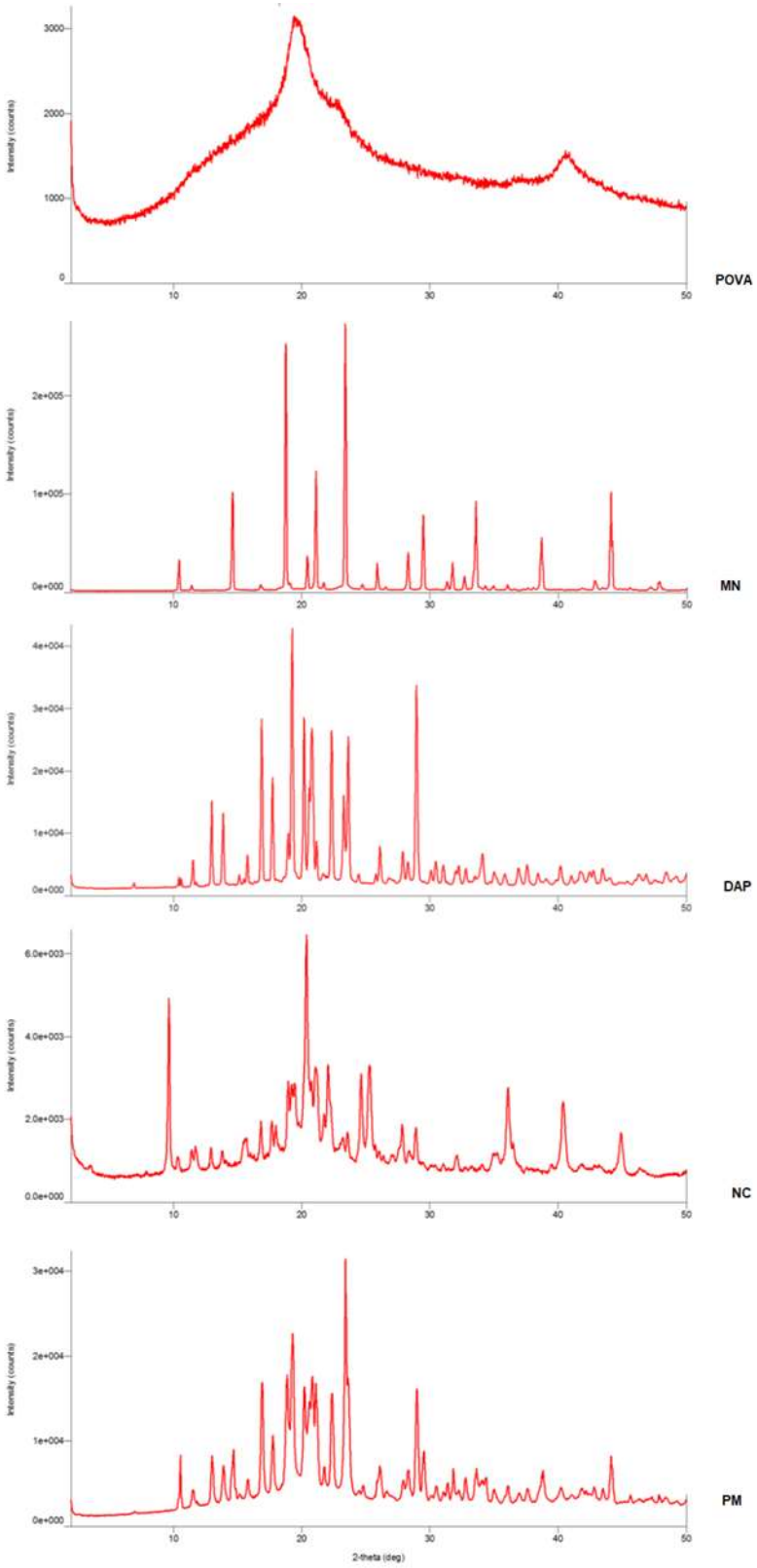

Source: the author

2.2.3.12. Verification of a spectrophotometric method for DAP quantification

The scanning was performed in the range 200-400nm, and the wavelengths corresponding to maximum absorbance were noted at 258 nm and 291 nm, according to figure 17. The working solution pH is 7.5, and considering DAP pKa (2.41), the molecules were neutral during the analysis. This study's wavelengths revealed for neutral DAP are consistent with those described in the literature (MOURA et al., 2020).

Figure 17: Absorption spectrum in the UV region for dapsone 10µg/ml in methanol:water.

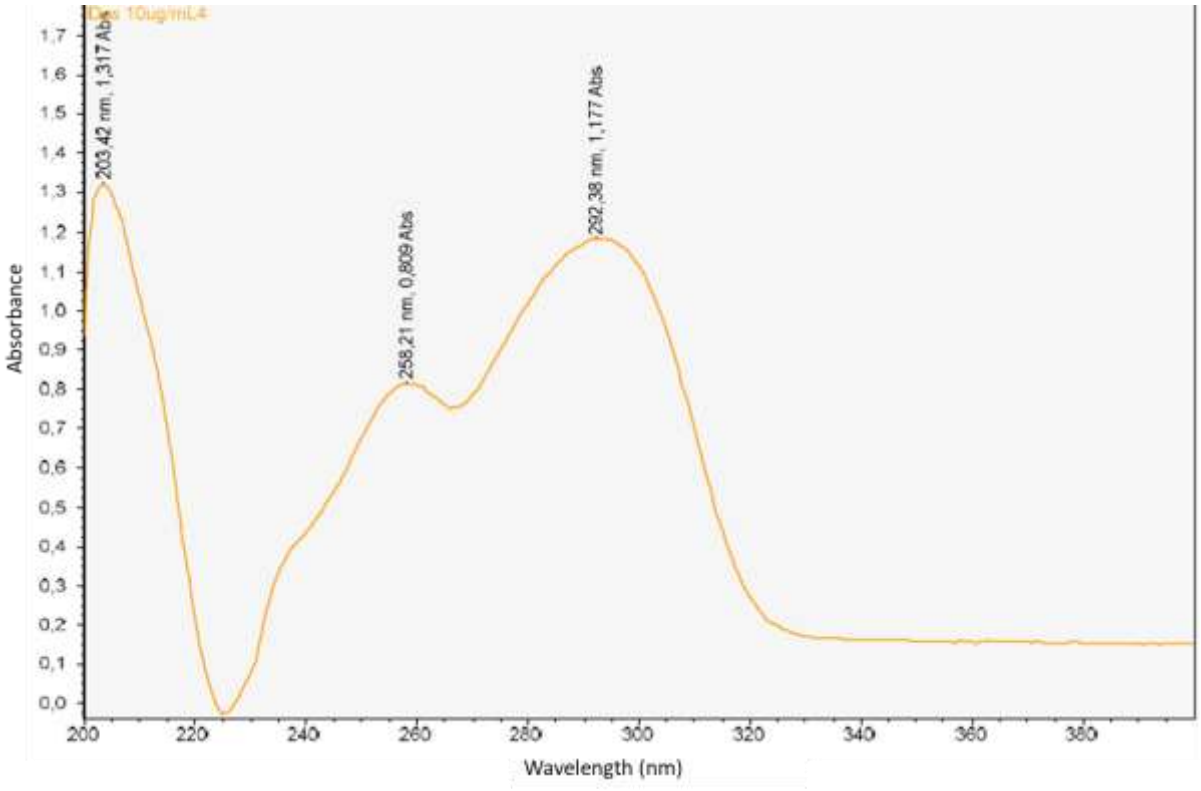

Source: the author

2.2.3.12.1. Linearity

Linearity was investigated at 291nm, using the stock solution, at different concentrations ranging from 2µg/mL to 8 µg/mL (in triplicate). The regression line obtained using the method of least squares is presented in figure 18. The regression

model details, such as equation, coefficient of determination (R^2), standard deviation (S), p-value, are described in Table 12.

The evaluation of the R^2 value (99.1%) indicates a good fit for the data in this model. The Anova p-value (0.0001) is less than the significance level (0.05), showing a statistically significant association between absorbance and concentration. Furthermore, the lack-of-fit <0.05 demonstrates that the error is not associated with the model. Moreover, the correlation coefficient (r=0.995) close to unit (r=1) means a good correlation for the model's linearity. Another factor that corroborates the linearity of the model is the regression coefficient (slope) being different from 0. In order to evaluate if the slope (0.1010) is statistically different from zero, t-value (17.09) should be compared to the critical value. The critical value, for 5 degrees of freedom (7 - 2), and considering 5% as significance level, is 2.015. Then, as the t-value (17.09) showed to be higher than the critical value (2.015), the H_0 hypothesis is rejected, and it is possible to confirm that the regression coefficient is statistically different from 0.

Figure 18: Regression line of the DAP standard solution - range of 2 to 8 µg/ml, at 291 nm.

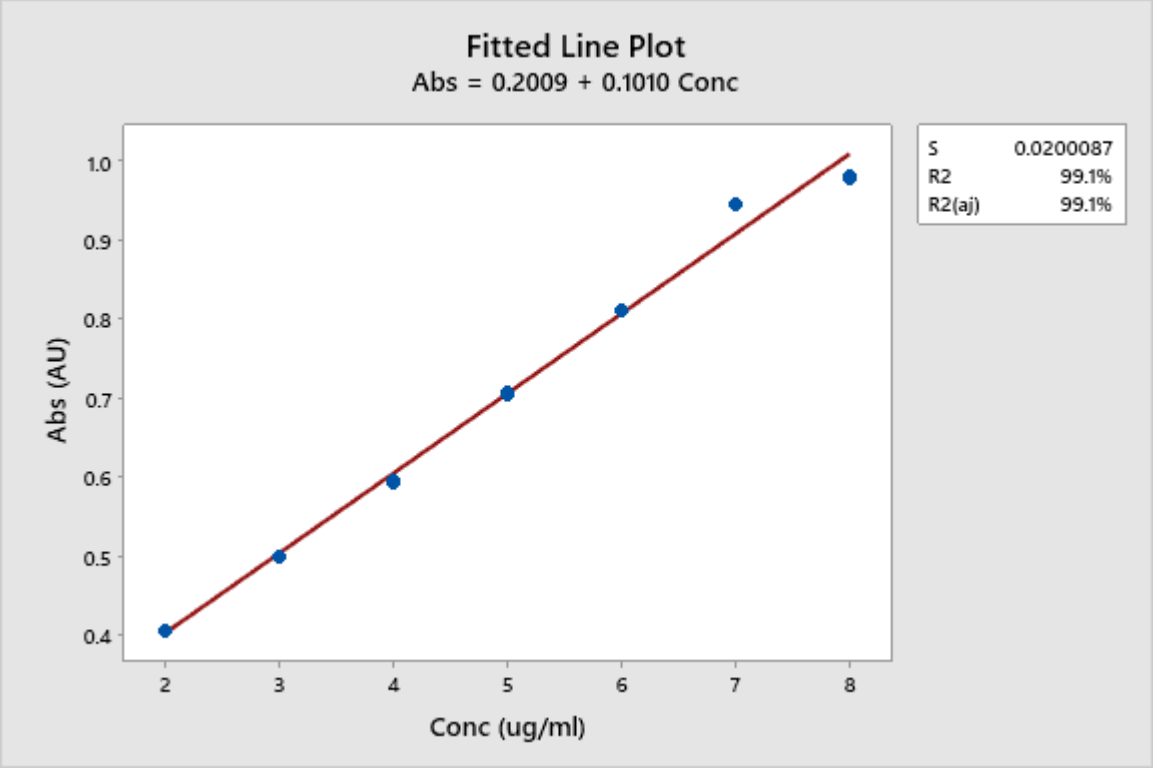

Source: the author

Table 12: Summary of model verification.

Parameter	Result
Range (µg/ml)	2.0 – 8.0
Regression equation	Abs = 0.2009 + 0.1010 Conc
Coefficient of determination (R^2)	99.1%
Correlation coefficient (r)	0.995
Standard deviation (σ, or S in the graph)	0.0200087
Anova p-value	0.0001
Lack-of-fit	0.0001
t-value	17.09

Abs: absorbance; Conc: concentration of DAP;

The residual plot, in figure 19, may help to determine the model's adequacy. The residual versus fit plot showed randomly distributed data, confirming the absence of a pattern during the analysis. The probability plot demonstrated an approximately straight line for the residuals without outliers.

Figure 19: Residual plot of regression model for DAP standard solution - range of 2 to 8 µg/ml, at 291 nm

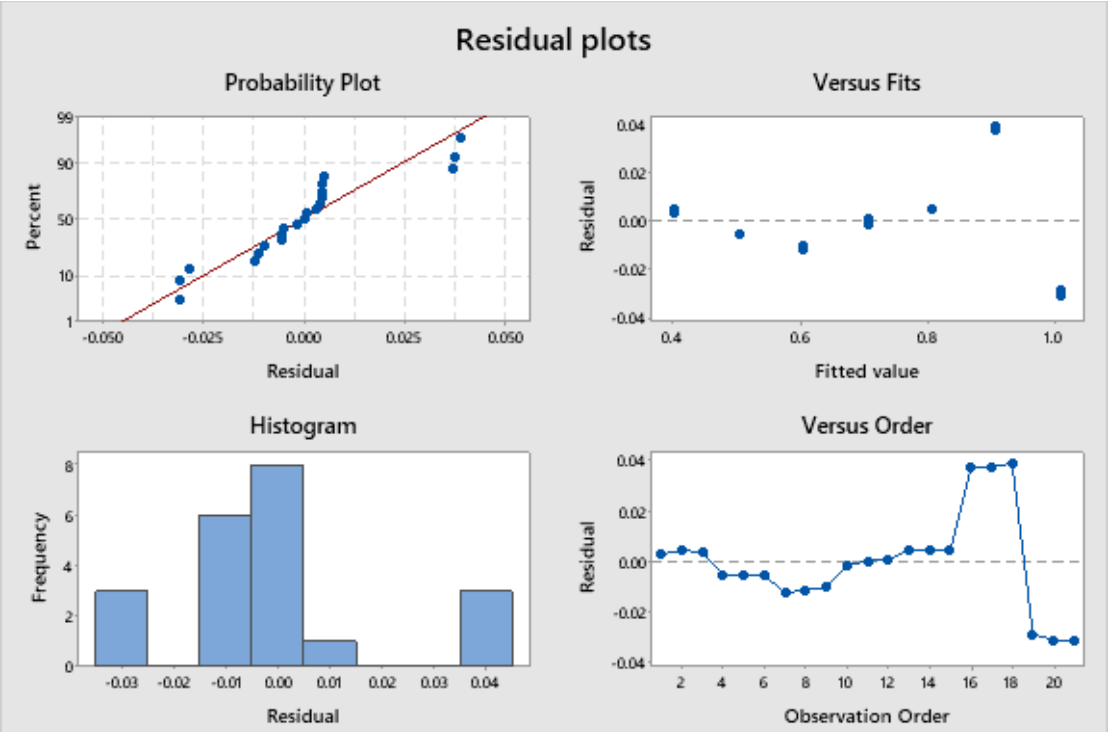

Source: the author

2.2.3.12.2. Detection limit and quantification limit

The detection limit (DL) and the quantification limit (QL) were mathematically determined based on the regression line parameters (Table 12). The DL is 0.654µg/ml, and the QL is 1.981µg/ml. Therefore, the spectrophotometric method was suitable since the lowest concentration in the calibration curve is higher than these limits.

2.2.3.12.3. Precision

a) Repeatability and Intermediate precision

Precision may be calculated through relative standard deviation (RSD) and was expressed in table 13. The acceptance criteria was RSD < 5.0%, according to FDA guidelines (FDA, 2020). All the RSD meets the acceptance criteria; therefore, the repeatability and intermediate precision present satisfactory results.

Table 13: Results obtained for method repeatability and intermediate precision.

Concentration (µg/mL)	Repeatability (RSD)	Intermediate precision (RSD)
2.0	-	3.23
5.0	1.16	0.10
8.0	-	0.05

2.2.3.12.4. Specificity

Figure 20 reveals the absorbance of POVA solution in the range of 200-400 nm. As demonstrated, the method presents low specificity due to the absorbance of POVA in the same DAP wavelength. Nevertheless, the ICH Q2 guideline predicts the possibility of method lack of specificity and suggests the application of analytical procedures. In this study, to eliminate the interference of POVA in the result, the same concentration of stabilizer was used as the blank solution.

Figure 20: Absorption spectrum in the UV region for POVA in methanol:water.

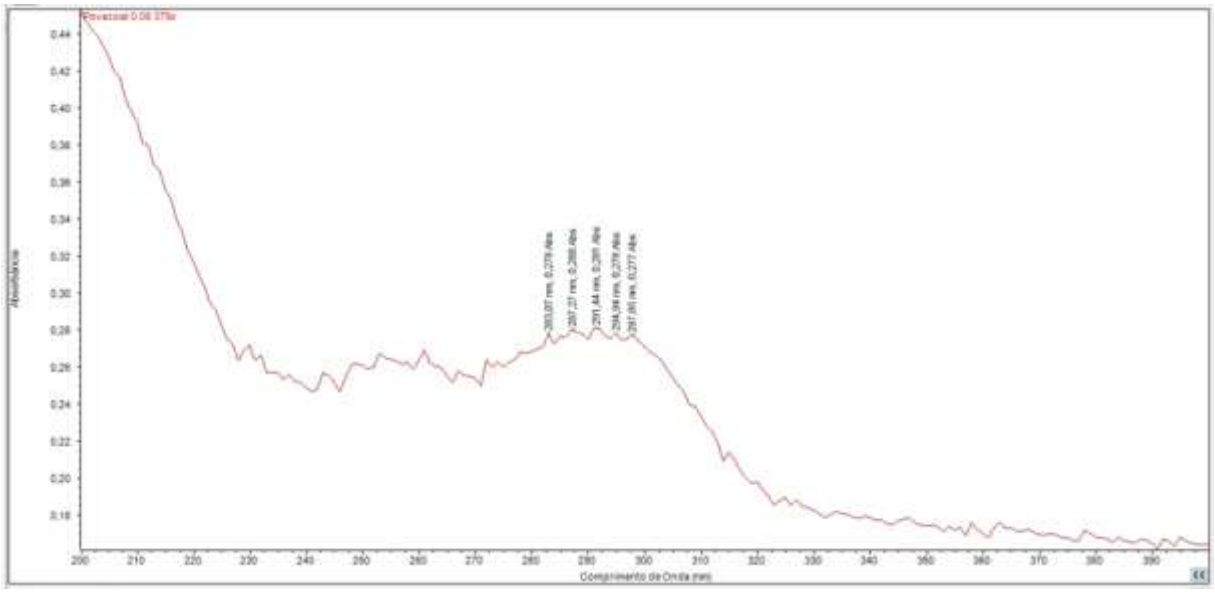

Source: the author

2.2.3.13. Saturation solubility test

Saturated solubility of the drug substance (DS), physical mixture (PM), as well as lyophilized nanocrystal (NC) was determined in different buffers (hydrochloric acid - pH 1.2 and acetate buffer - pH 4.5) and water (pH 6.5). The determination of saturation solubility is essential to prove the advantages of nanocrystals compared to micronized drug substances, but also to predict their *in vivo* performance (KALEPU; NEKKANTI, 2016). The results obtained are expressed in figure 21. The solubility obtained for DAP in water (0.193 mg/ml) was similar to the literature reference at 25ºC (MARTINS; CALDERINI; PESSINE, 2012). The time spent in sample preparation, such as centrifugation and filtration, caused a decrease in temperature, resulting in solubility closer to the values at 25ºC, including at the different buffers used (CHAVES et al., 2015).

Figure 21: Saturation solubility obtained by shake flask method in different media for dapsone raw material (DS), physical mixture (PM), and dapsone nanocrystals (NC).

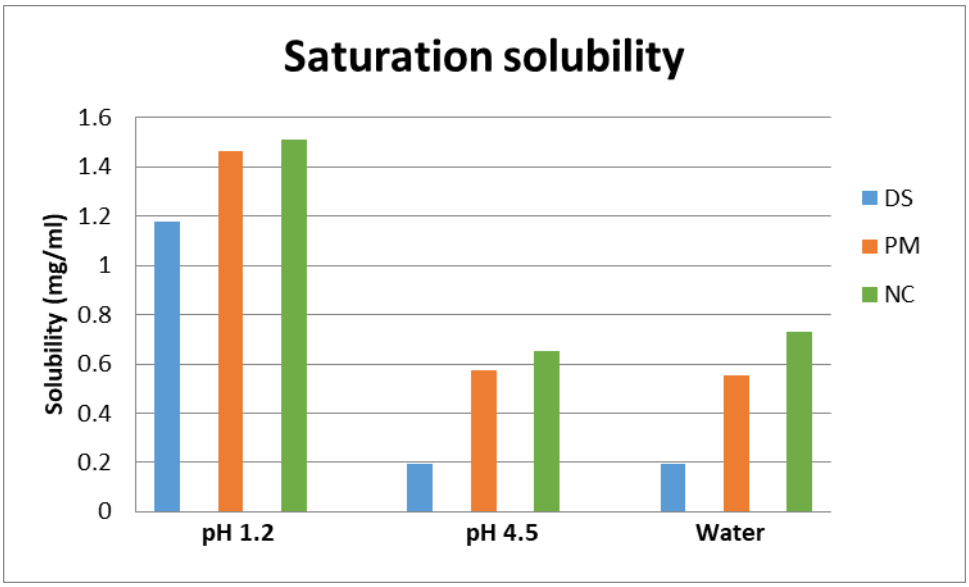

Source: the author

The highest values of saturation solubility were obtained at pH 1.2 due to the dapsone pka (2.41). Solubility results reflect what was expected during the solubility study planning, whereas the prevalence of ionized species at low pH increases the solubility. Therefore, the solubility enhancement is inversely proportional to the pH increase.

Dapsone nanocrystals presented an improvement of 1.28 in pH 1.2, 3.32 in pH 4.5, and 3.78 in water, compared to dapsone raw material. The majority presence of charged species can explain the lowest difference in acid pH. At other pHs, the difference between the media is minimal due to the non-ionized characteristics of the particles.

A change in the crystalline state of the drug substance may result in a saturation solubility increase, but in this study, as demonstrated by DSC and XRD, this characteristic remains unchanged (MAULUDIN; MÜLLER; KECK, 2009). On the other hand, the physical mixture result showed that the stabilizer must also have potentiated the increase of solubility. Thus, the saturation solubility improvement may result from the sum of the stabilizer choice and the development of nanocrystals.

2.2.3.14. Stability studies

Figure 22 presents the Z-ave, PdI, ZP, and standard deviations during the long-term and accelerated stability studies. Particle size presented monomodal distribution and PdI lower than 0.2 for both conditions studied. Additionally, for the long-term study, the difference of means significance was evaluated using ANOVA. The p-values of Z-ave, PdI, and ZP were respectively 0.071, 0.241, and 0.0001. Therefore, the difference between Z-ave and PdI from overtime was not statistically significant. The accelerated stability results varied a little over 90 days, but it was not possible to conduct a statistical analysis due to the low number of results.

On the other hand, for ZP the mean values showed a statistically significant difference. Nevertheless, POVA confers steric stability to formulation due to its increased molecular weight (type F = 40,000) and has less influence on the ZP values (CHEN et al., 2002; YUMINOKI et al., 2014). In summary, POVA is considered effective in providing stability to dapsone nanosuspension. It successfully prevents the occurrence of aggregation and the Ostwald ripening phenomenon under different storage conditions in the studied times.

Figure 22: Mean particle size (Z-ave), polydispersity index (PdI), and zeta potential (ZP) of dapsone nanosuspension for 4 months of storage at 30ºC/ 65% RH and 3 months at 40ºC/ 75% RH. (n=3)

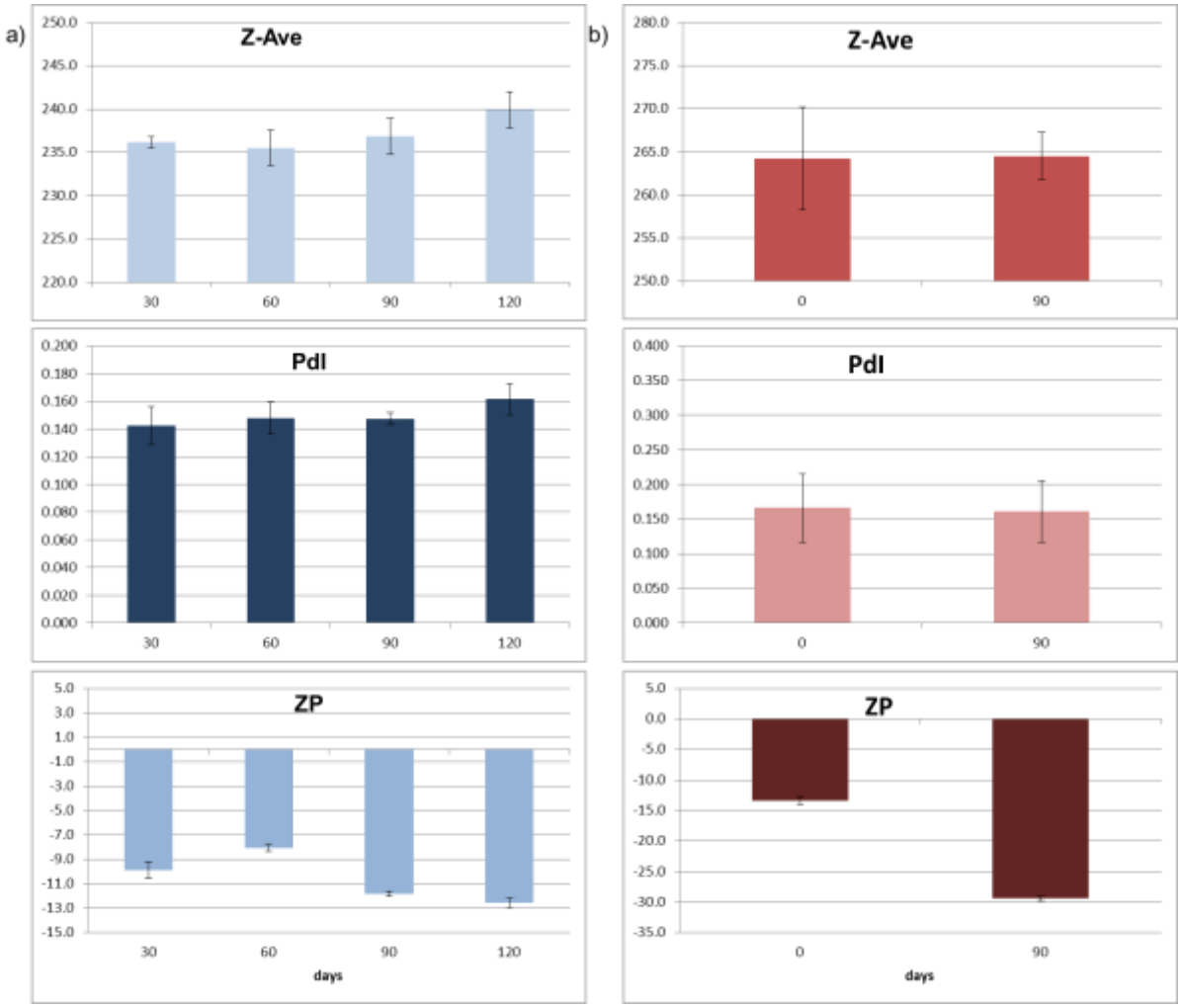

Source: the author

2.2.3.15. Toxicity on *Galleria mellonella* larvae

Aiming to assess the toxicity of free DAP and its nanocrystal formulation, 10 µL of the solutions were injected to obtain the following doses: 2000, 200, and 20 mg/kg of DAP nanocrystals; 200 mg/kg of free DAP and 100 mg/kg of POVA (Figure 23). The application of DAP nanocrystal at the highest dose (2000 mg/kg) was highly toxic, with 100% mortality of larvae 24 hours after injection. When reduced by 10 times (200 mg/kg), the nanocrystal presented its toxicity similar to the group containing only POVA at the same concentration, indicating that the toxicity is related

to the surfactant. At the lowest dose (20 mg/kg), 20% mortality of larvae was observed after five days of evaluation. After the evaluation period, free DAP at 200 mg/kg was not considered toxic, with 100% larvae survival.

Although the chosen surfactant may have contributed to the toxicity, the intrinsic characteristics of the nanocrystals must be considered. Even though it seems that DAP nanocrystals could be more toxic than the free drug, this may actually prove that the increase in solubility observed for the formulation is reflected in the larval toxicity, as observed in previous studies (LOU et al., 2009; GAO et al., 2011).

Figure 23: Survival (A) and morbidity (B) curves for evaluating the toxicity of free DAP, POVA, DAP nanocrystals tested at different doses in *Galleria mellonella* larvae.

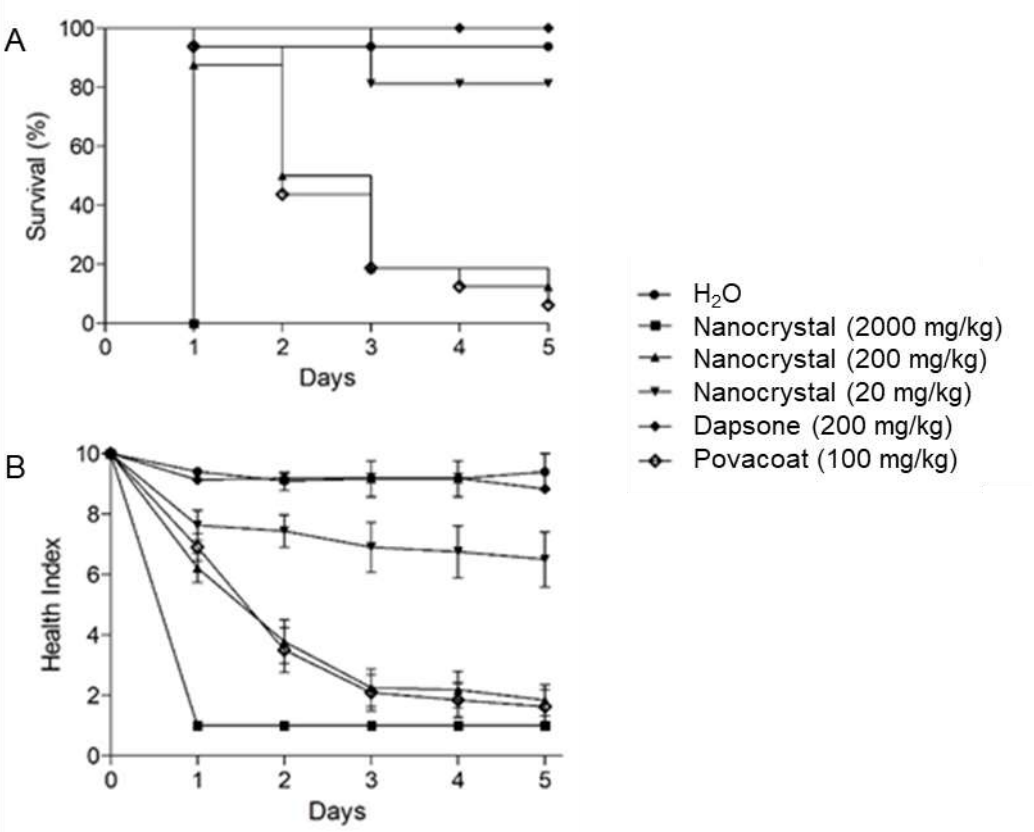

Source: the author

2.2.3.16. Scale-up from lab to pilot scale

Aiming to evaluate the feasibility of the top-down method to scale up, Labstar equipment was chosen (Figure 24), according to a previous study (GHOSH et al.,

2012). The resulting particles showed a monodisperse distribution, Z-ave smaller than 400 nm and PdI near 0.200 (Table 14). The values can be considered satisfactory as coming from an initial test, but they differ from the obtained values on the small-scale approach (about 200 nm). Particle size reduction is a complex process, which involves multiple essential factors, such as process parameters and formulation proportions. Thus, additional experiments are essential to obtain the same particle size from the lab-scale formulation.

On the other hand, the processing time was reduced almost 50-fold in the pilot scale, suggesting that a decrease in particle size does not always accompany the process time increase. Therefore, it is possible to produce DAP nanocrystal in just a few minutes, crucial for industrial production. Accordingly, the experiment proves the scalability of the small-scale wet bead milling to pilot scale, even if improvements are desirable.

Figure 24: LabStar Neos® agitator Bead Mill (NETZSCH-Feinmahltechnik GmbH) used to evaluate the scalability of small-scale wet bead milling for pilot scale.

Source: the author

Table 14: Mean particle size (Z-ave) and polydispersity index (PdI) obtained for pilot scale, according to milling process time.

Process time	Z-ave ± SD	PdI ± SD
30'	394.6 ± 27.0	0.244 ± 0.307
60'	336.9 ± 23.0	0.177 ± 0.032
90'	328.7 ± 15.0	0.196 ± 0.086
120'	314.6 ± 16.9	0.251 ± 0.059
150'	349.1 ± 12.1	0.157 ± 0.080
180'	346.6 ± 4.0	0.245 ± 0.016
210'	331.5 ± 10.4	0.164 ± 0.058

SD: standard deviation

2.3. CONCLUSION

The selection of stabilizers indicates Povacoat® as the suitable one.

The statistical approach through response surface methodology enables the evaluation of parameters which influence the response Z-ave: POVA concentration, stirring speed and process time.

The optimized formulation containing 4.0% of DAP and 2.0% of POVA presented particle size of 206.3 ± 6.7 and PdI of 0.132 ± 0.012.

The mean particle of optimized formulation was confirmed using three different techniques, reinforcing the reduction of particle size of 246-fold comparing to dapsone raw material.

The lyophilized formulation presented satisfactory mean particle size after reconstitution, showing the successful application of this method.

The DSC and DRX analysis indicate the crystalline pattern of dapsone nanocrystals.

Saturation solubility of nanocrystals presents a 3.78 increase in water compared to DAP raw material.

The long term stability of 4 months and accelerated of 3 months of DAP nanosuspension revealed formulation low variability in these timing intervals.

The *in vivo* test on *galleria mellonella* larvae indicates low toxicity of 20 mg/kg of formulation dose.

The attempt of scale up from lab to pilot scale showed promising results to obtain a commercial product.

Nanocrystals are a promising platform to developed innovative products with potential to improve the safety and efficacy of dapsone. The optimized formulation may decrease adverse effects occurrence, improving treatment adherence against leprosy.

2.4. REFERENCES

AGRAWAL, S.; PANCHAGNULA, R. Implication of biopharmaceutics and pharmacokinetics of rifampicin in variable bioavailability from solid oral dosage form. **Biopharmaceutics and Drug Disposition**, v. 26, n. 8, p. 321–334, 2005.

AGRAWAL, Y.; PATEL, V. Nanosuspension: An approach to enhance solubility of drugs. **Journal of Advanced Pharmaceutical Technology & Research**, v. 2, n. 2, p. 81, 2011.

ANJAN DE, SUDDHASATTYA DEY, PRASANNA KUMAR PRADHAN, FALGUNI CHAUDHARI, M. P. Estimation of Dapsone in Bulk & Dosage Form By Uv Spectroscopic. **Indo American Journal of Pharmaceutical Research**, v. 4, n. 1, p. 312–319, 2014.

BARRETO, T. L. et al. Miltefosine as an alternative strategy in the treatment of the emerging fungus Candida auris. **International Journal of Antimicrobial Agents**, v. 56, n. 2, 2020.

BASTIANI, F. W. M. D. S. DE. **Sistemas de liberação para anfotericina B e miltefosina no tratamento das candidíases**. 2018. Universidade de São Paulo, 2018.

BOLLA, G.; NANGIA, A. Clofazimine mesylate: A high solubility stable salt. **Crystal Growth and Design**, v. 12, n. 12, p. 6250–6259, 2012.

BOLUK, Y.; DANUMAH, C. Analysis of cellulose nanocrystal rod lengths by dynamic light scattering and electron microscopy. **Journal of Nanoparticle Research**, v. 16, n. 1, 2014.

BRASIL. **Resolução RDC nº 318, de 6 de novembro de 2019**.

BRUNI, G. et al. Physico-chemical characterization of anhydrous d-mannitol. **Journal of Thermal Analysis and Calorimetry**, v. 95, n. 3, p. 871–876, 2009.

CAMBAU, E. et al. Antimicrobial resistance in leprosy: results of the first prospective open survey conducted by a WHO surveillance network for the period 2009–15. **Clinical Microbiology and Infection**, v. 24, n. 12, p. 1305–1310, 2018.

CHAPPA, P. et al. Drug-Polymer Co-Crystals of Dapsone and Polyethylene Glycol: An Emerging Subset in Pharmaceutical Co-Crystals. **Crystal Growth and Design**, v. 18, n. 12, p. 7590–7598, 2018.

CHAVES, L. L. et al. Rational and precise development of amorphous polymeric systems with dapsone by response surface methodology. **International Journal of Biological Macromolecules**, v. 81, p. 662–671, 2015.

CHAVES, L. L. et al. PH-sensitive nanoparticles for improved oral delivery of dapsone: Risk assessment, design, optimization and characterization. **Nanomedicine**, v. 12, n. 16, p. 1975–1990, 2017.

CHAVES, L. L. et al. pH-responsive chitosan based hydrogels affect the release of dapsone: Design, set-up, and physicochemical characterization. **International Journal of Biological Macromolecules**, v. 133, p. 1268–1279, 2019.

CHEN, X. et al. Preparation of cyclosporine A nanoparticles by evaporative precipitation into aqueous solution. **International Journal of Pharmaceutics**, v. 242, n. 1–2, p. 3–14, 2002.

CHENG, M. et al. Fabrication of Fine Puerarin Nanocrystals by Box–Behnken Design to Enhance Intestinal Absorption. **AAPS PharmSciTech**, v. 21, n. 3, p. 1–12, 2020.

DANAEI, M. et al. Impact of particle size and polydispersity index on the clinical applications of lipidic nanocarrier systems. **Pharmaceutics**, v. 10, n. 2, p. 1–17, 2018.

DE ANDRADE, K. V. F. et al. Geographic and socioeconomic factors associated with leprosy treatment default: An analysis from the 100 Million Brazilian Cohort. **PLoS Neglected Tropical Diseases**, v. 13, n. 9, 2019.

DE CÁSSIA ZAGHI COMPRI, J. et al. Highly Water-Soluble Orotic Acid Nanocrystals Produced by High-Energy Milling. **Journal of Pharmaceutical Sciences**, v. 108, n. 5, p. 1848–1856, 2019.

DE SOUSA, V. et al. Development and characterization of a new oral dapsone nanoemulsion system: permeability and in silico bioavailability studies. **International Journal of Nanomedicine**, n. September, p. 5175, 2012.

DEPS, P. D. et al. Adverse effects from multi-drug therapy in leprosy: a Brazilian

study. **Leprosy review**, v. 78, n. 3, p. 216–22, 2007.

DESHIIKAN, S. R.; PAPADOPOULOS, K. D. Modified Booth equation for the calculation of zeta potential. **Colloid and Polymer Science**, v. 276, n. 2, p. 117–124, 1998.

EMEA. ICH Topic Q 2 (R1) Validation of Analytical Procedures: Text and Methodology. 121.

FDA. Guidance for Industry of New Drug Substances and Products Guidance for Industry Q1A (R2) Stability Testing of New Drug Substances and Products.

FDA. Methods, Method Verification and Validation, ORA Laboratory Manual Volume II. v. II, 2020.

GAN, C. Y.; ABDUL MANAF, N. H.; LATIFF, A. A. Optimization of alcohol insoluble polysaccharides (AIPS) extraction from the Parkia speciosa pod using response surface methodology (RSM). **Carbohydrate Polymers**, v. 79, n. 4, p. 825–831, 2010.

GAO, Y. et al. Preparation and characterization of intravenously injectable curcumin nanosuspension. **Drug Delivery**, v. 18, n. 2, p. 131–142, 2011.

GHOSH, I. et al. Optimization of formulation and process parameters for the production of nanosuspension by wet media milling technique: Effect of Vitamin e TPGS and nanocrystal particle size on oral absorption. **European Journal of Pharmaceutical Sciences**, v. 47, n. 4, p. 718–728, 2012.

GOULART, I. M. B. et al. Efeitos adversos da poliquimioterapia em pacientes com hanseníase: um levantamento de cinco anos em um Centro de Saúde da Universidade Federal de Uberlândia. **Revista da Sociedade Brasileira de Medicina Tropical**, v. 35, n. 5, p. 453–460, 26 abr. 2005.

GREBOGI, I. H. et al. Binary and ternary inclusion complexes of dapsone in cyclodextrins and polymers: Preparation, characterization and evaluation. **Journal of Inclusion Phenomena and Macrocyclic Chemistry**, v. 73, n. 1–4, p. 467–474, 2012.

HEUKELBACH, J. et al. Interruption and defaulting of multidrug therapy against leprosy: Population-based study in Brazil's Savannah region. **PLoS Neglected Tropical Diseases**, v. 5, n. 5, p. 4–9, 2011.

HUSSAIN, A. et al. In vitro - In vivo - In silico simulation studies of anti-tubercular drugs doped with a self nanoemulsifying drug delivery system. **RSC Advances**, v. 6, n. 95, p. 93147–93161, 2016.

ICH Q8. EMEA/CHMP, 2009, ICH Topic Q 8 (R2) Pharmaceutical Development, Step 5: Note for Guidance on Pharmaceutical Development.

IGE, P. P.; BARIA, R. K.; GATTANI, S. G. Fabrication of fenofibrate nanocrystals by

probe sonication method for enhancement of dissolution rate and oral bioavailability. **Colloids and Surfaces B: Biointerfaces**, v. 108, p. 366–373, 2013.

JACOB, S.; NAIR, A. B.; SHAH, J. Emerging role of nanosuspensions in drug delivery systems. **Biomaterials Research**, v. 24, n. 1, p. 1–16, 2020.

JUNGHANNS, J. U. A. H.; MÜLLER, R. H. Nanocrystal technology, drug delivery and clinical applications. **International Journal of Nanomedicine**, v. 3, n. 3, p. 295–309, 2008.

KALEPU, S.; NEKKANTI, V. Improved delivery of poorly soluble compounds using nanoparticle technology: a review. **Drug Delivery and Translational Research**, v. 6, n. 3, p. 319–332, 2016.

KARAKUCUK, A.; CELEBI, N. Investigation of Formulation and Process Parameters of Wet Media Milling to Develop Etodolac Nanosuspensions. **Pharmaceutical Research**, v. 37, n. 6, 2020.

KASZUBA, M. et al. Measuring sub nanometre sizes using dynamic light scattering. **Journal of Nanoparticle Research**, v. 10, n. 5, p. 823–829, 2008.

LESTARI, M. L. A. D.; MÜLLER, R. H.; MÖSCHWITZER, J. P. The Scalability of Wet Ball Milling for The Production of Nanosuspensions. **Pharmaceutical Nanotechnology**, v. 7, n. 2, p. 147–161, 2019.

LEWIS, G. A.; MATHIEU, D.; PHAN-TAN-LUU, R. **Pharmaceutical Experimental Design**. CRC Press, 1998. v. 92

LI, H. Z. et al. Nano carrier mediated co-delivery of dapsone and clofazimine for improved therapeutic efficacy against tuberculosis in rats. **Biomedical Research (India)**, v. 28, n. 3, p. 1284–1289, 2017.

LI, W. et al. Eutectics and Salt of Dapsone With Hydroxybenzoic Acids: Binary Phase Diagrams, Characterization and Evaluation. **Journal of Pharmaceutical Sciences**, v. 109, n. 7, p. 2224–2236, 2020.

LINDERSTRØM-LANG, C.; NAYLOR, R. 4,4′-Diaminodiphenyl sulphone: solubility and distribution in blood. **Biochemical Journal**, v. 83, n. 3, p. 417–420, 10 ago. 1962.

LOH, J. M. S. et al. Galleria mellonella larvae as an infection model for group A streptococcus. **Virulence**, v. 4, n. 5, p. 419–428, 2013.

LOU, H. et al. In vitro and in vivo antitumor activity of oridonin nanosuspension. **International Journal of Pharmaceutics**, v. 379, n. 1–2, p. 181–186, 2009.

MALAMATARI, M. et al. Pharmaceutical nanocrystals: production by wet milling and applications. **Drug Discovery Today**, v. 23, n. 3, p. 534–547, 2018.

MARTINS, M. H.; CALDERINI, A.; PESSINE, F. B. T. Host-guest interactions

between dapsone and β-cyclodextrin (Part II): Thermal analysis, spectroscopic characterization, and solubility studies. **Journal of Inclusion Phenomena and Macrocyclic Chemistry**, v. 74, n. 1–4, p. 109–116, 2012.

MAULUDIN, R.; MÜLLER, R. H.; KECK, C. M. Development of an oral rutin nanocrystal formulation. **International Journal of Pharmaceutics**, v. 370, n. 1–2, p. 202–209, 2009.

MELO, K. J. C. et al. Rifampicin nanocrystals: Towards an innovative approach to treat tuberculosis. **Materials Science and Engineering C**, v. 112, n. March, p. 110895, 2020.

MINISTÉRIO DA SAÚDE, A. N. D. V. S. **RESOLUÇÃO RDC Nº 166, DE 24 DE JULHO DE 2017**.

MOHAMMAD, I. S. et al. Drug nanocrystals: Fabrication methods and promising therapeutic applications. **International Journal of Pharmaceutics**, v. 562, n. December 2018, p. 187–202, 2019.

MÜLLER, R. H.; GOHLA, S.; KECK, C. M. State of the art of nanocrystals - Special features, production, nanotoxicology aspects and intracellular delivery. **European Journal of Pharmaceutics and Biopharmaceutics**, v. 78, n. 1, p. 1–9, 2011.

NOYES, A. A.; WHITNEY, W. R. The rate of solution of solid substances in their own solutions. **Journal of the American Chemical Society**, v. 19, n. 12, p. 930–934, 1897.

PATRAVALE, V. B.; DATE, A. A.; KULKARNI, R. M. Nanosuspensions: a promising drug delivery strategy. **Journal of Pharmacy and Pharmacology**, v. 56, n. 7, p. 827–840, 2004.

PENG, X. et al. Box–Behnken design based statistical modeling for the extraction and physicochemical properties of pectin from sunflower heads and the comparison with commercial low-methoxyl pectin. **Scientific Reports**, v. 10, n. 1, p. 1–10, 2020.

RAGHAVA SRIVALLI, K. M.; MISHRA, B. Drug nanocrystals: A way toward scale-up. **Saudi Pharmaceutical Journal**, v. 24, n. 4, p. 386–404, 2016.

RANJBAR, M. et al. Preparation of polyacrylamide/polylactic acid co-assembled core/shell nanofibers as designed beads for dapsone in vitro efficient delivery. **Artificial Cells, Nanomedicine and Biotechnology**, v. 47, n. 1, p. 917–926, 2019.

ROMERO, G. B.; KECK, C. M.; MÜLLER, R. H. Simple low-cost miniaturization approach for pharmaceutical nanocrystals production. **International Journal of Pharmaceutics**, v. 501, n. 1–2, p. 236–244, 2016.

SINGARE, D. S. et al. Optimization of formulation and process variable of nanosuspension: An industrial perspective. **International Journal of Pharmaceutics**, v. 402, n. 1–2, p. 213–220, 2010.

SINGH, B. et al. Developing oral drug delivery systems using formulation by design:

Vital precepts, retrospect and prospects. **Expert Opinion on Drug Delivery**, v. 8, n. 10, p. 1341–1360, 2011.

SINGH, H. et al. Nano-formulation of rifampicin with enhanced bioavailability: Development, characterization and in-vivo safety. **International Journal of Pharmaceutics**, v. 485, n. 1–2, p. 138–151, 15 maio 2015.

SPADARI, C. de C. et al. Alginate nanoparticles as non-toxic delivery system for miltefosine in the treatment of candidiasis and cryptococcosis. **International Journal of Nanomedicine**, v. 14, p. 5187–5199, 2019.

TALEKAR, S. D.; HAWARE, R. V.; DAVE, R. H. Evaluation of self-nanoemulsifying drug delivery systems using multivariate methods to optimize permeability of captopril oral films. **European Journal of Pharmaceutical Sciences**, v. 130, n. January, p. 215–224, 2019.

TUOMELA, A.; HIRVONEN, J.; PELTONEN, L. Stabilizing agents for drug nanocrystals: Effect on bioavailability. **Pharmaceutics**, v. 8, n. 2, 2016.
UNITED STATES PHARMACOPEIA AND NATIONAL FORMULARY. **Buffer solutions**, 2020.

VIEIRA, A. C. C. et al. Design and statistical modeling of mannose-decorated dapsone-containing nanoparticles as a strategy of targeting intestinal M-cells. **International Journal of Nanomedicine**, v. 11, p. 2601–2617, 2016.

XIA, D. et al. Preparation of stable nitrendipine nanosuspensions using the precipitation-ultrasonication method for enhancement of dissolution and oral bioavailability. **European Journal of Pharmaceutical Sciences**, v. 40, n. 4, p. 325–334, 2010.

YUMINOKI, K. et al. Preparation and evaluation of high dispersion stable nanocrystal formulation of poorly water-soluble compounds by using Povacoat. **Journal of Pharmaceutical Sciences**, v. 103, n. 11, p. 3772–3781, 2014.

YUMINOKI, K. et al. Application of povacoat as dispersion stabilizer of nanocrystal formulation. **Asian Journal of Pharmaceutical Sciences**, v. 11, n. 1, p. 48–49, 2016.

ZHANG, J. et al. Preparation of apigenin nanocrystals using supercritical antisolvent process for dissolution and bioavailability enhancement. **European Journal of Pharmaceutical Sciences**, v. 48, n. 4–5, p. 740–747, 2013.

3. APPENDIX A: Leprosy diagnosis and treatment: challenges and recent advances

Abstract

Leprosy has been known since 2000 BC, although it was not until 1981 that the WHO recommended an effective multidrug therapy (MDT) treatment capable of healing the patient and preventing the spread of the bacillus. Nevertheless, 208,641 new cases were reported from 161 Member States in 2018, with India leading the ranking (57.7%), followed by Brazil (13.7%) and Indonesia (8.2%). Leprosy elimination faces several challenges related to assertive diagnosis and poor patient compliance. Misdiagnosis may lead to insufficient therapy or overtreatment, endangering its completion by the patient. Early diagnosis is essential to prevent disabilities, commonly associated with leprosy stigma, and early diagnosis of household contacts. Modern methods with higher specificity, sensitivity nevertheless affordable have been proposed aiming to standardize the diagnosis. The MDT consists of dapsone, rifampicin, and clofazimine with different duration according to disease classification. MDT drugs face bioavailability constraints due to their low water solubility (Class II drugs, according to BCS). Innovative therapeutic strategies, as nanoparticle formulations, presented a modified drug release pattern, enabling dose adjustment. This strategy may minimize treatment-related adverse effects and reduce drug resistance, overcoming significant hurdles to treatment adherence. Therefore, this review is an effort to present the main challenges and recent advances on leprosy diagnosis and treatment, aiming to guarantee the early and reliable detection of the disease while underscoring the importance of innovative strategies for leprosy eradication.

Keywords: Leprosy, Clinical diagnosis, Multidrug therapy, Nanoparticle formulation, Treatment adherence

Funding statement: This work was supported by CAPES (Coordenação de Aperfeiçoamento de Pessoal de Nível Superior) – Finance code 001.

Conflict of interest: None declared.

Ethical approval: Not required.

1. Introduction

Leprosy is an ancient infectious-contagious and chronic disease caused by

intracellular bacterium *Mycobacterium leprae,* which has high infectivity and low pathogenicity [1]. This mycobacterium has a tropism for Schwann cells in nerves and macrophages in the skin, defining the main areas affected by them: nasal mucosa, peripheral nervous system, and dermis and epidermis [2]. The damage to peripheral nerves can cause sensory and motor impairment with deformities and disability [3]. It is transmitted by the aerosol spread of droplets from the nose and mouth, especially during close and prolonged contact with untreated patients [4,5].

In 2018, a total of 208,641 new cases were reported from 161 Member States, according to the World Health Organization (WHO). India, Brazil, and Indonesia were the first three countries in the number of new cases, responsible respectively for 57.7% (120,334), 13.7% (28,660), and 8.2% (17,017) of total globally reported cases. These three countries alone account for almost 80% of the new cases annually. Among countries of the Americas, Brazil presents the highest percentage, 92.5% in 2018, followed by Paraguay with 1.1% [6]. Alarming data have recently been reported showing the emergence and transmission of resistant strains of *M. leprae* in a unique and hyper-endemic population from the Brazilian Amazon [7].

Focusing on leprosy control, the WHO launched in April 2016 the guideline "Global Leprosy Strategy 2016–2020: accelerating towards a leprosy-free world", with one of the objectives of eliminating leprosy and visible deformities among children [8]. In 2018, India registered a decrease of nearly 10% of new leprosy cases among children, Brazil remains almost the same number, and Indonesia presented an increase of 6%, compared to 2017. In the same period, the new cases among children decreased by 6% globally [6]. The incidence of leprosy in children reveals the active foci of disease transmission, with early exposure to the bacillus. Furthermore, clinical diagnosis is difficult in this age group due to leprosy stigma for parents, and problems in promoting essential public health in some territories [9]. This rate of infected children measures the presence of the bacilli and the new endemic transmission force, informing the government about decisions regarding epidemiological surveillance [1].

Since 1997, the diagnosis recommended by WHO is mainly clinically based, dividing patients into two groups: multibacillary (MB) or paucibacillary (PB), according to the number of skin patches [10]. However, clinical diagnosis is questionable and depends on the medical experience and disease stage [11,12]. A misdiagnosis may cause under or overtreatment [13]. Thereby, to overcome this challenge, a

standardized laboratory diagnosis is a promising alternative.

The leprosy treatment is based on the multidrug prescription of dapsone, rifampicin, and clofazimine, according to leprosy classification [14]. Although this therapeutic regimen promotes healing, it still faces significant challenges, such as limited bioavailability of the drug substances, which may lead to variation in dose [15–18]. The severe adverse effects of the dose regimen lead to poor adherence to treatment may causing drug resistance and disease relapse [19–21]. To address those problems, innovative and inexpensive therapeutic strategies are urgently needed. This article is an effort to comprehensively review the challenges and recent advances of leprosy diagnosis and multidrug treatment aiming to improve patient therapy adherence while underscoring the importance of early and correct diagnosis.

2. Infection development

Leprosy is more alarming than it appears to be since it is the second mycobacteria disease most common in the world [22]. *Mycobacterium leprae* is an obligate intracellular parasite and acid-fast Gram-positive bacillus [3]. A second species of *Mycobacterium* was described as causing leprosy, *M. lepromatosis*. It may be responsible for the variations on clinical and geographic aspects of the disease, even it presents a common ancestor with *M. leprae* [23]. The impossibility of *M. leprae* to grow in a culture medium and lack of animal models challenges the study of its transmission and pathogenicity [3,24].

Leprosy transmission occurs by the uptake of nasal discharge on respiratory mucosa, the main ports of entry and exit to the disease [4]. It occurs through the contact of susceptible individuals with untreated patients [4,25]. Even that the population susceptibility to infection seems to be low (about 20%), a gene mutation in myeloid protein zero (MPZ) and in mannose-binding lectin 2 (MBL_2) receptors may increase the risk of *M. leprae* infection in family members of leprosy patients [22,25]. MPZ was expressed on myelinated Schwann cells, and MBL_2 plays a role in the activation of calcium-dependent lectin pathway, which acts in the first line of defense to face infections [22]. The gene mutations promote protein structural alterations, which may be crucial for the bacterial invasion of the host cell [22]. Besides, the exposure time and close contact is an aggravating factor for contamination [4]. Therefore, the household of patients present an elevated risk of contagion and can be suggested a combination of chemoprophylaxis and immunoprophylaxis [26].

Beyond these prevention methods, it seems to be increasingly important to detect subclinical leprosy cases through a diagnostic test [25].

An essential aspect of leprosy is the usually long incubation period between the infection and clinical manifestation of the disease, taking up to 30 years [3]. This extended period of incubation may hide a higher prevalence than we already know. Besides, this may result in the misrepresenting of the success of new public health policies since the results will be observed only a decade later [27].

The disease pathogenesis is not fully understood; meantime, recent works have progressed in elucidating different aspects of leprosy. Concerning metabolic alterations, the *M. leprae* infection shows to upregulate lipid metabolism, causing cell lipid accumulation in the form of lipid droplets [28]. They are sites of lipid mediators formation [28]. Some of these lipid mediators may induce down-regulation of innate and adaptive responses, which imbalance pro-inflammatory mediators, thus affecting leprosy pathogenesis [29]. When lipid droplet formation is inhibited, a pro-inflammatory profile is favored [30]. The inhibition described was observed in two different mechanisms, causing failure in Th1 response [31]. The first was the down-modulation of IL-10 production, a potent anti-inflammatory mediator [28]. In sequence, it causes the prostaglandin E_2 under-production by infected Schwann cells and macrophages [28]. Both mechanisms hinder infection control [31].

Nerve function impairment is the primary outcome of pathological processes in *M. leprae* infection [32]. Madigan and colleagues elucidated that the nerve damage and demyelination are initiated by infected macrophages that patrol axons and not by *M. leprae* itself. The *M. leprae*-specific PGL-1 (phenolic glycolipid) stimulates macrophages to overproduce reactive oxygen species (ROS), causing early damage to nerves regardless of their myelination [33]. This fact explains the common initial manifestation of leprosy that starts by affecting thermal sensations, mediated by nonmyelinated fibers.

The early innate immune-mediated nerve injury would progress through distinct mechanisms, and the patient immune response generated by them would determine the leprosy severity [33]. The disease is extraordinarily complex due to the modulation of immune response by the bacillus. During an extended period, it was known that a paradigm between Th1 and Th2 interaction determines the severity and manifestation that the disease would express [34]. The patients present a strong Th1 immune response, a high cell-mediated immunity, narrowing the disease progression

[35]. On the other hand, the Th2 response is predominantly humoral with high titles of antibodies and low cell-mediated immunity, impairing the control of bacilli multiplication, and causing disease aggravation [35]. However, recently it was identified that Th9, Th17, Th22, Treg, and different subsets of pro-inflammatory cytokines are also determinants to modulate leprosy [34,36]. Additionally, the role of B-cell in leprosy pathogenesis is being increasingly studied, and differently than was expected, they might influence the most severe form of the disease (lepromatous) as well as the mildest (tuberculoid) [36,37]. The B-cells may also be related to leprosy granulomas formation on the tuberculoid patients, according to immunohistochemical study on leprosy lesions [36]. Therefore, the infection evolution depends on the immune modulation caused by *M. leprae*, leading to a clinical spectrum [38].

3. Leprosy classification

Ridley and Jopling proposed in 1966 a classification based on immunity and considering clinical, histological, and bacteriological data [39]. Patients with a strong pro-inflammatory response, named Tuberculoid leprosy (TT), will present T helper-1 (Th1) and Th17 responses to control the infection; however, this vigorous T-cell response may destroy the body's own cells, mimicking autoimmunity [32]. This inflammatory response produces TNF-α and IFN-γ, inducing nitric oxide synthase, and free radicals generation by macrophages aiming bacillus elimination [34]. Moreover, in the other extreme, the no cell-mediated immunity manifests in Lepromatous leprosy (LL), with Th2 polarization, lacking *M. leprae*-specific T cells with high specific antibodies and increased levels of regulatory T cells [32,34]. On this anti-inflammatory behavior, the Th2 lymphocytes response induce the production of IL-4, IL-10, and TGF-β, which promote the bacillus survival through the macrophages inactivation; and down-regulate the Th1 response. Recently Th9, Th17, Th22, Treg responses were described, but their specific contribution in each disease form is not entirely understood [34]. This failure on the immune system allows the pathogen reproduction combined with minimal signals, furthering transmission.

In between these two extremes, representing the majority of the patients, are the patients classified as borderline: Borderline Tuberculoid (BT), Mid-borderline (BB), and Borderline Lepromatous (BL), respectively, presenting decreasing levels of cell-mediated immunity, and consequently increasing the bacillary load [32,39,40]. They

are immunologically unstable and present characteristics that oscillate between TT and LL form [34].

For therapy purposes, the WHO proposed a clinical classification in which patients are classified as Multibacillary (MB) (with more than five skin patches; including BB, BL, and LL) or Paucibacillary (PB) (1 to 5 skin patches; including TT and BT) [14,40,41]. This method is practical and inexpensive, primarily in regions with insufficient hospital infrastructure. However, this clinical diagnosis method only works on 70% of patients [42]. It was described that clinical diagnosis tends to overestimate MB cases, since than one-third of the MB patients clinically classified were classified as PB by the Ridley and Jopling classification [43]. These data reinforce the need for adequate diagnosis, to avoid overtreatment in PB patients, whereas misdiagnosed MB patient would not complete it [13].

Figure 1 illustrates the relationship between Ridley and Jopling leprosy classification and the WHO clinical classification added to the patient's expected immune response.

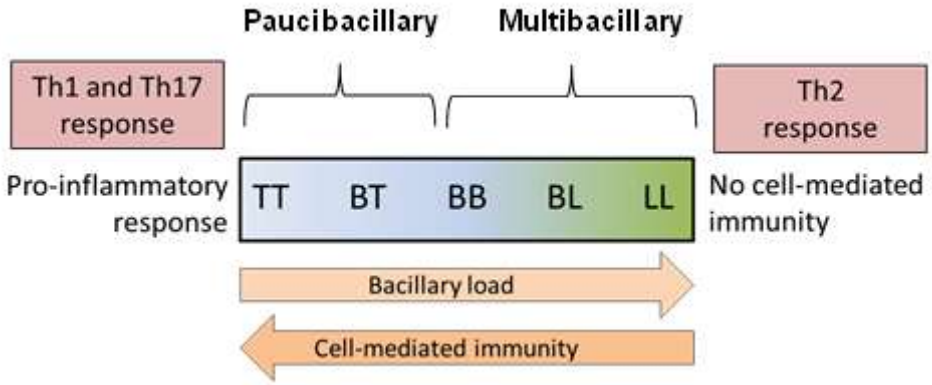

Figure 25. Leprosy classification X patient's immune response. According to Ridley and Joplin (1966), spectrum classification is a scale from Tuberculoid to Lepromatous with borderline designations located between them, considering the bacillary load. The bacillary load scale is opposite to cell-mediated immunity. For the Tuberculoid form, the Th1 and Th17 response prevail, a vigorous immune response, and for Lepromatous, the Th2 response is unresponsive to *M. leprae*. This classification was later replaced by the clinical examination to facilitate diagnosis, dividing patients into MB and PB, according to the number of skin lesions.

TT, Tuberculoid leprosy; BT, Borderline Tuberculoid; BB, Mid-borderline; BL, Borderline Lepromatous; LL, Lepromatous leprosy.

The assertive diagnosis is vital to decrease transmission since contaminated and untreated patients continue to disseminate the bacillus [4,44]. Additionally, early detection is essential to prevent physical disabilities [45]. The determination of a reliable laboratory diagnostic method proves to be necessary to subjugate the challenge of assertive and early diagnosis for leprosy patients.

4. Assertive and early diagnosis: the initial challenge

4.1. The clinical, microbiological and histopathological diagnosis method

The clinical diagnosis suggested by the WHO, based on counting the number of skin lesions, was encouraged mainly in regions where the microscopy analysis of skin smear was unavailable [46]. However, it is essential to consider the limitations of this method and the consequent impact on patient treatment. Pardillo and colleagues estimated a high percentage (31%–58%) of patients classified as PB while had PB leprosy according to Ridley and Jopling classification [13]. Besides the hurdle of under and overtreatment already discussed, the misclassification may trigger the drug resistance [13]. In Thailand, a higher rate of relapses on MB patients was observed, wrongly classified clinically as PB and undertreated [47].

In some doubtful cases, microbiological assessment of slit skin smears (SSSs) and histopathology should be considered [48]. The bacterial index reflects the quantitative bacillary load relevant to the Ridley and Jopling classification and may be useful to confirm MB diagnosis. On the other hand, due to its low sensitivity could not be assertive for PB cases, resulting even in a false negative [49,50]. The SSSs may be recommended, especially in areas with a high frequency of MB cases, in addition to clinical examination [13]. The histopathology may be performed in fragments of skin lesions or nerves and may disagree with the clinical aspect, indicating the evolution of the disease towards one of the two extremes [50].

Another objective from the guideline "Global Leprosy Strategy 2016–2020: accelerating towards a leprosy-free world” is to decrease the rate of newly diagnosed leprosy patients with visible deformities to less than 1 per million [8]. This target can be achieved through the early diagnosis and the management of complications due to leprosy reactions [8]. During the course of the disease and even after completing the treatment, 30-50% of borderline patients may present a sudden increase in pro-

inflammatory response [51]. This event results in termed Type I reactions, characterized by acute inflammation in skin lesions – infiltrations, edemas, or color change – or in nerves – neuritis – or both [44,52]. Type I reactions are associated with immune system changes, such as caused by antileprosy medications, pregnancy, or stress [53]. This acute reaction is mediated by a cellular response with serum cytokines levels (such as interferon-gamma and tumor necrosis factor-alpha) increased, and CD4+ T cells activated [53,54]. They are treated through inflammation control, using the medication as thalidomide, prednisone, or clofazimine [44,53].

In contrast, 20% of lepromatous patients, but not exclusively them, may undergo a Type II response mediated by immune complexes, termed erythema nodosum leprosum (ENL) [51]. The immune complex deposition is associated with systemic toxicity, through systemic vasculitis and panniculitis, which may result in several manifestations such as painful subcutaneous nodules, fever, malaise, orchitis, uveitis, neuritis and at times, frank glomerulonephritis [44,52,53]. Type II reactions are associated with humoral immune mechanisms, with an elevated level of tumor necrosis factor-alpha, neutrophilic infiltration increased, and complement deposition in the skin [53,54]. ENL was treated with immunosuppressants, such as prednisolone (high doses), thalidomide, and, with less effectiveness, clofazimine, pentoxifylline, colchicine, and chloroquine [44]. Disabilities associated with leprosy complications affect communities' economy and are the main reason for the leprosy stigma [55].

4.2. Serological methods towards standardized diagnosis

Recent diagnostic research attempts to identify specific molecular markers for *M. leprae* and develop a sensitive laboratory test to assist in the diagnosis of asymptomatic patients and progression prediction [50]. Early and adequate treatment plays a crucial role in containing disease transmission [50]. Although clinical and histopathological tests are helpful in the diagnosis of leprosy, they cannot confirm the PB suspected cases[56]. For this reason, the serological tests have presented as a promising alternative to diagnosis [52].

The immunodominant antigen of *M. leprae* more assessed is PGL-1, first described in Brennan & Barrow in 1980 [50,57]. The anti-PGL-1 antibodies indicate the bacillary load and can be helpful in leprosy classification. These antibodies may

also assist in the early identification of the risk of Type 1 reactions occur due to the high levels found in reaction episodes [50]. Anti-PGL-1 may identify the subclinical infection cases, so it can be used to detect susceptibility in close contacts [26,50]. Given the various advantages of using this method, there are significant disadvantages as its limited use in contacts living in endemic areas, as there is no significant difference concerning non-domestic contacts [50]. In addition to its limited use for diagnosing PB patients, this assay is not commercially available [48,52].

Natural disaccharide-octyl (NDO) is a synthetic mimetic of PGL-1, and conjugated with human serum albumin (BSA and HAS) may be an exciting alternative do standardized diagnosis. The single fusion protein Leprosy IDRI Diagnostic (LID)-1 also can be used as a carrier for NDO [48]. The quantification of antibodies against NDO-BSA, LID-1, and NDO-LID by ELISA are possibilities for a standard diagnostic test, with the latter showing more satisfactory results for MB and PB cases in different studies [48,52]. Moreover, the ready-to-use kit NDO-LID® is a low-cost and simplified test; unlike ELISA, it does not require a laboratory setup, being a promising alternative for early and differential leprosy diagnosis [52].

Historically, the inability of *M. leprae* to grow *in vitro* was the main hurdle to new diagnosis method development [58]. Since the bacillus genome was sequenced, it was possible to investigate molecular diagnosis methods [58,59]. In the last two decades, polymerase chain reaction (PCR) methods, through the amplification of *M. leprae* different gene targets, are especially crucial for the differential diagnosis for patients presenting negative bacillary load or non-conclusive histopathology [56,58]. Several genes such as 36-kDa antigen, 18-kDa antigen, 65-kDa antigen, the Ag 85B, 16S rRNA, and the repetitive sequences (RLEP) were studied [58]. This method may allow confirming PB cases, subclinical infection in household contacts, treatment monitoring, and determine the cure or MDT drugs resistance [50]. More recently, since 2011, quantitative PCR (qPCR) assays, using real-time quantitative fluorescence detection, have replaced the conventional PCR technique in several laboratories due to its higher specificity and sensitivity and faster turnaround time [58]. Nevertheless, it requires a well-equipped laboratory with high associated costs [60].

The use of the clinical diagnosis method alone presents several limitations, and, in some cases, the microbiological assessment and histopathology may not be sufficient. Thus, to achieve a differential diagnosis, subclinical case detection, and

early reactions prediction, it is necessary to use more modern and sensitive techniques as serological and molecular methods. The anti-PGL-1 detection and the NDO-LID® kit may be useful for regions with a less developed laboratory structure, ordinarily absent in endemic areas. On the other hand, the qPCR assays show to be more specificity and sensitivity, which would be desirable for the principal diagnosis challenges. However, qPCR assays are costly, limiting its use.

5. Leprosy treatment and efforts to overcome its challenges

5.1. Overview of current treatment

Since 1981, the WHO has recommended multidrug therapy (MDT) regimens to minimize resistance to the single drugs themselves used as monotherapy [61]. MDT consists of dapsone, rifampicin, and clofazimine, with a different duration between clinical classifications [62]. The inclusion of clofazimine in PB treatment occurred in 2018 by the WHO, and it is still the subject of considerable discussion among clinicians [63]. This measure was precisely taken to reduce the impact of misdiagnosis [62]. MDT posology is shown in Table 1.

Table 1. Doses of MDT medications and treatment duration (for adults), recommended by the WHO, according to clinical classification.

Classification	Drug substance (mg)			Duration (months)
	Dapsone (daily)	Rifampicin (monthly)	Clofazimine (daily/ monthly)	
Multibacillary	100	600	50/300	12
Paucibacillary	100	600	50/300	6

Source: Adapted from [63]

The three drugs that compose MDT treatment present complementary therapeutic targets, as represented in Figure 2.

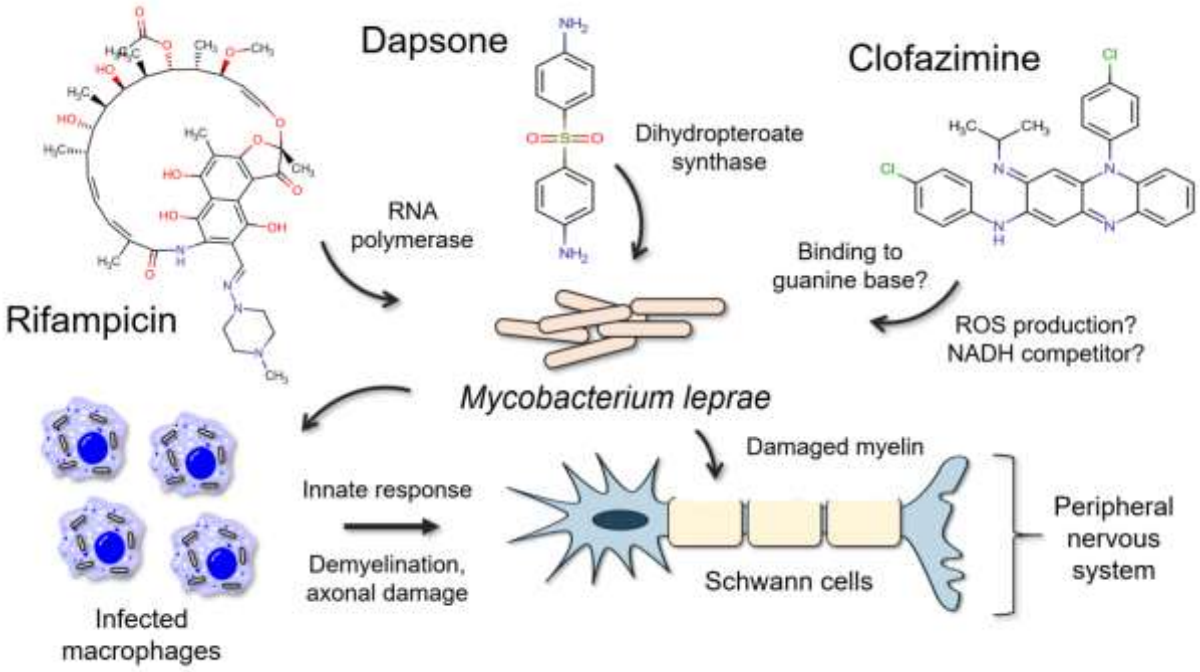

Figure 2. Drugs used against *M. leprae* and respective therapeutic targets. *M. leprae* attacks Schwann cells, which causes damage to myelin in the peripheral nervous system. This damage results in thermal and touch sensory sensitivity impairment. Early innate response from infected macrophages might cause demyelination and axonal damage. The mechanism might be due to reactive nitrogen species production. Rifampicin is a substrate to RNA polymerase, blocking bacterial protein synthesis. Dapsone is analog of para-aminobenzoic acid, acting as a substrate to dihydropteroate synthase, resulting in folic acid production inhibition and DNA synthesis. The mechanism of clofazimine is still unknown. This drug might act directly on the DNA by ROS production or binding to guanine bases. CFZ also might act as a competitive substrate of NADH, impairing ATP production. Molecular structures obtained from Chemicalize.com.

Dapsone (DAP, $C_{12}H_{12}N_2O_2S$) is a structural analog of para-aminobenzoic acid (PABA) presenting bacteriostatic action [64,65]. It acts as a competitive inhibitor of dihydropteroate synthase enzyme (DHPS), decreasing or blocking bacterial folic acid synthesis [64]. DAP also has anti-inflammatory, antibacterial, antiprotozoal, and antifungal activities [66]. DAP can be indicated for the treatment of malaria, rheumatoid arthritis, granuloma annulare, dermatitis herpetiformis, and other vesiculobullous diseases [66].

Rifampicin (RIF, $C_{43}H_{58}N_4O_{12}$) is a semi-synthetic derivative of rifamycin B and shows bactericidal action [67]. It is a macrocyclic antibiotic used mainly against mycobacterial infections (e.g., tuberculosis and leprosy) and a wide range of Gram-positive and Gram-negative bacteria [68]. RIF acts forming a stable drug-enzyme complex with RNA polymerase enzyme, suppressing chain formation during the bacteria's RNA synthesis, leading to cell death [67,69]. This drug plays a crucial role in leprosy treatment because it renders the majority of bacilli non-viable within a few

days of treatment, even though it may fail in some cases [70]. This failure is commonly associated with drug resistance or recurrence [70]. The elimination of these bacilli is expected through the combination of clofazimine/dapsone in a few months [71].

Clofazimine (CFZ, $C_{27}H_{22}Cl_2N_4$) is a phenazine derivative, active in *M. leprae* dapsone-resistant cases, working slowly on bacillus and destroying 99% of them in approximately five months [70]. CFZ is a repository drug, thus continuing to be stored in the body after administration and slowly excreted [71]. This feature explains the additional administration of CFZ monthly dose to ensure optimal concentration maintenance in case of a daily missed dose [71]. Additionally, CFZ has critical anti-inflammatory activity, being used in leprosy reactions to manage the corticosteroid doses [53,70]. The CFZ exact mechanism of action is not entirely understood, but it probably acts in different targets [72]. Mirnejad and colleagues summarize some of them. CFZ starts acting in the outer membrane, through the inhibition of respiratory bacillus chain and ion transporters. The CFZ self-oxidizes instead of NADH, causing the reduction of ATP for cellular processes. Additionally, CFZ may bind to bacterial DNA guanine selectively, and its redox potential may lead to reactive oxygen species generation [72].

These three MDT drugs are classified as Class II drug substances, according to Biopharmaceutics Classification System (BCS), presenting low solubility in water and high permeability, impairing its bioavailability [15–17]. This feature is the limiting factor for oral drug absorption and may aggravate the occurrence of adverse effects, increases resistance development, finally resulting in treatment abandonment.

Despite the solubility challenge, the MDT still faces the emergence of resistance in some patients. For DAP, 55% of monitored patients developed resistance in research in Malaysia [73]. Point mutations in codon 55 and 53 from the *folp1 M. leprae* gene encode DHPS are responsible for that [65]. It is currently possible to test the drug susceptibility in a rapid DNA-based PCR direct sequencing method [74], which represents a significant advance to avoid relapses in leprosy treatment. Similarly, the *rpoB* gene, which encodes the β subunit of the RNA polymerase, is responsible for the bacterial mutation in RIF resistance cases [35]. Furthermore, the percentage of rifampicin resistance reported differs, but it is less than 5% [73,75]. Assuming that the rifampicin resistance rate in the non-compliant patient was 89%, treatment compliance seems to be related to and the occurrence of RIF resistance [76]. Unlike the previous two drugs, resistance is less critical for CFZ, being observed in only 0.2% of patients [73]. Bacillus survival may be due to the several mechanisms of action attributed to CFZ [77].

In contrast, adverse effects are predominantly common for CFZ. A reddish-brown skin discoloration, which is common when using iminophenazine dye, is manifested in 75-100% of patients [70,77]. Even after completing the treatment, the altered skin may take over three years to return to its healthy appearance. Ichthyosis and dryness are less prevalent, and erythroderma, acneiform eruptions, monilial cheilosis, subacute intestinal obstruction, corneal xerosis, and Bull's-eye retinopathy are rare [77]. Patients under DAP treatment can present skin hyperpigmentation,

hemolytic anemia, methemoglobinemia, hepatotoxicity, peripheral neuropathy, and rarely agranulocytosis and toxic epidermal necrolysis [69,78]. DAP-related adverse severe effects are Steven-Johnson syndrome, toxic epidermal necrolysis, or dapsone hypersensitivity syndrome [78]. DAP may induce a dose-dependent reaction, in which its metabolites produce ROS that will cause hemolysis [79]. Like the other drug formulations, adverse effects may be observed for RIF, limiting its use and provoking abandoning treatment before its completion [64]. Hepatotoxicity, thrombocytopenia, orange discoloration (of sweat, saliva, urine, feces, and tears), rash, adrenal insufficiency, and pseudo-influenza syndrome are more commonly related [64,80]. Rarely related are shocks, respiratory insufficiency, and renal failure [64]. Despite the occurrence of serious adverse effects such as those described, the addition of CFZ to the PB treatment to reverse a possible misdiagnosis may be questionable and may act oppositely, causing the treatment dropout by the patient.

5.2. Innovative *pharmaceutical strategies*

Adequate therapy ensures interruption of bacillus transmission, and treatment completion reduces motor and neurological impairment. However, treatment dropout is typical for leprosy due to severe and frequent adverse effects and drug resistance occurrence [61,64]. The most significant hurdle in the pharmaceutical area is to improve leprosy treatment without investing a considerable amount of resources, making the access unfeasible.

An attractive and less costly strategy to overcome the treatment challenges is the repurposing of drugs. Thalidomide is one of the best cases of successful repurposing project. It was initially used as a sedative, followed by a withdrawal from the market due to the severe teratogenic effects caused, and subsequently in 1998 was approved to treat ENL, an aggravating reaction of leprosy [81]. Thalidomide severe adverse effects related, even worse than those that can occur with MDT drugs, may difficult its uses. Moreover, unfortunately, since the thalidomide, no drug repositioning study has been underscored for the leprosy treatment.

Accordingly, the therapeutic efficacy improvement of MDT drugs already used may contribute to treatment compliance. Nanostructured systems have been developed aiming at a modified drug release profile, as in the case of RIF solid lipid nanoparticle (RIF-SLN) and polymeric nanoparticles of CFZ and DAP [82,83]. These nanoparticles provided a controlled release for both drugs (82% for DAP and 68% for CFZ, after 24h, compared to nearly 100% for both free drugs, after 4h) and no sign of cytotoxicity *in vitro* for intravenous administration route [83]. RIF-SLN showed an extended and triphasic release behavior, achieving 70% after nine days, compared to more than 90% of free RIF in 24h. SLN presented no toxicity in rats for the oral administration route, and the product plasma levels were 8.16 times higher than free RIF, reinforcing its efficacy [82].

The sustained release promoted by these nanostructured systems may reduce the adverse effects of MDT drugs and overcome the resistance occurrence [84,85]. In general, SLNs present an additional advantage compared to polymeric

nanoparticles, since its lipid matrix is composed of physiologically tolerated lipid components, decreasing the potential toxicity of adjuvants [86]. The drugs sustained drug circulation time may even result in lower doses and frequency of administration [85], which would further minimize the adverse effects and resistance associated with them. All the mentioned benefits, such as reduction of dose and interval between them, adverse effects, and resistance, can increase patient adherence to treatment and allow the decreased transmission of the bacillus.

6. Final considerations

Despite being an ancient disease, leprosy eradication is still a challenge for some countries, mainly due to the difficulties related to correct diagnosis and treatment conclusion. Proper diagnosis allows for adequate treatment, avoiding insufficient therapy, overtreatment, and bacillus resistance. The clinical diagnosis, currently recommended, is subjective and prone to mistakes. The microbiological and histological may not be sufficient to differentiate the disease forms. Therefore, the development of standardized and affordable laboratory tests, such as serological ones, may enable the correct diagnosis and classification of patients. As for the therapy, MDT has been used for decades; however, their limited bioavailability, the occurrence of serious adverse effects, and bacterial resistance remain to be addressed. Accordingly, nano-based drug delivery systems may offer promising alternatives to conventional therapy. This strategy aimed to overcome poor-water solubility of drug substances, through the sustained release of MDT drugs (dapsone, rifampicin, and clofazimine). The plasma concentration enhancement may reduce the dose administered to the patient and the interval between them, possibly minimizing their severe adverse effects and decreasing bacillus resistance. The achievement of these goals might improve patient compliance, minimizing the bacillus spread by untreated patients, bringing global leprosy elimination closer.

Acknowledgements: The authors thank Jim Hesson of Academic English Solutions for the English language editing services of this manuscript (https://www.academicenglishsolutions.com).

References

1. Schneider PB, Freitas BHBM de. Tendência da hanseníase em menores de 15 anos no Brasil, 2001-2016. Cad Saude Publica. 2018 Mar 12;34(3).

2. Tiwari V, Malhotra K, Khan K, Maurya PK, Singh AK, Thacker AK, et al. Evaluation of polymerase chain reaction in nerve biopsy specimens of patients with Hansen's disease. J Neurol Sci. 2017;380:187–90. Available from: http://dx.doi.org/10.1016/j.jns.2017.07.038

3. Britton WJ, Lockwood DN. Leprosy. Lancet. 2004 Apr;363(9416):1209–19. Available from: https://linkinghub.elsevier.com/retrieve/pii/S0140673604159527

4. Cunha C, Pedrosa VL, Dias LC, Braga A, Chrusciak-Talhari A, Santos M, et al. A historical overview of leprosy epidemiology and control activities in amazonas, brazil. Rev Soc Bras Med Trop. 2015;48(September 2014):55–62.

5. Mane Abhay B. Leprosy on the rise in India: need to adopt enhanced strategy for its control. Prim Heal Care Open Access. 2014;04(1):1–2.

6. WHO. Weekly epidemiological record - Global leprosy update, 2018: moving towards a leprosy-free world. 2019. Available from: http://www.who.int/wer

7. Rosa PS, Espindula HRSD, Melo ACL, Fontes ANB, Amanda J, Belone AFF, et al. Emergence and transmission of drug / multidrug-resistant Mycobacterium leprae in a former leprosy colony in the Brazilian Amazon © The Author (s) 2019 . Published by Oxford University Press for the Infectious Diseases Society of America . This is an Ope. 2019;

8. WHO. Global Leprosy Strategy 2016-2020: accelerating towards a leprosy-free world. Vol. 1, Weekly Epidemiological record. 2016. Available from: http://apps.who.int/iris/bitstream/10665/205149/1/B5233.pdf?ua=1

9. de Souza EA, Ferreira AF, Boigny RN, Alencar CH, Heukelbach J, Martins-Melo FR, et al. Leprosy and gender in Brazil: Trends in an endemic area of the Northeast region, 2001-2014. Rev Saude Publica. 2018;52.

10. World Health Organization. Who Expert Committee on Leprosy. World Health Organization - Technical Report Series. Geneva; 1998. Available from: https://apps.who.int/iris/handle/10665/42060

11. Gupte MD, Anantharaman DS, Nagaraju B, Kannan S, Vallishayee RS. Experiences with Mycobacterium leprae soluble antigens in a leprosy endemic population. Lepr Rev. 1990;61(2):132–44.

12. Yan W, Xing Y, Yuan LC, De Yang R, Yue Tan F, Zhang Y, et al. Application of RLEP real-time PCR for detection of m. leprae DNA in paraffin-embedded skin biopsy specimens for diagnosis of paucibacillary leprosy. Am J Trop Med Hyg. 2014;90(3):524–9.

13. Pardillo FEF, Fajardo TT, Abalos RM, Scollard D, Gelber RH. Methods for the Classification of Leprosy for Treatment Purposes. Clin Infect Dis. 2007;44(8):1096–9.

14. Yawalkar SJ. Leprosy for Medical Practitioners and Paramedical Workers. Vol. 8, JAMA: The Journal of the American Medical Association. American Medical Association (AMA); 2009 Nov.

15. LINDERSTRØM-LANG C, NAYLOR R. 4,4′-Diaminodiphenyl sulphone: solubility and distribution in blood. Biochem J. 1962 Aug 10;83(3):417–20.

16. Agrawal S, Panchagnula R. Implication of biopharmaceutics and pharmacokinetics of rifampicin in variable bioavailability from solid oral dosage form. Biopharm Drug Dispos. 2005;26(8):321–34.

17. Bolla G, Nangia A. Clofazimine mesylate: A high solubility stable salt. Cryst Growth Des. 2012;12(12):6250–9.

18. Goldman P. Effect of bioavailability on Dose-Response relationships. Am J Med. 1984;77(5 SUPPL. 1):47–51.

19. Girão RJS, Soares NLR, Pinheiro JV, Oliveira GDP, De Carvalho SMF, De Abreu LC, et al. Leprosy treatment dropout: A sistematic review. Int Arch Med. 2013;6(1):1–9.

20. Honrado ER, Tallo V, Balis AC, Chan GP, Cho SN. Noncompliance with the World Health Organization-Multidrug Therapy Among Leprosy Patients in Cebu, Philippines: Its Causes and Implications on the Leprosy Control Program. Dermatol Clin. 2008;26(2):221–9.

21. Kaimal S, Thappa D. Relapse in leprosy. Indian J Dermatol Venereol Leprol. 2009;75(2):126–35.

22. Cardona-Pemberthy V, Rendón M, Beltrán JC, Soto-Ospina A, Muñoz-Gomez A, Araque-Marín P, et al. Genetic variants, structural, and functional changes of Myelin Protein Zero and Mannose-Binding Lectin 2 protein involved in immune response and its allelic transmission in families of patients with leprosy in Colombia. Infect Genet Evol. 2018 Jul 1;61:215–23.

23. Han XY, Seo YH, Sizer KC, Schoberle T, May GS, Spencer JS, et al. A new Mycobacterium species causing diffuse lepromatous leprosy. Am J Clin Pathol. 2008;130(6):856–64.

24. Mohanty PS, Bansal AK, Naaz F, Arora M, Gupta UD, Gupta P, et al. Multiple strain infection of Mycobacterium leprae in a family having 4 patients: A study employing short tandem repeats. PLoS One. 2019 Apr 1;14(4).

25. Blok DJ, de Vlas SJ, Geluk A, Richardus JH. Minimum requirements and optimal testing strategies of a diagnostic test for leprosy as a tool towards zero transmission: A modeling study. Yang R, editor. PLoS Negl Trop Dis. 2018 May 25;12(5):e0006529. Available from: https://dx.plos.org/10.1371/journal.pntd.0006529

26. Palit A, Kar HK. Prevention of transmission of leprosy: The current scenario. Indian J Dermatol Venereol Leprol. 2020;86(2):115–23.

27. Medley GF, Blok DJ, Crump RE, Hollingsworth TD, Galvani AP, Ndeffo-Mbah ML, et al. Policy lessons from quantitative modeling of leprosy. Clin Infect Dis. 2018 Jun 1;66:S281–5.

28. Mattos KA, Lara FA, Oliveira VGC, Rodrigues LS, D'Avila H, Melo RCN, et al. Modulation of lipid droplets by Mycobacterium leprae in Schwann cells: A putative mechanism for host lipid acquisition and bacterial survival in phagosomes. Cell Microbiol. 2011;13(2):259–73.

29. Silva CAM, Belisle JT. Host lipid mediators in leprosy: The hypothesized contributions to pathogenesis. Front Immunol. 2018;9(FEB).

30. Mattos KA, D'Avila H, Rodrigues LS, Oliveira VGC, Sarno EN, Atella GC, et al. Lipid droplet formation in leprosy: Toll-like receptor-regulated organelles involved in eicosanoid formation and Mycobacterium leprae pathogenesis. J Leukoc Biol. 2010;87(3):371–84.

31. de Macedo CS, Lara FA, Pinheiro RO, Schmitz V, de Berrêdo-Pinho M, Pereira GM, et al. New insights into the pathogenesis of leprosy: Contribution of subversion of host cell metabolism to bacterial persistence, disease progression, and transmission. F1000Research. 2020;9.

32. Geluk A. Correlates of immune exacerbations in leprosy. Vol. 39, Seminars in Immunology. Academic Press; 2018. p. 111–8.

33. Madigan CA, Cambier CJ, Kelly-Scumpia KM, Scumpia PO, Cheng TY, Zailaa J, et al. A Macrophage Response to Mycobacterium leprae Phenolic Glycolipid Initiates Nerve Damage in Leprosy. Cell. 2017 Aug 24;170(5):973-985.e10.

34. Antonio J, Quaresma S. Leprosy As a Complex infection : Breakdown of the Th1 and Th2 immune Paradigm in the immunopathogenesis of the Disease. Front Immunol |. 2017;8(November):18–21.

35. Reibel F, Cambau E, Aubry A. Update on the epidemiology, diagnosis, and treatment of leprosy. Vol. 45, Medecine et Maladies Infectieuses. Elsevier Masson SAS; 2015. p. 383–93.

36. Fabel A, Maria A, Brunasso G, Schettini AP, Cota C, Puntoni M, et al. Pathogenesis of Leprosy : An Insight Into B Lymphocytes and Plasma Cells. Am J Dermatopathol. 2019;41(6):422–7.

37. Fachin LRV, Soares CT, Belone A de FF, Trombone APF, Rosa PS, Guidella CC, et al. Immunohistochemical assessment of cell populations in leprosy-spectrum lesions and reactional forms. Histol Histopathol. 2017;32(4):385–96.

38. De Sousa JR, Pagliari C, De Almeida DSM, Barros LFL, Carneiro FRO, Dias LB, et al. Th9 cytokines response and its possible implications in the immunopathogenesis of leprosy. J Clin Pathol. 2017 Jun 1;70(6):521–7.

39. Ridley, D S ; Jopling WH. Classification of Leprosy According to Immunity. Int J o Lepr. 1966;34(3):255–73. Available from: http://www.ncbi.nlm.nih.gov/pubmed/5950347

40. Legua P. Leprosy. Int J Infect Dis. 2018 Aug;73(2018):66. Available from: http://dx.doi.org/10.1016/j.ijid.2018.04.3573

41. World Health Organization. Chemotherapy of Leprosy. WHO Tech. Rep. Ser. Geneva; 1994. Available from: https://www.who.int/lep/resources/Chemotherapy.pdf

42. Moura RS de, Calado KL, Oliveira MLW, Bührer-Sékula S. Leprosy serology using PGL-I: a systematic review. Rev Soc Bras Med Trop. 2008;41 Suppl 2:11–8. Available from: http://www.ncbi.nlm.nih.gov/pubmed/19618069

43. Rodrigues Júnior IA, Gresta LT, Noviello M de LM, Cartelle CT, Lyon S, Arantes RME. Leprosy classification methods: A comparative study in a referral center in Brazil. Int J Infect Dis. 2016 Apr 1;45:118–22.

44. Walker SL, Lockwood DNJ. Leprosy. Clin Dermatol. 2007 Mar 6;25(2):165–72. Available from: https://linkinghub.elsevier.com/retrieve/pii/S0738081X06000666

45. Rao Pn, Suneetha S. Current situation of leprosy in India and its future implications. Indian Dermatol Online J. 2018;9(2):83. Available from: http://www.idoj.in/text.asp?2018/9/2/83/227794

46. Lastória JC, de Abreu MAMM. Leprosy: Review of the epidemiological, clinical, and etiopathogenic aspects - Part 1. An Bras Dermatol. 2014;89(2):205–18.

47. Dasananjali K, Schreuder PAM, Pirayavaraporn C. A Study on the Effectiveness and Safety of the WHO/MDT Regimen in the Northeast of Thailand; A Prospective Study, 1984-1996. Int J Lepr Other Mycobact Dis. 1997;65(1):28–36.

48. Jian L, Xiujian S, Yuangang Y, Yan X, Lianchao Y, Duthie MS, et al. Evaluation of antibody detection against the NDO-BSA, LID-1 and NDO-LID antigens as confirmatory tests to support the diagnosis of leprosy in Yunnan province, southwest China. Trans R Soc Trop Med Hyg. 2020;114(3):193–9.

49. Ministério da Saúde. Diretrizes para vigilância, atenção e eliminação da hanseníase como problema de saúde pública 2016. Brasília: MINISTÉRIO DA SAÚDE; 2016. 58 p. Available from: http://editora.saude.gov.br

50. Lastória JC, de Abreu MAMM. Leprosy: A review of laboratory and therapeutic aspects - Part 2. An Bras Dermatol. 2014;89(3):389–401.

51. Fava VM, Dallmann-Sauer M, Schurr E. Genetics of leprosy: today and beyond. Hum Genet. 2019;(0123456789). Available from:

https://doi.org/10.1007/s00439-019-02087-5

52. Devides AC, Rosa PS, de Faria Fernandes Belone A, Coelho NMB, Ura S, Silva EA. Can anti–PGL-1 and anti–NDO-LID-1 antibody titers be used to predict the risk of reactions in leprosy patients? Diagn Microbiol Infect Dis. 2018 Jul 1;91(3):260–5.

53. Eichelmann K, González González SE, Salas-Alanis JC, Ocampo-Candiani J. Leprosy. An Update: Definition, Pathogenesis, Classification, Diagnosis, and Treatment. Actas Dermo-Sifiliográficas (English Ed. 2013 Sep;104(7):554–63. Available from: https://linkinghub.elsevier.com/retrieve/pii/S1578219013001431

54. Balagon MVF, Gelber RH, Abalos RM, Cellona R V. Reactions following completion of 1 and 2 year multidrug therapy (MDT). Am J Trop Med Hyg. 2010;83(3):637–44.

55. Lockwood DNJ. Chronic aspects of leprosy-neglected but important. Trans R Soc Trop Med Hyg. 2019;113(12):812–6.

56. Barbieri RR, Manta FSN, Moreira SJM, Sales AM, Nery JAC, Nascimento LPR, et al. Quantitative polymerase chain reaction in paucibacillary leprosy diagnosis: A follow-up study. PLoS Negl Trop Dis. 2019 Mar 1;13(3):1–12.

57. Brennan PJ, Barrow WW. Evidence for species-specific lipid antigens in Mycobacterium leprae. Int J Lepr. 1980;48(4):382–7.

58. Ribeiro-alves M, Sarno EN, Ozo M. Evaluation of qPCR-Based Assays for Leprosy Diagnosis Directly in Clinical Specimens. PLoS Negl Trop Dis. 2011;5(10):1–8.

59. Garnier T, Churcher C, Harris D, Cole ST, Eiglmeier K, Parkhill J, et al. Massive gene decay in the leprosy bacillus. Nature. 2001;409:1007–11.

60. Soto A, Torres Muñoz P. Leprosy Diagnosis: An Update on the Use of Molecular Tools Lucrecia. Mol Biol. 2015;04(04).

61. Cambau E, Perani E, Guillemin I, Jamet P, Ji B. Multidrug-resistance to dapsone, rifampicin, and ofloxacin in Mycobacterium leprae. Lancet. 1997 Jan;349(9045):103–4. Available from: https://linkinghub.elsevier.com/retrieve/pii/S0140673605608884

62. World Health Organization. Guidelines for the Diagnosis, Treatment and Prevention of Leprosy Report of the literature review ii. 2018; Available from: https://apps.who.int/iris/handle/10665/274127

63. Alemu Belachew W, Naafs B. Position statement: LEPROSY: Diagnosis, treatment and follow-up. J Eur Acad Dermatology Venereol. 2019;33(7):1205–13.

64. Goulart IMB, Arbex GL, Carneiro MH, Rodrigues MS, Gadia R. Efeitos adversos da poliquimioterapia em pacientes com hanseníase: um levantamento de cinco anos em um Centro de Saúde da Universidade Federal de Uberlândia. Rev Soc Bras Med Trop. 2005 Apr 26;35(5):453–60.

65. Kai M, Matsuoka M, Nakata N, Maeda S, Gidoh M, Maeda Y, et al. Diaminodiphenylsulfone resistance of Mycobacterium leprae due to mutations in the dihydropteroate synthase gene. FEMS Microbiol Lett. 1999 Aug 15;177(2):231–5.

66. Fernandes TRM de O, De Jesus BN, Barreto TT, Pereira A de A. Dapsone-induced agranulocytosis in patients with Hansen's disease. Vol. 92, Anais Brasileiros de Dermatologia. Sociedade Brasileira de Dermatologia; 2017. p. 894–7.

67. Angiolini L, Agnes M, Cohen B, Yannakopoulou K, Douhal A. Formation, characterization and pH dependence of rifampicin: heptakis(2,6-di-O-methyl)-β-cyclodextrin complexes. Int J Pharm. 2017;531(2):668–75. Available from: http://dx.doi.org/10.1016/j.ijpharm.2017.06.015

68. Angiolini L, Cohen B, Douhal A. Ultrafast dynamics of the antibiotic Rifampicin in solution. Photochem Photobiol Sci. 2019;18(1):80–91.

69. Guragain S, Upadhayay N, Bhattarai BM. Adverse reactions in leprosy patients who underwent dapsone multidrug therapy: A retrospective study. Clin Pharmacol Adv Appl. 2017 Jun 29;9:73–8.

70. Cruz RC da S, Penna MLF, Talhari S, Bührer-Sékula S, Penna GO. Leprosy: Current situation, clinical and laboratory aspects, treatment history and perspective of the uniform multidrug therapy for all patients. An Bras Dermatol. 2017 Nov 1;92(6):761–73.

71. World Health Organization. The final push strategy to eliminate leprosy as a public health problem: questions and answers. Vol. 73, WHO. 2003. Available from: https://apps.who.int/iris/handle/10665/63271

72. Mirnejad R, Asadi A, Khoshnood S, Mirzaei H, Heidary M, Fattorini L, et al. Clofazimine: A useful antibiotic for drug-resistant tuberculosis. Biomed Pharmacother. 2018 Sep 1;105:1353–9.

73. Dalawi I, Tang MM, Osman AS, Ismail M, Abu Bakar RS, Dony JF, et al. Drug resistance pattern of Mycobacterium leprae from mouse footpad cultivation between 1997 to 2013 in Malaysia. Lepr Rev. 2017;88(4):463–77. Available from: https://www.scopus.com/inward/record.uri?eid=2-s2.0-85044312433&partnerID=40&md5=a85fa5433b73163c631ee7c687fc20f4

74. PVS P. Recent Advances in Diagnostic Techniques and New Hope towards

Leprosy Elimination in the Post Elimination Era. Clin Dermatology Ther. 2016 Jun 4;4(1):1–8. Available from: http://www.heraldopenaccess.us/fulltext/Clinical-Dermatology-&-Therapy/Recent-Advances-in-Diagnostic-Techniques-and-New-Hope-towards-Leprosy-Elimination-in-the-Post-Elimination-Era.php

75. Cambau E, Saunderson P, Matsuoka M, Cole ST, Kai M, Suffys P, et al. Antimicrobial resistance in leprosy: results of the first prospective open survey conducted by a WHO surveillance network for the period 2009–15. Clin Microbiol Infect. 2018 Dec 1;24(12):1305–10.

76. Siskawati Y, Effendi EH, Legiawati L, Menaldi SL. Poor treatment compliance leads to a higher mutation for rifampicin resistance in multibacillary leprosy patients. Med J Indones. 2018 Dec 31;27(4):237.

77. Kar HK, Gupta R. Treatment of leprosy. Clin Dermatol. 2015 Jan 1;33(1):55–65.

78. Bhengra MP, Kumar P, Sundar Chaudhary S. An unusual case of dapsone hypersensitivity syndrome in a leprosy patient. Vol. 26, Journal of Pakistan Association of Dermatologists. 2016.

79. Reilly TP, Woster PM, Svensson CK. Methemoglobin formation by hydroxylamine metabolites of sulfamethoxazole and dapsone: implications for differences in adverse drug reactions. J Pharmacol Exp Ther. 1999;288(3):951–9. Available from: http://www.ncbi.nlm.nih.gov/pubmed/10027831

80. Howard P, Twycross R, Grove G, Charlesworth S, Mihalyo M, Wilcock A. Rifampin (INN Rifampicin). Vol. 50, Journal of Pain and Symptom Management. Elsevier Inc.; 2015. p. 891–5.

81. Jourdan JP, Bureau R, Rochais C, Dallemagne P. Drug repositioning: a brief overview. J Pharm Pharmacol. 2020;1–7.

82. Singh H, Jindal S, Singh M, Sharma G, Kaur IP. Nano-formulation of rifampicin with enhanced bioavailability: Development, characterization and in-vivo safety. Int J Pharm. 2015 May 15;485(1–2):138–51.

83. Li HZ, Ma SH, Zhang HM, Liu JM, Wu YX, Cao PQ, et al. Nano carrier mediated co-delivery of dapsone and clofazimine for improved therapeutic efficacy against tuberculosis in rats. Biomed Res. 2017;28(3):1284–9.

84. Huang G, Zhang N, Bi X, Dou M. Solid lipid nanoparticles of temozolomide: Potential reduction of cardial and nephric toxicity. Int J Pharm. 2008;355(1–2):314–20.

85. Huh AJ, Kwon YJ. “Nanoantibiotics”: A new paradigm for treating infectious

diseases using nanomaterials in the antibiotics resistant era. J Control Release. 2011;156(2):128–45. Available from: http://dx.doi.org/10.1016/j.jconrel.2011.07.002

86. Pushpendra J, Amit M, K. Y, K. P, S. B. Formulation Development and Characterization of Solid Lipid Nanoparticles Containing Nimesulide. Int J Drug Deliv Technol. 2009;1(1):24–7.

4. APPENDIX B: Innovative drug delivery systems for leprosy treatment

Introduction

Leprosy is one of the oldest human epidemic diseases and is still endemic in some world regions.[1,2] The last WHO report, from 2018, counted 208,641 new cases globally, with India, Brazil, and Indonesia concentrating 166,011, approximately 80% of the cases.[2] Dapsone (DAP), rifampicin (RIF), and clofazimine (CFZ) compose the Multidrug Therapy (MDT), which on implementation in the 1980s was responsible for the reduction of leprosy new cases.[3-5] According to the diagnosis and classification of the disease, the treatment duration varies from 6 to 12 months.[6]

Low adherence to therapy is one of the main hurdles to leprosy elimination since the disease requires prolonged treatment.[7] A complex interaction of factors such as socioeconomic condition, inadequate health care services, and MDT drugs is associated with poor adherence.[7] Among the factors associated with MDT drugs are the resistance and adverse effects occurrence.[8-10] The first extensive study from the endemic countries revealed that 8.0% of *M. leprae* strains presented mutations, resulting in MDT resistance.[9] In contrast, a comprehensive study of drugs adverse effects has not been conducted yet. However, a retrospective study conducted in a Brazilian state revealed 37.9% of patients manifesting at least one adverse effect MDT-related.[11]

An alternative treatment to WHO-MDT consists of rifampicin, ofloxacin (OFL), and minocycline (MINO), known as ROM. This MDT substitute is based on the bactericidal/bacteriostatic activity of both drugs, OFL and MINO.[12] Although the resistance rate of ofloxacin (1.3%) is relevant, ROM-drugs usually present mild adverse effects.[9,13]

In common, most drugs used for the treatment of leprosy presents low water solubility, which limits their bioavailability.[14–16] Accordingly, the administration of high doses required for reaching therapeutic blood levels aggravates adverse effects. Additionally, drugs poor water solubility may trigger high variability in the serum drug concentration, increasing the likelihood of bacterial resistance.[17–19] Also, RIF and CFZ bioavailability may be limited, respectively, by stomach degradation and recrystallization depending on pH.[11,20,21] Unlike the other drugs, MINO presents high water solubility, being the intestinal permeability its limitation.[22]

Aiming to address these problems, new formulations have been proposed for leprosy therapy. This article is an effort to highlight the most recent advances in drug delivery systems to overcome the hurdles related to low MDT adherence.

Innovative pharmaceutical strategies towards enhancement of therapeutic efficacy

Recent advances in drug delivery systems may overcome solubility impairment, common in pharmaceutical development.[23] The oral formulations proposed for MDT drugs focused on two main strategies: increasing the apparent drug water solubility or modifying the drug release.

Figure 1 summarizes the improvements and the expected results of MDT innovative formulations. *In vitro* evaluation, *in vivo, and in silico* performances of these preparations are provided in Table S1 (supplemental material), if available, showing their potential therapeutic efficacy. As the following steps, well-established clinical tests will play a key role in ensuring their relevance for patients. Aiming to reach the market, a collaborative effort between government and private companies is essential.

- Drug water solubility enhancement

For DAP, innovative formulations obtained through the synthesis of chemical derivatives of DAP (salt and cocrystal) and solid dispersion were proposed aiming at water solubility enhancement.[24–26] For example, the solid dispersion provided a solubility of more than 7.5-fold compared to free DAP.[24] This improvement may lead to dose reduction.

The RIF solubility improvement was achieved through its nanocrystals, solid dispersion, vesicle systems (liposphere, niosome, and liposome), and complex preparations.[20,27–33] RIF nanocrystals enable a formulation containing a 2-fold increase of drug concentration. This innovative preparation leads to an administration of half of the dose.[27] Apart from dose reduction, nanocrystals allow an increase in intestine cells permeation due to their characteristic of adherence enhancement.[27] RIF absorption may be reduced in half by food, which may also be mitigated by nanocrystals.[27,34]

CFZ innovative preparations include synthetic chemical derivatives of CFZ (salt and complex) and nanotechnology-based delivery (nanoparticle and nanoporous silica particle).[35–38] Amongst them, nanoporous silica particles increased the drug solubility in water and the permeability of intestinal cells, respectively, by

20-fold and 5-fold, both compared to free-drug.[37] These factors can lead to a significant reduction in the dose for the therapeutic efficacy.

The formulations proposed to overcome OFL solubility limitations are cocrystal and cyclodextrin complex.[39,40] Most of them were developed as topical preparations due to their frequent use on ophthalmic diseases. MINO does not present aqueous solubility issues.[22] Instead, strategies for this drug are based on release modifications, aiming to improve its permeability.

- **Modified drug release**

Modified release strategy aims to modulate drug release from the dosage form. For instance, the enteric release is designed to deliver the drug in the intestine, protecting it from gastric pH. The extended release controls the drug delivery immediately following oral administration.[29,30] The enteric release is especially relevant for RIF and CFZ due to their chemical instability in acidic conditions.[41,42]

DAP modified-release was proposed using different strategies such as polymeric nanoparticles, hydrogels, and nanofibers.[43–45] *In vivo* results of polymeric nanoparticles proved that the sustained co-delivery of DAP and CFZ could reduce their doses.[43] For RIF, strategies included nanoparticles (solid lipid, polymeric, and lecithin), complex, and hydrogel beads.[17,18,46-47] A formulation presenting a profile with an initial burst followed by the sustained release is desirable. It was found in over 65% (4 of 6) (Table S1) of proposed RIF studies.[46-49] Also, studies have shown favorable *in vivo* or *in silico* results. Among these, the increase in peak plasma concentration (Cmax) is up to seven times higher than the free drug, [17,18] using the solid lipid nanoparticle strategy.[17] Further, RIF plasma concentration was sustained above the MIC for five days, compared to two days of free drug (Table S1). These notable performances can reduce the dose and the occurrence of adverse effects.[17]

Nano-based drug delivery systems have been approved by regulatory agencies and prescribed in the last decades, reinforcing their efficacy and safety.[50,51] For instance, liposomal amphotericin B (AmBisome®) has been used to treat leishmaniasis successfully.[52] Nevertheless, the particle size and shape can impact the nanoparticle distribution.[53] For example, nanorods may accumulate in organs related to the immune response and blood clearance, namely lymph nodes, spleen, liver, and bone marrow.[54] Consequently, risk assessment and quantification methods

have been increasingly explored aiming to predict nanomedicine effects for patients.[54,55]

CFZ, in turn, can recrystallize outside of a pH range from 2 to 4, which compromises absorption.[56] Polymeric nanoparticles, alginate, pepsin, and mesoporous silica are examples of carriers developed to modify the release of CFZ.[37,42,56-58] Polymeric nanoparticles presented sustained release and lower cellular toxicity in Caco-2 and HT29-MTX cells, compared to the free drug. Accordingly, these studies showed the success of the strategy to avoid CFZ recrystallization.[42]

Strategies for OFL consisted of cellulose conjugate, nanofibers, polymeric complex, and nanoparticles.[59-63] *In vivo* studies using nanofibers showed that the formulation might act as an OFL reservoir, increasing its residence time in the gastrointestinal tract. Besides, an *in vitro* study showed significant mucoadhesion using a strip of rats gastric mucosal membrane and improved efficacy against microorganisms, such as *E. coli, E. faecalis, S. aureus, and P. aeruginosa*. Therefore, these studies represent advances to provide formulations with a better oral absorption profile in leprosy treatment.[60]

Formulations containing MINO were mainly developed for topical application, focused on periodontal diseases. However, the modified release approach might be considered to overcome its permeability issue. Hydrogel, nanoparticles, solid lipid nanoparticles, and polymeric nanoparticles were proposed to achieve this goal.[64-67]

Final considerations

Leprosy elimination involves a series of treatment-related challenges, leading to poor patient adherence. The MDT drugs are distributed free of charge; however, their low water solubility, severe adverse effects, and resistance occurrence still represent obstacles to completing treatment. Aiming to overcome these hurdles, innovative drug delivery systems were proposed in the last years with two main targets: water solubility improvement and sustained drug release. The solubility enhancement may reduce the administered dose to the patient, which may suppress adverse effects occurrence. A modified drug release approach may increase the interval between doses, causing a decline in bacterial resistance and adverse effect occurrence. Both might improve the patient adherence to treatment, diminishing bacillus spread by

untreated patients. A reinvention of leprosy treatment may promote patient healing and interrupt the transmission, two essential goals towards a leprosy free-world.

References:

1. Fischer M. Leprosy – an overview of clinical features, diagnosis, and treatment. *JDDG - J Ger Soc Dermatology*. 2017;15:801-827.

2. WHO. Weekly Epidemiological Record - Global Leprosy Update, 2018: Moving towards a Leprosy-Free World.; 2019.

3. Benjak A, Avanzi C, Singh P, Loiseau C, Girma S, Busso P, et al. Phylogenomics and antimicrobial resistance of the leprosy bacillus Mycobacterium leprae. *Nat Commun*. 2018;9:1-11.

4. Soares LS, Moreira R, Vilela V V., Alves MJ, Pimentel AF, Ferreira AP, et al. The impact of multidrug therapy on the epidemiological pattern of leprosy in Juiz de Fora, Brazil. *Cad saúde pública / Ministério da Saúde, Fundação Oswaldo Cruz, Esc Nac Saúde Pública*. 2000;16:343-350.

5. Ramasoota P, Intaratitaya T. Progress and impact of multidrug therapy (MDT) implementation to leprosy control in Thailand. *Japanese J Lepr*. 1995;64:214-219.

6. Farah Naaz, Partha Sarathi Mohanty, Avi Kumar Bansal, Dilip Kumar UDG. Challenges beyound elimination in leprosy. *Int J Mycobacteriology*. 2017;6:222-228.

7. Heukelbach J, Chichava OA, de Oliveira AR, Häfner K, Walther F, de Alencar CHM, et al. Interruption and defaulting of multidrug therapy against leprosy: Population-based study in Brazil's Savannah region. *PLoS Negl Trop Dis*. 2011;5:4-9.

8. De Andrade KVF, Nery JS, Pescarini JM, Ramond A, de Souza Teles Santos CA, Ichihara MY, et al. Geographic and socioeconomic factors associated with leprosy treatment default: An analysis from the 100 Million Brazilian Cohort. *PLoS Negl Trop Dis*. 2019;13:1-18.

9. Cambau E, Saunderson P, Matsuoka M, Cole ST, Kai M, Suffys P, et al. Antimicrobial resistance in leprosy: results of the first prospective open survey conducted by a WHO surveillance network for the period 2009–15. *Clin Microbiol Infect*. 2018;24:1305-1310.

10. Deps PD, Nasser S, Guerra P, Simon M, Birshner RDC, Rodrigues LC. Adverse effects from multi-drug therapy in leprosy: a Brazilian study. *Lepr Rev*. 2007;78:216-222.

11. Goulart IMB, Arbex GL, Carneiro MH, Rodrigues MS, Gadia R. Efeitos adversos da poliquimioterapia em pacientes com hanseníase: um levantamento de cinco anos em um Centro de Saúde da Universidade Federal de Uberlândia. *Rev Soc Bras Med Trop*. 2005;35:453-460.

12. World Health Organization. WHO model prescribing information : drugs used in leprosy. 1998:1-28.

13. Pai V. Second-line anti-leprosy drugs: Indian experience. *Indian J Drugs Dermatology.* 2020;6(1):1-4.

14. LINDERSTRØM-LANG C, NAYLOR R. 4,4′-Diaminodiphenyl sulphone: solubility and distribution in blood. *Biochem J*. 1962;83:417-420.

15. Agrawal S, Panchagnula R. Implication of biopharmaceutics and pharmacokinetics of rifampicin in variable bioavailability from solid oral dosage form. *Biopharm Drug Dispos*. 2005;26:321-334.

16. Bolla G, Nangia A. Clofazimine mesylate: A high solubility stable salt. *Cryst Growth Des*. 2012;12:6250-6259.

17. Singh H, Jindal S, Singh M, Sharma G, Kaur IP. Nano-formulation of rifampicin with enhanced bioavailability: Development, characterization and in-vivo safety. *Int J Pharm.* 2015;485:138-151.

18. Hussain A, Singh SK, Singh N, Prasad Verma PR. In vitro - In vivo - In silico simulation studies of anti-tubercular drugs doped with a self nanoemulsifying drug delivery system. *RSC Adv*. 2016;6:93147-93161.

19. Monteiro LM, Lione VF, do Carmo FA, do Amaral LH, da Silva JH, Nasciutti LE, et al. Development and characterization of a new oral dapsone nanoemulsion system: permeability and in silico bioavailability studies. *Int J Nanomedicine.* 2012;7:5175-5182.

20. Angiolini L, Agnes M, Cohen B, Yannakopoulou K, Douhal A. Formation, characterization and pH dependence of rifampicin: heptakis(2,6-di-O-methyl)-β-cyclodextrin complexes. *Int J Pharm.* 2017;531:668-675.

21. Bannigan P, Durack E, Mathur H, Rea MC, Ross RP, Hudson SP. Delivery of a hydrophobic drug into the lower gastrointestinal system via an endogenous enzyme-mediated carrier mechanism: An in vitro study. *Eur J Pharm Biopharm*. 2018;133:12-19.

22. Papich MG, Martinez MN. Applying Biopharmaceutical Classification System (BCS) Criteria to Predict Oral Absorption of Drugs in Dogs: Challenges and Pitfalls. *AAPS J.* 2015;17(4):948-964.

23. Rodriguez-Aller M, Guillarme D, Veuthey JL, Gurny R. Strategies for formulating and delivering poorly water-soluble drugs. *J Drug Deliv Sci Technol*. 2015;30:342-351.

24. Chaves LL, Vieira ACC, Ferreira D, Sarmento B, Reis S. Rational and precise development of amorphous polymeric systems with dapsone by response surface methodology. *Int J Biol Macromol*. 2015;81:662-671.

25. Li W, Shi P, Jia L, Zhao Y, Sun B, Zhang M, et al. Eutectics and Salt of Dapsone With Hydroxybenzoic Acids: Binary Phase Diagrams, Characterization and Evaluation. *J Pharm Sci.* 2020;109:2224-2236.

26. Chappa P, Maruthapillai A, Voguri R, Dey A, Ghosal S, Basha MA. Drug-Polymer Co-Crystals of Dapsone and Polyethylene Glycol: An Emerging Subset in Pharmaceutical Cocrystals. *Cryst Growth Des.* 2018;18:7590-7598

27. Melo KJC, Henostroza MAB, Löbenberg R, Bou-Chacra NA. Rifampicin nanocrystals: Towards an innovative approach to treat tuberculosis. *Mater Sci Eng C*. 2020;112:110895.

28. Oh CM, Siow CRS, Heng PWS, Chan LW. Impact of HPMC on the physical properties of spray-congealed PEG microparticles and its swelling effect on rifampicin dissolution. *Drug Dev Ind Pharm*. 2016;42:403-411.

29. Singh C, Koduri LVSK, Bhatt TD, Jhamb SS, Mishra V, Gill MS, et al. In Vitro-In Vivo Evaluation of Novel Co-spray Dried Rifampicin Phospholipid Lipospheres for Oral

Delivery. *AAPS PharmSciTech*. 2017;18:138-146.

30. Khan DH, Bashir S, Figueiredo P, Santos HA, Khan MI, Peltonen L. Process optimization of ecological probe sonication technique for production of rifampicin loaded niosomes. *J Drug Deliv Sci Technol*. 2019;50:27-33.

31. Khan DH, Bashir S, Khan MI, Figueiredo P, Santos HA, Peltonen L. Formulation optimization and in vitro characterization of rifampicin and ceftriaxone dual drug loaded niosomes with high energy probe sonication technique. *J Drug Deliv Sci Technol*. 2020;58:101763.

32. Bapolisi AM, Nkanga CI, Walker RB, Krause RWM. Simultaneous liposomal encapsulation of antibiotics and proteins: Co-loading and characterization of rifampicin and Human Serum Albumin in soy-liposomes. *J Drug Deliv Sci Technol*. 2020;58:101751.

33. Luciani-Giacobbe LC, Ramírez-Rigo M V., Garro-Linck Y, Monti GA, Manzo RH, Olivera ME. Very fast dissolving acid carboxymethylcellulose-rifampicin matrix: Development and solid-state characterization. *Eur J Pharm Sci*. 2017;96:398-410.

34. Howard P, Twycross R, Grove G, Charlesworth S, Mihalyo M, Wilcock A. Rifampin (INN Rifampicin). *J Pain Symptom Manage*. 2015;50:891-895.

35. Sousa ML, Sarraguça MC, Oliveira dos Santos A, Sarraguça JMG, Lopes J, S Ribeiro PR. A new salt of clofazimine to improve leprosy treatment. *J Mol Struct*. 2020;1214.

36. Salim M, Ramirez G, Clulow AJ, Zhang Y, Ristroph KD, Feng J, et al. Solid-State Behavior and Solubilization of Flash Nanoprecipitated Clofazimine Particles during the Dispersion and Digestion of Milk-Based Formulations. *Mol Pharm*. 2019;16:2755-2765.

37. Sabrina V, Xin X, Joana C-G, Priscille B, Marie-Françoise B-C, Margareta A. Clofazimine encapsulation in nanoporous silica particles for the oral treatment of antibiotic-resistant Mycobacterium tuberculosis infections. *Nanomedicine*. 2017;12:831-844.

38. Li S, Chan JYW, Li Y, Bardelang D, Zheng J, Yew WW, et al. Complexation of clofazimine by macrocyclic cucurbit[7]uril reduced its cardiotoxicity without affecting the antimycobacterial efficacy. *Org Biomol Chem*. 2016;14:7563-7569.

39. Suresh A, Gonde S, Mondal PK, Sahoo J, Chopra D. Improving solubility and intrinsic dissolution rate of ofloxacin API through salt formation via mechanochemical synthesis with diphenic acid. *J Mol Struct.* 2020;1221:128806.

40. Misiuk W, Jozefowicz M. Study on a host-guest interaction of hydroxypropyl-β-cyclodextrin with ofloxacin. *J Mol Liq.* 2015;202:101-106.

41. Arca HÇ, Mosquera-Giraldo LI, Pereira JM, Sriranganathan N, Taylor LS, Edgar KJ. Rifampin Stability and Solution Concentration Enhancement Through Amorphous Solid Dispersion in Cellulose ω-Carboxyalkanoate Matrices. *J Pharm Sci.* 2018;107(1):127-138.

42. Chaves LL, Costa Lima SA, Vieira ACC, Barreiros L, Segundo MA, Ferreira D, et al. Development of PLGA nanoparticles loaded with clofazimine for oral delivery: Assessment of formulation variables and intestinal permeability. *Eur J Pharm Sci.* 2018;112:28-37.

43. Li HZ, Ma SH, Zhang HM, Liu JM, Wu YX, Cao PQ, et al. Nano carrier mediated co-

delivery of dapsone and clofazimine for improved therapeutic efficacy against tuberculosis in rats. *Biomed Res.* 2017;28:1284-1289.

44. Chaves LL, Silveri A, Vieira ACC, Ferreira D, Cristiano MC, Paolino D, et al. pH-responsive chitosan based hydrogels affect the release of dapsone: Design, set-up, and physicochemical characterization. *Int J Biol Macromol*. 2019;133:1268-1279.

45. Ranjbar M, Khazaeli P, Pardakhty A, Tahamipour B, Amanatfard A. Preparation of polyacrylamide/polylactic acid co-assembled core/shell nanofibers as designed beads for dapsone in vitro efficient delivery. *Artif Cells, Nanomedicine Biotechnol*. 2019;47:917-926.

46. Chokshi N V., Khatri HN, Patel MM. Formulation, optimization, and characterization of rifampicin-loaded solid lipid nanoparticles for the treatment of tuberculosis. *Drug Dev Ind Pharm*. 2018;44:1975-1989.

47. Rani S, Gothwal A, Pandey PK, et al. HPMA-PLGA Based Nanoparticles for Effective In Vitro Delivery of Rifampicin. *Pharm Res*. 2019;36:1-12.

48. Farnia P, Velayati A, Mollaei S, Ghanavi J. Modified rifampin nanoparticles: Increased solubility with slow release Rate. *Int J Mycobacteriology*. 2017;6:171.

49. Patil JS, Jadhav SM, Mandave SV, Vilegave KV, Dhadde SB. Natural Gellan gum (Phytagel®) based novel hydrogel beads of rifampicin for oral delivery with improved functionality. *Indian J Pharm Educ Res*. 2016;50:S159-S167.

50. Duncan R, Gaspar R. Nanomedicine(s) under the Microscope. Mol Pharm. 2011 Dec 5;8(6):2101-41. Available from: https://pubs.acs.org/doi/10.1021/mp200394t

51. Foulkes R, Man E, Thind J, Yeung S, Joy A, Hoskins C. The regulation of nanomaterials and nanomedicines for clinical application: Current and future perspectives. Biomater Sci. 2020;8(17):4653-64.

52. Balasegaram M, Ritmeijer K, Lima MA, Burza S, Ortiz Genovese G, Milani B, et al. Liposomal amphotericin B as a treatment for human leishmaniasis. Expert Opin Emerg Drugs. 2012;17(4):493-510.

53. Yang H, He H, Tong Z, Xia H, Mao Z, Gao C. The impact of size and surface ligand of gold nanorods on liver cancer accumulation and photothermal therapy in the second near-infrared window. J Colloid Interface Sci. 2020;565:186-96. Available from: https://doi.org/10.1016/j.jcis.2020.01.026.

54. Morales-Dalmau J, Vilches C, Sanz V, De Miguel I, Rodríguez-Fajardo V, Berto P, et al. Quantification of gold nanoparticle accumulation in tissue by two-photon luminescence microscopy. Nanoscale. 2019;11(23):11331-9.

55. Accomasso L, Cristallini C, Giachino C. Risk assessment and risk minimization in nanomedicine: A need for predictive, alternative, and 3Rs strategies. Front Pharmacol. 2018;9(MAR):1-7.

56. Bannigan P, Durack E, Mathur H, Rea MC, Ross RP, Hudson SP. Delivery of a hydrophobic drug into the lower gastrointestinal system via an endogenous enzyme-mediated carrier mechanism: An in vitro study. *Eur J Pharm Biopharm.* 2018;133:12-19.

57. Angiolini L, Valetti S, Cohen B, Feiler A, Douhal A. Fluorescence imaging of antibiotic clofazimine encapsulated within mesoporous silica particle carriers: Relevance to drug delivery and the effect on its release kinetics. *Phys Chem Chem Phys*. 2018;20:11899-

11911.

58. Meng Y, Wu C, Zhang J, Cao Q, Liu Q, Yu Y. Amphiphilic alginate as a drug release vehicle for water-insoluble drugs. *Colloid J*. 2015;77:754-760.

59. Amin M, Abbas NS, Hussain MA, Edgar KJ, Tahir MN, Tremel W, et al. Cellulose ether derivatives: a new platform for prodrug formation of fluoroquinolone antibiotics. *Cellulose.* 2015;22(3):2011-2022.

60. Vashisth P, Raghuwanshi N, Srivastava AK, Singh H, Nagar H, Pruthi V. Ofloxacin loaded gellan/PVA nanofibers - Synthesis, characterization and evaluation of their gastroretentive/mucoadhesive drug delivery potential. *Mater Sci Eng C*. 2017;71:611-619.

61. Solovskii M V., Borisenko MS, Vlasova EN, Tarabukina EB, Zakharova N V., Prazdnikova TA. Polymeric Complexes of Ofloxacin and Their Activity Against Tuberculosis Mycobacteria. *Pharm Chem J*. 2017;51(4):250-253.

62. Pathania D, Gupta D, Agarwal S, Asif M, Gupta VK. Fabrication of chitosan-g-poly(acrylamide)/CuS nanocomposite for controlled drug delivery and antibacterial activity. *Mater Sci Eng C*. 2016;64:428-435.

63. Marslin G, Revina AM, Khandelwal VKM, Balakumar K, Sheeba CJ, Franklin G. PEGylated ofloxacin nanoparticles render strong antibacterial activity against many clinically important human pathogens. *Colloids Surfaces B Biointerfaces*. 2015;132:62-70.

64. Guo J, Sun H, Lei W, et al. MMP-8-Responsive Polyethylene Glycol Hydrogel for Intraoral Drug Delivery. *J Dent Res*. 2019;98(5):564-571.

65. Chen Q, Shah KN, Zhang F, Salazar AJ, Shah PN, Li R,et al. Minocycline and Silver Dual-Loaded Polyphosphoester-Based Nanoparticles for Treatment of Resistant Pseudomonas aeruginosa. *Mol Pharm.* 2019;16(4):1606-1619.

66. Valdes C, Bustos G, Martinez JL, Laurido C. Antinociceptive antibiotics-loaded into solid lipid nanoparticles of prolonged release: Measuring pharmacological efficiency and time span on chronic monoarthritis rats. *PLoS One*. 2018;13(4):1-15.

67. Holmkvist AD, Friberg A, Nilsson UJ, Schouenborg J. Hydrophobic ion pairing of a minocycline/Ca2+/AOT complex for preparation of drug-loaded PLGA nanoparticles with improved sustained release. *Int J Pharm*. 2016;499(1-2):351-357.

Table S1: Innovative pharmaceutical preparations for solubility/ drug release improvement of leprosy drugs (dapsone, rifampicin, clofazimine, ofloxacin, and minocycline).

DS	Innovative formulations	*In vitro* evaluation (Drug release/ Solubility assessment)	*In vivo*/ *in silico*/ *in vitro* performance	Ref.
DAP	Solid dispersion (SD)	Drug release was nearly 1.9-fold compared to physical mixture and 7.5-fold compared to pure DAP (in first 10 min).	-	24
DAP and CFZ	Polymeric nanoparticles	Sustained release: after 24h, 82% of DAP and 68% of CFZ.	NP was more effective than the same dose of the drugs.	43
DAP	Cocrystal	Best solubility achieved: 1.5 times, compared to pure DAP.	-	26
DAP	Hydrogel	In the first hours, up to 5%, after 4h 10% and sustained release (up to 20%) in the next 22h.	-	44
DAP	Nanofibers	After 400 min, 77.71%, compared to 80.61% of DAP nanoemulsion.	-	45
DAP	Salt and Eutectics	Dissolution rate of salt nearly 2-fold and eutectics 1.7-fold than pure DAP (in first 10 min).	-	25
RIF	Solid lipid nanoparticles (SLN)	Drug release was 70.12% after 9 days while free RIF was more than 90% in 24h.	*In vivo* studies: Cmax in plasma, SLN: 15.12 µg/ml, Free RIF: 2.27 µg/ml. Relative bioavailability was improved 8.16 times (compared to free RIF), with sustained levels for 5 days.	17
RIF	Particulate hydrogel beads	Constant and sustained drug level throughout 24 h, with highest amount of drug released of 71.49%.	-	49
RIF	Solid dispersion	Drug release was 82.3%, compared to 32.7% of RIF powder (at 60 min, pH 6.8).	-	28
RIF	Solid lipid nanoparticle (SLN)	85% within approximately 6 min at both pHs performed (1.2 and 6.8).	*In vivo-in silico* assessment: AUC and Cmax increased by 3.72 and 5.22 fold compared to the RIF suspension. GastroPlus™ predicted maximum compartmental absorption from proximal and distal portions of the intestine.	18
RIF	Chitosan/gelatin/lecithin nanoparticles	Drug release was more than 3-fold up compared to free drug, at higher concentration of lecithin (2.0 g), in pH 7.2.	-	48
RIF	Carboxymethylcellulose complex	Drug release was 99 ± 3% at 15 min, compared to two commercial medicines of less than 80% and approximately 90%.	-	33
RIF	Phospholipid lipospheres	The best formulation presented solubility of 350.9 ± 23 µg/mL compared to 105.1 ± 12 µg/mL of pure drug.	Antimycobacterial activity enhanced compared to pure drug. Peak plasma concentration (Cmax) was 109.92 ± 25 µg/mL compared to 54.31 ± 18 µg/mL of pure drug.	29

DS	Innovative formulations	*In vitro* evaluation (Drug release/ Solubility assessment)	*In vivo/ in silico/ in vitro* performance	Ref.
			The AUC was 406.92 ± 18 µg h/L compared to 147.72 ± 15 µg h/L of pure drug.	
RIF	DIMEB complex	Improved solubility, at pH 7.4, achieving the equilibrium in approximately 9h.	-	20
RIF	Solid lipid nanoparticles (SLN)	Biphasic profile: initial burst followed by sustained pattern (up to 90% drug in 120 h).	-	46
RIF	Niosome	Between 61.69% and 75.90%, compared to 32.43% of pure RIF (after the first 2h).	-	30
RIF	Co-polymeric nanoparticles (NP)	Solubility improved 65-fold compared to pure drug. Controlled release achieving up to 70 h, compared to 6h of pure drug.	-	47
RIF	Niosome	Achieving 80% of drug release compared to 40% of pure drug, over 12h.	-	31
RIF	Liposomes	Drug release achieved 95% released after only 5 h, compared to nearly nearly 70% of free drug.	-	32
RIF	Nanocrystals	Nanocrystals showed up to 1.74-fold on solubility compared to commercial product.	-	27
CFZ	Alginate-mediated carrier	The release rate decreases upon increasing alginate concentrations.	-	58
CFZ	Complex formation	Increased approximately 0.53-fold of the maximum solubility compared to CB[7].	The analysis of MIC50 between complex and free drug did not show significant statistical difference.	38
CFZ	Nanoporous silica particles	Solubility was increased by 20-fold in simulated gastric fluid.	Permeation studies (using Caco-2 intestinal cells) showed more than 5-fold increased intestinal permeation in comparison to the free drug (below the detection limit).	37
CFZ	Enzyme-mediated carrier	Only CFZ binded to pepsin remains in solution in the intestinal environment (pH~5.4)	-	56
CFZ	Polymeric nanoparticle	Sustained pattern, about 30% at the end of the experiment (buffer solution - pH 6.8 for 8 h, at 37°C).	-	42
CFZ	Mesoporous silica particles (MPS)	At pH 4.1, maximum of 29% for ho-MSP (more hydrophobic) and 46% for hi-MSP. At pH 6.8: rapid release from hi-MSP, with 2 times higher initial release, compared to ho-MSP. However, both released nearly 10%.	-	57

DS	Innovative formulations	*In vitro* evaluation (Drug release/ Solubility assessment)	*In vivo/ in silico/ in vitro* performance	Ref.
CFZ	Nanoparticle (NP)	The NP, mainly in presence of fat, was faster dissolved compared to drug substance or to Lamprene®.		36
CFZ	Salt	Improvement of 5-fold on solubility compared to the free drug.	-	35
OFL	Cocrystal salt	After 1h, the amount of dissolved from cocrystal was more than 3-fold, compared to pure drug.	-	39
OFL	Inclusion complex	Solubility increased 3.7-fold compared to pure drug.	-	40
OFL	Nanoparticle cellulose conjugates	Nanoparticles showed sustained release proved in a pharmacokinetic study.	AUC was 1.6–2.3 times higher than controls rabbits.	59
OFL	Nanofibers	Initial rapid release (> 50% of drug released within 4 h), followed by a slow and sustained release phase.	Enhanced *in vitro* antimicrobial activity, and *in vivo* mucoadhesion and gastro-retention in rats.	60
OFL	Polymeric complex	Release of 45 – 57% in 50h.	Formulations demonstrated activity against *M. tuberculosis* in *in vitro* microbiological studies.	61
OFL	Nanoparticle (NP)	Maximum drug release of 76% observed after 18 h (ph 2.2).	Proven antibacterial activity against *E. coli*.	62
OFL	PEGylated nanoparticle (NP)	The best nanoparticles obtained released 96% of OFL in 36h. Free drug was released 100% in less than 4h.	Better bactericidal activity compared to free drug. And inhibition of *Bacillus subtilis* resistance.	63
MINO	Hydrogel	Initial burst release with subsequent release control, achieving 100% only after more than 48h.	-	64
MINO	Nanoparticle	Drug release achieved nearly 90% only after more than 10h. Free drug achieve the same percentage within 1h.	Antimicrobial activity was comparable to the free drug.	65
MINO	Solid lipid nanoparticle (SLN)	*In vitro* release was kept continuous during 7 days.	SLN was twice as efficient as free drug, in animal tests.	66
MINO	Polymeric nanoparticles	The NP presented an initial burst during 24h and a linear release over 30 days, compared to more than 98% within two days of free drug.	-	67

DS: Drug Substance; Ref: References; DAP: Dapsone; RIF: Rifampicin; CFZ: Clofazimine; OFL: Ofloxacin; MINO: Minocycline; h: hours.

5. APPENDIX C: Statistical process control of manufacturing tablets for antiretroviral therapy

ABSTRACT

In this study, the process of lamivudine (3TC) and zidovudine (AZT) (150 + 300 mg) tablets was evaluated using statistical process control (SPC) tools. This medicine is manufactured by Fundação para o Remédio Popular “Chopin Tavares de Lima” (FURP) laboratory, and it is distributed free of charge to patients infected with HIV by the Ministry of Health DST/AIDS national program. Data of 529 batches manufactured from 2012 to 2015 were collected. The critical quality attributes (CQAs), weight variation, uniformity of dosage units, and dissolution were evaluated. The process stability was assessed using control charts, and the capability indices Cp, Cpk, Pp, and Ppk were evaluated. 3TC dissolution data from 2013 revealed a non-centered process and lack of consistency compared to the other years, showing Cpk and Ppk lower than 1.0 and the chance of failure of 2,483 in 1,000,000 tablets. Dissolution data from 2015 showed the process improvement, revealed by Cpk and Ppk equal to 2.19 and 1.99, respectively. Overall, the control charts and capability indices showed the variability of the process and special causes. Additionally, it was possible to point out the opportunities for process changes, which are fundamental for understanding and supporting a continuous improvement environment.

Keywords: capability indices; control charts; HIV treatment; manufacturing process; quality tools.

INTRODUCTION

Despite the Brazilian government's efforts to control acquired immunodeficiency syndrome (AIDS), the number of infected patients has increased. Between 1980 and June 2019, 966,058 cases were reported in the country. Although the new HIV infections index has been decreasing in the previous five years - national detection rate of 0.18 cases per 1,000 population in 2018 [1] -.globally, this index has remained stable at the same period - nearly 0.23 per 1,000 uninfected population [2].

Fighting HIV requires the combination of at least three antiretrovirals, being two from different classes. The most common antiretroviral therapy is the combination of zidovudine (AZT), a reverse transcriptase inhibitor, and lamivudine (3TC), a nucleic acid synthesis inhibitor. AZT and 3TC are prodrugs and must be metabolized to their triphosphates metabolites for pharmacologic activity [3].

Lamivudine and zidovudine (150 + 300 mg) immediate-release tablets are manufactured using direct compression method by Fundação para o Remédio Popular “Chopin Tavares de Lima” (FURP) in Brazil. The medicines are distributed free of charge through the Health Ministry DST/AIDS program [4]. One of the features of this therapy is the significant intersubject variability of treatment [5]. AZT has been associated with hematologic toxicity, including neutropenia and severe anemia, being these effects concentration-dependent. Additionally, the highest prescribed dose should be administered in patients with an average weight above 40 kg, aiming to minimize these adverse effects [6]. Thus, the product quality consistency is critical to minimize unacceptable *in vivo* variability and, consequently, therapeutic drug failure.

The current Good Manufacturing Practices (cGMP) from the FDA requires statistical process control (SPC) quality tools to measure and analyze the process variability. They are also recommended by other pharmaceutical regulatory guidelines, such as the ICH Pharmaceutical Quality System Q10 guideline [7,8]. The manufacturers must gain enough process knowledge by detecting sources, variability amplitude, and their impact on product quality attributes. This is a paradigm shift in process evaluation towards a rational scientific-based approach, in contrast with the standard practice, which covers a mere comparison of the data collected with the CQA’s specification [9,10].

Among the statistical tools, the control charts and the capability indices (i.e., Cp, Cpk, Pp, and Ppk) allow evaluating the process consistency. It is considered stable if only common causes of variation are present, revealed by the control charts (CC) [11,12] in which the values are distributed in random order. In contrast, when special causes of variation are present (non-random distribution), the process is considered unpredictable. The process capability indices measure the ability to manufacture products that meet specifications. These indices are a ratio of variability and the CQA specification, and it can be applied to estimate the probability of producing out-of-specification (OOS) products. The capability indices Cp and Cpk calculation requires normally distributed data and a stable (stochastic) variation. These tools can be introduced at any time in the product's lifecycle, following a quality by design (QbD) approach, and may support continued process verification and annual product quality review [8,13].

The present study aimed to provide insights into the 3TC + AZT tablet manufacturing process variability by retrospective data analysis of 529 batches

manufactured by FURP between 2012 and 2015. For this purpose, the following CQAs were evaluated: weight variation, uniformity of dosage units, and dissolution.

MATERIALS AND METHODS

Materials:

FURP kindly provided the retrospective data of 529 batches of 3TC + AZT tablets manufactured between 2012 and 2015. Weight variation, uniformity of dosage units, and dissolution were the CQAs selected. Table 1 shows the number of batches by year.

Methods:

FURP performed the manufacturing process, and all CQAs quality control testing and the methods are summarized below:

3TC and AZT tablets (150 + 300 mg) manufacturing process

The direct compression process was used to manufacture the tablets. The drug substances and excipients were previously sieved, transferred to a 200.0 kg capacity V-blender (Treu® São Paulo), with later blend homogenization by 15 minutes at 13 rpm cycles. Magnesium stearate was also sieved and added to the other components of the formulation in V-blender and mixed for an additional five minutes. The powder blend was manually transferred to the gravity feeder, and the compression was performed in a 25-station rotary tableting machine, model N25 (Neuberger® São Paulo). The speed was 35,000 tablets/hour. After the end of the compression, the cores were transferred to a coating pan machine (150.0 kg) (Lawes Cota 150®São Paulo). An aqueous suspension sprayed the cores for film coating. The parameters used on coating step were: spray gun nozzle of 1.2 mm diameter, a gun-to-bed distance of 25 cm, atomizing air pressure of 36 psi, 8 rpm pan coating rotation speed, 65ºC inlet air temperature, 45 to 48ºC tablet bed temperature, and coating time between 45 and 60 minutes.

Critical Quality Attributes (CQAs)

- *Weight variation.* The weight variation of 3TC + AZT tablets was performed according to the Brazilian Pharmacopoeia 5ed. chapter 5 (general methods) [14]. Briefly, a total of 20 tablets per batch were weighted using a digital balance (Mettler Toledo® Model AL204). The criteria are met when no more than two tablets differ from the mean by ±5%, and no unit differs in weight more than ±10% of the mean.

- *Uniformity of dosage units.* The uniformity of dosage units of 3TC + AZT tablets was accessed according to the Brazilian Pharmacopoeia 5ed. chapter 5 (general methods) [14]. Briefly, for each batch, ten tablets were weighed individually (Mettler Toledo® Model AL204). The results were expressed as the amount of drug per tablet. The acceptance value (AV) was calculated using the equation: AV = (M – X) + ks, where M reference batch, X is mean batch for batch assay, k is the acceptability constant, and s is the standard deviation. The specifications were (90-110%) [14]. The HPLC method parameters for 3TC + AZT quantification were: HPLC LC-20AT, Shimadzu®, column Phenomenex C18 250 x 4.6 mm, 0.1 M ammonium acetate buffer, methanol and acetic acid (65:35:0.1) mobile phase, 270 nm wavelength.

- *Dissolution*. Dissolution tests of the 3TC + AZT tablets were performed according to the Brazilian Pharmacopoeia 5ed. [14]. Briefly, the conditions were: USP apparatus 2, 50 rpm, 900 mL, and 37.0 ± 0.5 °C purified water, using DTS, Ethik Technology® dissolution system. After 60 minutes, 5 mL aliquots of the dissolution medium were withdrawn and diluted with the mobile phase. The quantification was performed as described in the uniformity of dosage units method. The values were expressed as a percentage of the declared content drug. The first stage's tolerance limit is not less than 80% (Q + 5%) of 3TC and AZT.

Statistical analysis

The process stability and process capability of the CQAs of the 3TC + AZT tablets were performed using, respectively, control charts and capability indices [15,16]. Histogram evaluation and Anderson-Darling tests were performed to evaluate the normal data distribution. The process stability was evaluated using individual observations with moving range charts, the tool stage in temporal sequence, considering one year as a subgroup. This chart is created using the difference of consecutive batches. The process capability was evaluated by the capability charts and

the capability indices: Cp (process capability), Cpk (process capability adjusted for non-centered distribution), Pp (potential or global capability of the process), and Ppk (potential process capability adjusted for non-centered distribution) [17]. The within and global standard deviations were compared to verify the process capability, the sources of variation, and the variation within subgroups [16,18,19]. Statistical analysis of data was performed using Minitab 18 software (Minitab, State College, PA).

RESULT AND DISCUSSION

Weight variation evaluation:

Assumption of data normality

The histogram evaluated the normality of the data. The data distribution in Figure 1 revealed a symmetrical, bell-shaped, and unimodal curve (Gaussian curve). These features and the mean (666.48 mg) close to the median (666.50 mg) suggest the data normality. Moreover, the standard deviation can be evaluated to assume a normal distribution. The 68-95-99.7 empiric rule is another method the access data normality. This study revealed 69.26% of data within the limits of one standard deviation (σ), 95.46% within two σ, and 99.73% within three σ [16].

The weight variation data by year is described in Table 2. The analysis for each year revealed that the values were close to the target (666.5 mg).

In addition to the histogram (fig. 1), the normal distribution of the weight variation data was assessed using the Anderson-Darling (AD) test [20,21]. The results of the AD test were presented in Figure 2 and Table 3. The p-values were below the significance level (α = 0.05) for all years. It implies the rejection of the null hypothesis (H0: the data follow a normal distribution). Consequently, the alternative hypothesis H1 (H1: the data does not follow a normal distribution) was accepted. Therefore, this test suggests that the weight variation data does not follow a normal distribution [20].

The AD test compares the sum of squares differences between the empirical data and the hypothetical distribution. AD uses the data without grouping, which means that the test is sensitive to inconsistencies at the distribution tails rather than near the median. So, it accentuates the discrepancies in the tails [21,22]. Thus, the batches' weight tablet values in the tails significantly influence the assumption of normality (fig. 2). The data normality was assumed despite the AD test result due to histogram

evaluation, mean and median comparison, and standard deviation 68-95-99.7 empiric rule (fig. 1).

Process stability evaluation

The control chart of weight variation (fig. 3) was performed using the tool stages, which allows the data evaluation in a historical ordered way (by year). Lower and upper control limits (657.82 and 675.16 mg, respectively) were calculated considering three standard deviation intervals (fig. 3). The Brazilian Pharmacopoeia 5ed. [14] sets up the variation limits of ± 5% for coated tablets weighing more than 300 mg, which means values between 633 and 700 mg. However, in the present study, they were 650 and 683 mg (variation ± 2.5%), respectively. The tight specification is an internal manufacturer procedure implemented to ensure product effectiveness, safety, and quality.

Six batches were detected out of the control limits (OCL) (individuals values chart), known as special causes. Four in 2012, one in 2013, and one in 2014. No OCL was observed in 2015. Five of the six batches were found below the lower control limit (LCL). However, these batches met the internal specification limits. In the moving range chart, the OCL showed high variability between successive batches, mostly in 2012. No OCL was detected in 2013 and 2014, and only one event was detected in 2015 (fig. 3). However, it is essential to point out that the six detected OCL comprises only 1% of the 529 batches manufactured in the four-year period, which shows the weight variation's practical stability.

A possible explanation for the observed OCL can be related to operator performance and manufacturing issues, including equipment and pharmaceutical inputs. The tablet machine used is hand-feeding equipment, making this step a potential source of variability. Moreover, the observed variability might justify the implementation of more advanced technology, for example, a forced feeder machine. Additionally, the detected variability may be due to powder flow characteristics, the components' cohesiveness, and the particles' irregular shape. Thus, forced feeding using suitable blade-containing equipment is recommended. In this case, a 45-angle blade can be selected for powders with reduced density for moving the powder downwards. This configuration can improve the matrix's filling for formulations with low powder flow, resulting in standard deviation minimization up to 75% [23].

Process capability evaluation

The process capability indices describe the ability of the process of manufacturing products within the specification limits. These indices are accurate when the data follows a normal distribution. The indices Cp and Pp do not consider whether the mean is close to the target. Cpk and Ppk are defined as the rate between the unilateral process capability index and the specification limit (upper or lower) closest to the average. Overall, Cp measures the potential capability of the process, while Cpk measures effective capability. The capability indices Cpk and Ppk are calculated with different standard deviations, respectively σ **(**within) and **s** (overall). The σ is used to calculate the control limits and calculate Cp and Cpk, also called short-term process performance indices or potential capability [16]. The ***s*** is used to calculate Pp and Ppk, which are indices of long-term process performance or global capability.

When the values of Cp and Cpk are similar, the process is centralized, which means that the process average is close to the target and under statistical control (only common causes of variability are present). The process is considered capable of manufacturing within specification limits when Cpk > 1.0, being an ideal Cpk ≥ 2.0. When it is between 1.34 and 1.99, the process is considered suitable; values between 1.0 and 1.33 show that the process requires corrective action, and values less than 1.0 denote a not capable process. If it is equal to 1.0, then 99.73% of the values lie within the specification limits [24]. Thus, 0.27% of the units manufactured may be out of specification (example: in 1000.000 units manufactured, 2,700 units OOS). Figure 4 shows the process capability evaluation for the four years with values of Pp and Ppk of 1.88 (***s*** = 2.92) and Cp and Cpk of 1.89 and 1.92, respectively (σ = 2.86). This result revealed process centralization and its consistency under the statistical control for this CQA. The process failure probability, in the four years, was two tablets in 100,000,000 manufactured units.

The capability indices were also calculated by year, as shown in Table 4. Cpk ranged from 1.79 to 2.03, and Ppk from 1.75 to 2.11. Standard deviations σ were in the range of 2.65 to 3.04, and 2.51 to 3.12 for ***s***. However, only 2015 showed Cp = Cpk and Pp = Ppk and Cpk = Ppk, showing the process's consistency. Botelho, R.S. et al. [10] revealed Cp and Cpk of 1.00 and 0.98, respectively, for the weight variation data of three consecutive batches of furosemide (40 mg) tablets. These values showed a high probability of process failure (2,751 PPM). In this study, the probability of obtaining results outside the specification limits was substantially lower (0.02 PPM).

When the indices were calculated with overall data (no year stage), Cp and Cpk indices were equal, 1.89, and Cpk was almost equal to Ppk (1.89 and 1.88, respectively). This result showed a centralized and under statistical control process. Thus, the analysis by year can expose the opportunities for process improvement. These opportunities are the centralization of the process, special causes investigation, and even technology modernization.

Uniformity of dosage units evaluation:

Assumption of data normality

Histogram and Anderson-Darling test were evaluated as previously described in weight variation analysis (fig. S1 and Table S1). Histograms with unimodal distribution and bell-shaped symmetry were observed for both drug substances. The mean and median values were similar, with the maximum difference for 3TC of 0.39 mg, in 2015 (Table S2). The mean and median difference of AZT data was only 0.14 mg in 2012. Reduced values for AZT standard deviations (SD) were detected from 2012 to 2014. In 2015, SD was similar to the two previous years, respectively, 1.94 and 1.96.

In addition to the histogram, the data were evaluated for their distribution using the Anderson-Darling test (fig. S2 and Table S1). The p-values for both drug substances were lower than the level of significance ($\alpha = 0.05$). These results indicated that the data do not follow a normal distribution. However, it is possible to observe that the extreme values (from tails) for AZT are closer to the adjusted distribution line (fig. S2). Figures S1, S2, and Tables S1, S2 can be found in the supplemental material.

Process stability evaluation

Figure 5 shows the control charts for individual observations. The 3TC UCL and LCL were 94.27 and 104.12%. For AZT, the UCL and LCL were 95.49 and 103.58%, respectively. For this CQA, the specification limits are 90 and 110% [14].

Ten batches above the UCL (102.94%) and six below the LCL (96.24%) were found (fig. 5). In 2012, nine OCL were found, being six above the UCL and three below the LCL. Five batches out of the control limits (OCL) were observed in 2013, two above the UCL and three below the LCL. In 2014, only two batches were observed below the

LCL. In 2015, no OCL was observed. However, all of them are within the specification limits. Figure 5 also shows a lower variability in 2013 when compared with other years.

The special causes mentioned above could be easily detected using these control charts. Consequently, this tool can be used to support a search for the source of variation and apply corrective actions. Control charts can help in the prevention of non-conforming units when a variability increase trend is found. Thus, this tool can support process variability elimination or its reduction as much as possible [15].

Besides, Figure 5 shows the moving range (MR). The highest UCL was detected in 2015, respectively, 6.0 and 5.0% for 3TC and AZT. The most substantial variability in the MR was detected in 2014; batch 419 showed higher values for both drugs, 3TC and AZT, 6.3 and 7.3%, respectively. Twenty-three OCL of 3TC make up only 4.3% of the 526 batches, and for AZT, twelve OCL are only 2.2% of the total.

Process capability evaluation

Table 5 shows the process capability indices for uniformity of dosage units. Since 3TC indices are not very close, they revealed the need for process centralization. The minor difference between Cp and Cpk was 0.05 in 2014, and a significant difference was observed in 2013 (0.44). On the other hand, the best values for process consistency were observed in 2015, when the difference between Cpk and Ppk was only 0.29. The worst value was found in 2013, with a difference of 1.38. The Cpk and Ppk divergences indicated that the process was not operated predictably over time. Considering the worst index (Ppk: 1.58), the probability of process failure was 116 tablets in 100,000,000 units manufactured in 2015 for 3TC.

The Cp and Cpk, Pp, and Ppk of AZT (Table 5) also revealed the need for process centralization when the process is observed by year. The lowest difference between Cp and Cpk was 0.08 in 2014, while the highest difference was in 2013 (0.61). Considering the lower Ppk (1.62), the probability of failure of the process was 68 tablets in 100,000,000 units manufactured in 2015. Although in 2015, the 3TC Ppk was close to AZT, the probability of failure in the uniformity of the dosage units for lamivudine is 1.7 times greater than zidovudine. Likewise, the Cp and Cpk indices from the uniformity of dosage units of furosemide tablets (40 mg) and captopril (25 mg) also revealed a non-centralized process. Cp and Cpk were 1.43 and 1.27 and 1.69 and 1.83, respectively [10,24].

The 3TC + AZT tablets are 67.5% of drug substances (22.5% of 3TC and 45% of AZT). Therefore, differences in the powder densities and particle size distribution of drug substances may cause segregation of the powder blend from the feeding to the compression chamber. This potential failure must be investigated and avoided by controlling the particle size distribution in the blend, flow time evaluation, and morphological analysis of the particles. Crowley (2018) used multivariate models to evaluate the negative impact of non-uniform moisture on compaction performance. Besides, the variability between four batches of microcrystalline cellulose prepared from different wood pulp was analyzed, revealing a considerable influence of the excipient's origin on the compaction ability [25].

Dissolution evaluation:

Assumption of data normality

Histogram and Anderson-Darling tests were evaluated to access data normality as earlier described (fig. S3, S4, and Table S3 of the supplemental material). Histogram showed curves with unimodal data distribution and bell-shaped symmetry for both drug substances and cores and coated tablets (fig. S3 and fig. S4). 3TC and AZT dissolution data showed close means and medians for all years (Table S4). A reduction trend in the standard deviation of 3TC was detected in 2014. Minor values were found in 2015 for both drug substances (2.74 for 3TC and 2.38 for AZT).

Data normality was also evaluated using the Anderson-Darling test (fig. S5 and Table S3). The values for both drug substances were lower than the level of significance (α = 0.05). These results show that the data do not follow a normal distribution. Similarly, the core tablets did not show normal data distribution (fig. S6). However, as in earlier evaluations, the data was assumed normally distributed. Figures S3, S4, S5, and Tables S3 and S4 can be found in the supplemental material.

Process stability evaluation

Figure 6a shows the control chart of 3TC. In 2012, five batches presented values below the LCL. No batches were detected above UCL as expected due the to uniformity of dosage units results. In 2013, higher variability was found compared to other years, with results tending to be lower than the mean, signaled by the LCL below the lower

specification limit (LSL). For 2014, two batches were below the LCL and none in 2015. Similar behavior was observed for the 3TC cores (fig. S7).

Figure 6b shows the control chart from 3TC in 2013, with a monthly stage. This chart shows the batches in detail for coated tablets. Between February and November 2013, eighty-eight batches were manufactured. The first fifteen batches showed the highest process variability. From batches sixteen to sixty-two, 3TC dissolution was close to the target. It means a centralized process with reduced variability. The variability has increased from sixty-three to seventy-four batches, and from batches seventy-five to eighty-eight, the variability decreased.

For the same drug, two batches were found below the LCL in 2014. In 2015, no OCL was found. The LCL and UCL of coated tablets were, respectively, 87.0% and 103.5% (2012), 78.1 and 105.9% (2013), 87.3 and 103.6% (2014) and 88.8 and 103.8% (2015). For the cores, these values were very close (LCL= 89.29% and UCL= 102.3%) (fig. S7). These values, except the UCL in 2013, are within the limit of specification [14].

Figure 7 shows the control chart of AZT for coated tablets. In 2012, a more significant number of lots presented OCL results in comparison to other years: four below the LCL and one above the UCL. Even so, this quantity was considerably low regarding the entire batches produced in the period (n=249). Interestingly, in the same period, the cores showed only one result below LCL and one above the UCL (fig. S8). It is necessary to reinforce that even though some results have shown values out of the control limits, all meet the specification.

Figures 6a, 6b, 7, S7, and S8 show the moving range charts. The highest UCL was found in 2013 for 3TC and AZT. The moving range values above the UCL showed high variability between successive batches.

Process capability evaluation

Table 4 summarizes the dissolution (3TC and AZT) capability process for the period 2012-2015. The process capability of 3TC shows that the process is not centralized for coated tablets or cores (Table 6 and S5). Ppk and Cpk, were: 1.63 and 1.96 (2012); 1.00 and 0.94 (2013); 1.45 and 1.91 (2014) and 1.99 and 2.19 (2015) for coated tablets. These indices showed a minimum difference of 0.06 in 2013. The differences between Cpk and Ppk indicated that the process was not operated predictably during the evaluated period. The lowest 3TC Cpk index for coated (0.94) revealed the

probability of failure of 1,339 tablets in 1,000,000 units manufactured in 2013. This probability of failure suggests urgent improvement of process centralization and special causes elimination.

According to Tables 6, S5, and Figures 8 and S9, the process capability of AZT shows that the process is also not centered. For coated tablets, the Ppk and Cpk indices were: 2.02 and 2.50 (2012); 1.86 and 1.86 (2013); 1.92 and 2.28 (2014); and 2.36 and 2.62 (2015). These indices were equal in 2013 (1.86) and had a maximum difference of 0.48 in 2012. The differences between Cpk and Ppk indicated that the process was not operated consistently. Considering the lowest index (Ppk = 1.86), the probability of failure of the process was 1 in 100,000,000 units manufactured in 2013.

The overall Cpk values for coated tablets were 1.50 for 3TC and 1.98 for AZT, denoting AZT's better performance. Even for the evaluation by year, the AZT Cpk values are higher than 3TC, confirming the difference between the drug substances. Significant variability for both drugs on coated tablets was observed in 2013, with the total variation (***s***) of 4.02 and 2.90 for 3TC and AZR, respectively. The within subgroup variation (σ) was also elevated in 2013 (4.28 for 3TC and 2.90 for AZT). In parallel, the lowest variation was observed in 2015 for both drug substances.

As the statistical analysis of the dissolution of the coated tablets and the 3TC and AZT cores (150 + 300 mg) showed virtually no difference in results (Tables 6 and S5), the higher variability of 3TC from dissolution might be related to the uniformity of dosage units results. However, this CQA showed a lower variability in the year 2013 (Table 5, fig. 5). The capability indexes of uniformity of dosage showed high Cp and Cpk, Pp, and Ppk, all above 1.58. This performance reinforced that the uniformity of dosage units did not influence 3TC and AZT dissolution variability in 2013.

Regarding the cores' coating, a slight difference between the results before and after the coating process was expected. This behavior may be explained by the function of the dry film used in the coating process. The excipient Opadry II was hypromellose-based, and its function is to mask the unpleasant taste of 3TC and AZT [26,27]. Therefore, in this case, the coating did not influence the dissolution of the coated tablets.

The excipients croscarmellose sodium, microcrystalline cellulose, silicon dioxide, hypromellose, and magnesium stearate represent only 32.5% of the total tablet mass. Considering the higher amount of drug substances in the formulation, differences in 3TC or AZT particles' physical characteristics such as size, shape,

density, and polymorphism may contribute to drug dissolution failures and increase the process variability [23].

CONCLUSION

This study allowed understanding the 3TC + AZT tablet manufacturing process variability by retrospective data analysis of 529 batches considering the following CQAs: weight variation, uniformity of dosage units, and dissolution. The analysis of weight variation highlighted a better understanding of the process performance over time. For this CQA, the process stability was revealed, presenting low process failure probability. Nevertheless, some opportunities for improvement can be pointed out. Corrective actions such as the training of operators can be applied immediately. Besides, implementing a forced feeder machine may improve matrix filling during direct compression minimizing its variability.

For uniformity of dosage units, 3TC and AZT's capability indices revealed the need for process centralization. Special causes were progressively eliminated over the years and were not detected in 2015. If process refinements are still desired, it is recommended to investigate the impact of powder density, particle morphology, and origin of excipients on the uniformity of dosage units. Besides, controlling the particle size during the blend and the flow time through a forced feeder machine implementation may centralize the process.

The dissolution process capability allowed discriminating the performance of the two drug substances. This difference permits drive the efforts towards 3TC improvements. Moreover, the dissolution results showed no significant difference before and after the coating process. Also, the large amount of drug substances in the tablet and their physical characteristics may be further investigated to mitigate the process variation.

Lamivudine and zidovudine AIDS treatment requires product quality consistency to minimize intersubject variability and, consequently, therapeutic drug failure. Control charts and capability indices allowed variation detection, understanding, and assessing their sources on product attributes. Therefore, this approach revealed opportunities for process improvement, aiming to reduce risks to the patients.

Acknowledgements: This work was supported by CAPES (Coordenação de Aperfeiçoamento de Pessoal de Nível Superior) – Finance code 001

Declaration of interest statement: No potential conflict of interest was reported by the author(s).

Abbreviations: 3TC: lamivudine; AZT: zidovudine; AD test: Anderson Darling test; AM: average moving range; CC: control charts; Cp: process capability; Cpk: process capability based on unilateral dispersion; CPL: process capability based on lower control limit; CPU: process capability based on upper control limit; LCL: lower control limit; LSL: lower specification limit; OCL: out of control limits; Pp: global capability of the process, Ppk: global process capability based on unilateral dispersion; PPL: global process capability based on lower control limit; PPM: parts of failure per million of manufactured units; PPU: global process capability index based on upper control limit; UCL: upper control limit; USL: upper specification limit;

REFERENCES

1. BRASIL. Boletim Epidemiológico HIV / Aids | 2019. Boletim Epidemiológico HIV/AIDS. 2019. Available from: http://www.aids.gov.br/pt-br/pub/2019/boletim-epidemiologico-de-hivaids-2019
2. WHO. Number of new HIV infections Estimates by WHO region. 2019. Available from: https://apps.who.int/gho/data/node.main.HIVINCIDENCE
3. Anderson PL, Rower JE. Zidovudine and Lamivudine for HIV Infection. Clin Med Rev Ther. 2010;2:115–27.
4. BRASIL. Tratamento para o HIV | Departamento de Doenças de Condições Crônicas e Infecções Sexualmente Transmissíveis. Ministério Da Saúde. 2019. Available from: http://www.aids.gov.br/pt-br/publico-geral/o-que-e-hiv/tratamento-para-o-hiv
5. Flynn PM, Rodman J, Lindsey JC, Robbins B, Capparelli E, Knapp KM, et al. Intracellular pharmacokinetics of once versus twice daily zidovudine and lamivudine in adolescents. Antimicrob Agents Chemother. 2007;51(10):3516–22.
6. Fauchet F, Treluyer JM, Frange P, Urien S, Foissac F, Bouazza N, et al. Population pharmacokinetics study of recommended zidovudine doses in HIV-1-infected children. Antimicrob Agents Chemother. 2013;57(10):4801–8.
7. GUIDELINE IHT. PHARMACEUTICAL QUALITY SYSTEM Q10. 2008. p. 1–17. Available from: https://database.ich.org/sites/default/files/Q10 Guideline.pdf
8. FDA. Guidance for Industry - Process Validation: General Principles and Practices. Current Good Manufacturing Practices (CGMP). 2011. p. 1–19. Available from: https://www.fda.gov/downloads/drugs/guidances/ucm070336.pdf
9. Samohyl RW. Controle Estatístico de Processo e Ferramentas da Qualidade. In: M.M. Carvalho, E.P. Paladin and E.P. Paladini, Eds E, editor. Gestão da qualidade: teoria e casos. Rio de Janeiro: Elsevier; 2009. p. 261–300.
10. de Souza Botelho T, Tavares VF, Dal Curtivo CP, Sarolli SRB, Fernandes MA, Donaduzzi CM, et al. A Statistical approach to: Evaluating the manufacture of furosemide tablets. Pharm Technol. 2011;35(3):112–21.
11. Dudek-Burlikowska M. Quality estimation of process with usage control charts

type X-R and quality capability of process Cp, Cpk. J Mater Process Technol. 2005;162–163:736–43.
12. Kotz S, Johnson NL. Process capability indices - A review, 1992-2000. J Qual Technol. 2002;34(1):2–19.
13. FDA. Pharmaceutical Quality System Elements: Product Quality Management. 2011. Available from: https://www.fda.gov/files/drugs/published/Product-Quality-Management.pdf
14. ANVISA. Métodos Gerais. In: Farmacopeia Brasileira. 5th ed. São Paulo; 2010.
15. Shah S, Shridhar P, Gohil D. Control chart : A statistical process control tool in pharmacy. Asian J Pharm. 2010;4(3):184–92.
16. Chatterjee M, Chakraborty AK. Some process capability indices for unilateral specification limits—Their properties and the process capability control charts. Commun Stat - Theory Methods. 2016;45(24):7130–60.
17. Kashif M, Aslam M, Rao GS, Al-Marshadi AH, Jun CH. Bootstrap Confidence Intervals of the Modified Process Capability Index for Weibull distribution. Arab J Sci Eng. 2017;42(11):4565–73.
18. Chopra V, Bairagi M, Trivedi P, Nagar M. A case study: Application of statistical process control tool for determining process capability and sigma level. PDA J Pharm Sci Technol. 2012;66(2):98–115.
19. Kovářík; M, Sarga L. Process Capability Indices for Non-Normal Data. 2014;11:419–29.
20. Montgomery DC. Introdução ao controle estatístico da qualidade. Vol. 7. Rio de Janeiro; 2015.
21. Anderson TW, Darling DA. A Test of Goodness of Fit. J Am Stat Assoc. 1954;49(268):765–9.
22. Yap BW, Sim CH. Comparisons of various types of normality tests. J Stat Comput Simul. 2011;81(12):2141–55.
23. Kirsch D. Fixing tableting problems. Pharm Technol. 2015;39(5):58–9.
24. Dal Curtivo CP, Funghi NB, Tavares GD, Barbosa SF, Löbenberg R, Bou-Chacra NA. The critical role of NIR spectroscopy and statistical process control (SPC) strategy towards captopril tablets (25 mg) manufacturing process understanding: A case study. Pharm Dev Technol. 2015;20(3):345–51.
25. Crowley ME. A study of microcrystalline cellulose variability and how this impacts compaction performance. University College Cork; 2018.
26. Schiffman SS, Zervakis J, Shaio E, Heald AE. Effect of the nucleoside analogs zidovudine, didanosine, stavudine, and lamivudine on the sense of taste. Nutrition. 1999;15(11–12):854–9.
27. Nishiyama T, Ogata T, Ozeki T. Preparation of bitter taste-masking granules of lafutidine for orally disintegrating tablets using water-insoluble/soluble polymer combinations. J Drug Deliv Sci Technol. 2016;32:38–42. Available from: http://dx.doi.org/10.1016/j.jddst.2016.01.005

6. APPENDIX D: Cancer treatment in the lymphatic system: A prospective targeting employing nanostructured systems

ABSTRACT

Cancer related to lymphangiogenesis has gained a great deal of attention in recent decades ever since specific markers of this intriguing system were discovered. Unlike the blood system, the lymphatic system has unique features that can advance cancer in future metastasis, or, conversely, can provide an opportunity to prevent or treat this disease that affects people worldwide. The aim of this review is to show the recent research of cancer treatment associated with the lymphatic system, considered one of the main gateways for disseminating metastatic cells to distant organs. Nanostructured systems based on theranostics and immunotherapies can offer several options for this complex disease. Precision targeting and accumulation of nanomaterials into the tumor sites and their elimination, or targeting the specific immune defense cells to promote optimal regression of cancer cells are highlighted in this paper. Moreover, therapies based on nanostructured systems through lymphatic systems may reduce the side effects and toxicity, avoid first pass hepatic metabolism, and improve patient recovery. We emphasize the general understanding of the association between the immune and lymphatic systems, their interaction with tumor cells, the mechanisms involved and the recent developments in several nanotechnology treatments related to this disease.